TRANSPORTATION RESEARCH RECORD 612

Subsidence Over Mines and Caverns, Moisture and Frost Actions, and Classification

TRANSPORTATION RESEARCH BOARD

COMMISSION ON SOCIOTECHNICAL SYSTEMS
NATIONAL RESEARCH COUNCIL

NATIONAL ACADEMY OF SCIENCES
WASHINGTON, D.C. 1976

Transportation Research Record 612
Price $3.60
Edited for TRB by Frances R. Zwanzig

subject areas
21 photogrammetry
33 construction
61 exploration-classification (soils)
62 foundations (soils)
64 soil science

Transportation Research Board publications are available by ordering directly from the board. They may also be obtained on a regular basis through organizational or individual supporting membership in the board; members or library subscribers are eligible for substantial discounts. For further information, write to the Transportation Research Board, National Academy of Sciences, 2101 Constitution Avenue, N.W., Washington, D.C. 20418.

Notice

The project that is the subject of this report was approved by the Governing Board of the National Research Council, whose members are drawn from the councils of the National Academy of Sciences, the National Academy of Engineering, and the Institute of Medicine. The members of the committee responsible for the report were chosen for their special competence and with regard for appropriate balance.

This report has been reviewed by a group other than the authors according to procedures approved by a Report Review Committee consisting of members of the National Academy of Sciences, the National Academy of Engineering, and the Institute of Medicine.

The views expressed in this report are those of the authors and do not necessarily reflect the view of the committee, the Transportation Research Board, the National Academy of Sciences, or the sponsors of the project.

Library of Congress Cataloging in Publication Data
National Research Council. Transportation Research Board.
Subsidence over mines and caverns, moisture and frost actions, and classification.

(Transportation research record; 612)
Twelve reports prepared for the 55th annual meeting of the Transportation Research Board.
1. Subsidences (Earth movements)–Congresses. 2. Earth movements and building–Congresses. I. Title. II. Series.
TE7.H5 no. 612 [QE600] 380.5'08s [551.3] 77-23116
ISBN 0-309-02588-5

Sponsorship of the Papers in This Transportation Research Record

GROUP 2–DESIGN AND CONSTRUCTION OF TRANSPORTATION FACILITIES
W. B. Drake, Kentucky Department of Transportation, chairman

Construction Section
Robert D. Schmidt, Illinois Department of Transportation, chairman

Committee on Earthwork Construction
David S. Gedney, Federal Highway Administration, chairman
Joseph D'Angelo, Edward N. Eiland, L. F. Erickson, Charles H. Haney, Jr., Erling Henrikson, William P. Hofmann, John R. Kohnke, W. F. Land, Charles H. Shepard, Edgar H. Stickney, Walter C. Waidelich, Glen R. Watz

Soil Mechanics Section
John A. Deacon, University of Kentucky, chairman

Committee on Subsurface Drainage
George W. Ring III, Federal Highway Administration, chairman
Charles C. Calhoun, Jr., Harry R. Cedergren, Barry J. Dempsey, Ernest L. Dodson, Edward N. Eiland, David S. Gedney, Alfred W. Maner, Glen L. Martin, K. H. McGhee, Lyndon H. Moore, Lyle K. Moulton, William B. Nern, Travis W. Smith, W. T. Spencer, William D. Trolinger, Walter C. Waidelich, Clayton E. Warner, Thomas F. Zimmie

Soil and Rock Properties and Geology Section
L. F. Erickson, Idaho Department of Highways, chairman

Committee on Exploration and Classification of Earth Materials
Robert L. Schuster, U.S. Geological Survey, Denver, chairman
Martin C. Everitt, Edward A. Fernau, Frank L. Jagodits, Robert B. Johnson, Robert D. Krebs, Donald E. McCormack, Olin W. Mintzer, R. Woodward Moore, Frank R. Perchalski, David L. Royster, Alex Rutka, J. Chris Schwarzhoff, Robert B. Sennett, Preston C. Smith, Sam I. Thornton, J. Allan Tice

Committee on Soil and Rock Properties
T. H. Wu, Ohio State University, chairman
William F. Brumund, Richard W. Christensen, George B. Clark, Charles L. Emery, James P. Gould, Ernest Jonas, Charles C. Ladd, G. A. Leonards, Victor Milligan, John D. Nelson, Gerald P. Raymond, Hassan A. Sultan, David J. Varnes, Harvey E. Wahls, John L. Walkinshaw

Committee on Frost Action
Arthur L. Straub, Clarkson College of Technology, chairman
Barry J. Dempsey, Wilbur J. Dunphy, Jr., L. F. Erickson, Wilbur M. Haas, Glenn E. Johns, Thaddeus C. Johnson, Alfreds R. Jumikis, Miles S. Kersten, Clyde N. Laughter, George W. McAlpin, Richard W. McGaw, Stephen F. Obermeier, Marvin D. Oosterbaan, Robert G. Packard, Edward Penner, Harold R. Peyton, Alex Rutka

Committee on Engineering Geology
David L. Royster, Tennessee Department of Transportation, chairman
Robert C. Deen, Ernest Dobrovolny, Martin C. Everitt, Leonard H. Guilbeau, Robert B. Johnson, John D. McNeal, Adrian Pelzner, Charles S. Robinson, Dwight A. Sangrey, Jerome R. Saroff, Robert L. Schuster, Robert B. Sennett, Travis W. Smith, Berke L. Thompson, J. Allan Tice, A. Keith Turner

John W. Guinnee and William G. Gunderman, Transportation Research Board staff

Sponsorship is indicated by a footnote on the first page of each report. The organizational units and the officers and members are as of December 31, 1975.

Contents

Part 1
Subsidence Over Mines and Caverns

Mechanisms of Subsidence Due to Underground Openings

George F. Sowers, Department of Civil Engineering, Georgia Institute of Technology, Atlanta

Subsidence from underground defects is an increasing problem, and effective preventive or corrective measures depend on knowing the mechanism causing the failure. Too often, however, the mechanism is ignored or diagnosed from the appearance of the ground surface, leading to routine indiscriminate treatment such as filling the depression or draining any water, which can be successful, ineffective, or harmful, depending on the mechanism involved. A number of types of openings are involved: open excavations, leaking sewers and culverts, solution channels in limestones, enlarged joints, faults, mines, tunnels, porous lava, erosion caves, voids between boulders, and voids between large debris. The mechanisms responsible include stratum thinning (including consolidation, collapse, or plastic flow), chemical and biochemical action (including burning), lateral strain, loss of lateral support, collapse of an opening, and raveling or erosion. Various combinations of openings and mechanisms can produce similar effects, but the necessary corrective measures are often different. Moreover, subsidences due to other mechanisms often resemble those from openings. This paper briefly discusses these to show their similarities and differences.

On June 22, 1975, both the eastbound and westbound lanes of Interstate 4 northeast of Lakeland, Florida, suddenly collapsed. Fortunately, no one was hurt and it was possible to fill the openings, repave the surface, and put the highway back in operation with little inconvenience to the public.

Aerial reconnaissance of the area disclosed a saucer-like circular depression that was centered in the median with its perimeter extending beyond the right-of-way, and an elongated system of similar depressions leading toward the area on both sides of the highway. The cause of the subsidence had been the collapse of underground cavities in the sandy soil that had developed by roofing and doming action above solution channels in the porous limestone 16 m (50 ft) below.

Unfortunately, this is not an isolated case. Failures due to sinkhole action in areas underlain by limestone are well known. In such areas, their frequency of occurrence is such that they are almost ignored as engineering problems. Sinks also occasionally occur in areas underlain by volcanic rocks, and are common in iron and coal mining regions. While the locations, mechanisms, the rates of failure, and warnings of trouble available to the public vary greatly, there is one thing in common among many of these failures—nearby openings in the soil or rock. These openings may be natural or man-made; they may be large or small. They take many forms: pores between solid particles, covered openings such as tunnels and caves, and open cuts.

Failure occurs through numerous independent and interdependent mechanisms. The surface effects of many of these mechanisms are so similar that the cause of a subsidence is sometimes misdiagnosed and the remedial action is then ineffective. This paper summarizes the forms of openings that have been the focal points for surface subsidences, describes the various mechanisms by which failure eventually develops, and points out places where confusion in diagnosing the type of opening and the mechanism of failure has led to continuing trouble.

TYPES OF OPENINGS

There are numerous types of openings beneath the ground surface that have been the focal point of ground surface subsidence. These are illustrated by diagrams in Figure 1.

Cuts and Open Excavations

The simplest underground opening is a nearby excavation or cut (Figure 1a). There is no general relation between the depth and size of the excavation, the material, and the distance to the point of subsidence, although there is generally little trouble if the distance from the excavation is several times the excavation depth. However, quarries less than 60 m (200 ft) deep near Birmingham, Alabama, have been related to sinkhole development as far as 1.6 km (1 mile) away.

Sewers and Culverts

Leaking sewers and culverts (Figure 1b) are common and underrated sources of trouble. Most city sewers are beneath the streets; culverts are necessary for

Publication of this paper sponsored by Committee on Engineering Geology.

Figure 1. Types of underground openings.

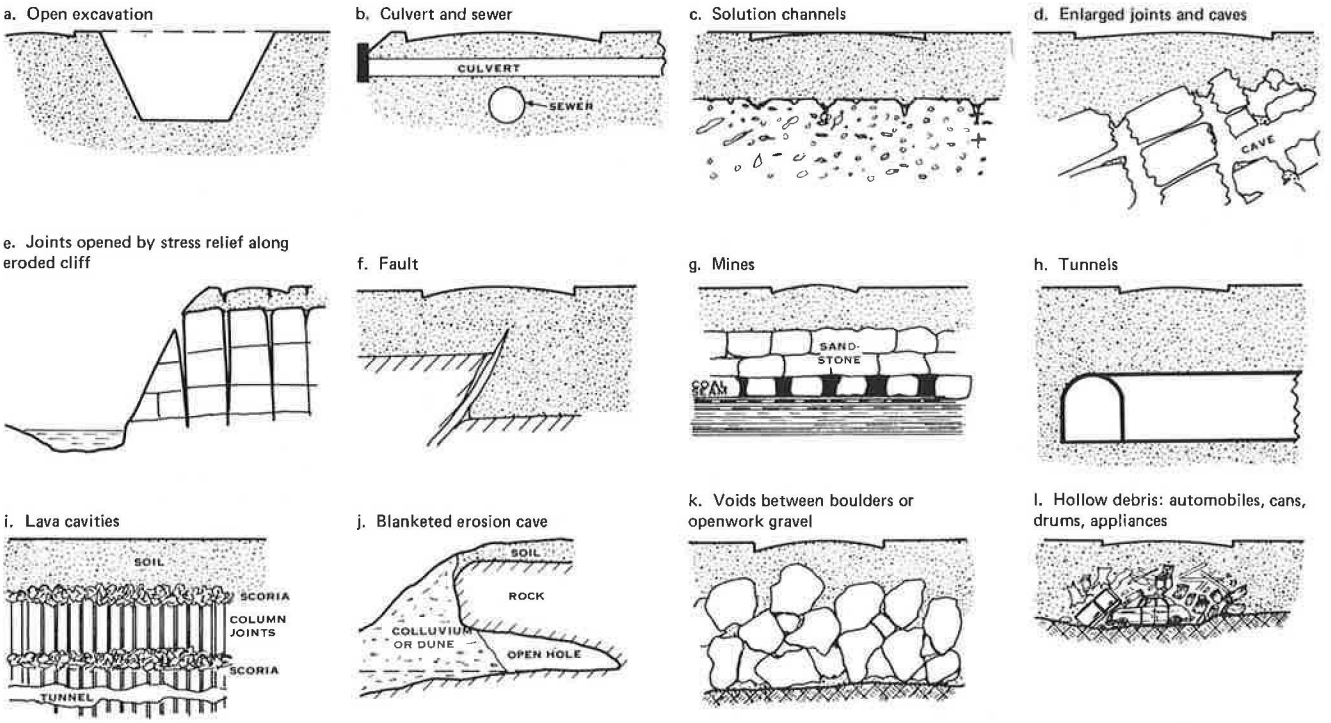

drainage under railroads, highways, and airport runways. There appears to be no relation between the size of the sewer or culvert and the size of a related subsidence. For example, a dropout 2.5 m (8 ft) in diameter and 6 m (20 ft) deep occurred directly over a 15-cm (6-in) sewer below a poorly consolidated fill. The only requirement for trouble is a leak or opening into the sewer through which soil can be eroded.

Solution Channels

Solution channels in soluble formations, in particular limestones and dolomites, and also to some extent calcareous sands and gypsum, are the most familiar form of underground opening leading to serious subsidences. These channels can arise in two ways: from primary porosity between mineral grains (Figure 1c) and from solution-enlarged joints and bedding planes that form slots and underground caves (Figure 1d). The softer, poorly consolidated limestones of the southeastern coastal plain and the margins of the Caribbean Sea exhibit primary porosity: They have voids between spherical oolitic particles, irregular channels between coral fragments, and lens-like openings between fragments of shells, and water can circulate through the pores to enlarge them and give the rock the texture of petrified sponge. This creates numerous interlaced solution channels, ranging from 1 mm (a small fraction of an inch) to as much as 1 m (3 ft) in diameter. When the rock is highly soluble and there is some concentration of flow, as near Ocala, Florida, the solution channels may become caves 10 m (33 ft) or more in diameter.

The more indurated limestones, as well as the porous limestones, can become cracked or jointed from differential consolidation, flexure, folding, and faulting. The rock mass then consists of a series of discrete blocks, the size of which depends on the joint and bedding plane spacing. Water circulating around these blocks will then enlarge the openings to form vertical slots and horizontal lenticular cavities, and vertical chimneylike channels will develop where the slots intersect. The rapid circulation of water may enlarge the channels to form caves as wide as 10 m (33 ft). Some of these caves, such as the Luray Caverns in Virginia, Mammoth Cave in Kentucky, and Carlsbad Caverns in New Mexico, are well known. However, these cave systems are but a fraction of the solution openings that are found throughout limestones (7, 8).

These openings are of greatest potential danger when they are covered by a blanket of residual soil or subsequent deposits such as the old beach sands in Florida. The cavity (the source of trouble) is hidden from view, but if it is close enough to the ground surface, it can easily become the focal point for a subsidence. If the solution channels are hidden by thick deposits of reasonably competent rock, as occurs in the Appalachian ridge and Shenandoah Valley, or if some of the limestones are covered by younger shales and sandstones, the potential for future subsidence is much less severe. There appears to be no simple rule for establishing the degree of risk in each case. Experience in the area is the most reliable index.

Open Joints

Joints that have become enlarged due to local flexure or stress relief are another type of opening (Figure 1e). These are generally much smaller than the previously described openings and occur in localized belts adjacent to deep valleys or zones of severe structural distress, or adjacent to deep, steep cuts (1).

Faults

Faults (Figure 1f) may similarly produce networks of underground openings; however, the grinding and sliding action associated with faulting seldom produces large open voids. In some instances of normal faulting where the earth is subject to tension, or in irregular strike slip faulting, localized narrow openings sometimes develop. Faulting in limestone can lead to enlarged solution chan-

nels similar to those that develop along joints and bedding planes, but the weathering of the fractured materials in many fault surfaces may produce zones that are less porous than any of the surrounding formations.

Mines

Mines (Figure 1g) are a major source of both sudden and continuing subsidence (2). The risk depends on a number of factors (3): (a) the width and height of the mine openings, (b) the percentage of pillar left to support the mine roof, (c) the thickness of rock and soil above the mine compared to the size of mine opening, and (d) the engineering properties of the soils and rocks present.

Small, deep mines seldom cause ground surface subsidence, but large, shallow mines can produce major areas of subsidence. There are, however, exceptions: The gold mines near Johannesburg, South Africa, several hundred meters below the surface, have triggered disastrous subsidences, although the intervening rocks fully support the mine opening. These subsidences have been triggered by drainage from the mines and resemble the cave collapse that occurs in shallow limestones or the raveling failures that occur in residual soils.

Tunnels

Tunnels (Figure 1h) are similar to mines. However, except for urban subways and sewers, there is seldom great risk of damage above them because they are generally built beneath inaccessible areas. Thus, the collapse of a tunnel is of less consequence to the general public than it is to those who are using it. On the other hand, failures of tunnels in cities have produced large local subsidences.

Lava Cavities

Cavities of many forms occur in lavas (Figure 1i). There are blow holes from gases in the harder lavas, enlarged joints due to cooling, scoriaceous zones of high primary porosity, and tension cracks from movement of the solidifying lava, all of which create zones of localized high porosity. The larger openings are seldom more than a few meters (about 10 ft) across. The primary porosity of scoriaceous lava generally occurs in strata 1 to 2 m (3 to 6 ft) thick between more competent rock layers with well-developed joints perpendicular to the layer.

Erosion Caves

Caves produced by erosion (Figure 1j) are another type of localized underground opening and are generally formed by the action of wind, waves, or underground streams on poorly indurated formations. For example, weak sandstones along the sea coast are frequently undercut to form sea caves, and wind erosion in desert areas produces similar enlarged underground openings. These openings are seldom serious hazards to construction, although they can cause localized subsidence if they are subsequently buried by younger formations. They occur in areas of old sea and river terraces or shifting sand dunes that bury the old caves beneath younger deposits.

Concentrated seepage through enlarged joints or solution channels in limestone can cause erosion of adjacent, poorly cemented formations. For example, in a small cave system in north Alabama, water flowing under pressure through the limestone has produced narrow, tall, wedge-shaped channels in the soft sandstone above. Some of these channels lead to the surface and have been the cause of local subsidence.

Voids Between Large Solid Bodies

The voids between large solid masses in fills are a man-made system of underground openings. One example of this is that of large boulders obtained from blasting rock having insufficient fine fragments to fill the voids between the boulders (Figure 1k). A second type is that of the irregular voids between fragments of debris, stumps, and other rubbish that make up waste fills. A third type is that of large, hollow metallic bodies (such as cans, bottles, oil drums, old refrigerators, stoves, and even railroad tank cars) that have been buried in the ground (Figure 1l).

Thus, there is a wide variety of underground openings—some are geologic, others are man-made. The mechanisms by which they cause subsidence are described in the following section. Various combinations of these mechanisms may combine with different types of openings to create complex subsidence conditions that are difficult to anticipate and just as difficult to treat. Regardless, the understanding and treatment of a subsidence must begin with knowledge of the character of the opening that is the ultimate source of the subsidence, and of the failure that created it.

MECHANISMS OF SUBSIDENCE

There are many mechanisms of subsidence. In most cases, water is involved in some way. It weakens many soils and some poorly cemented rocks and serves as an agent of internal erosion; conversely, loss of moisture destroys the apparent cohesion that holds some fine-grained cohesionless soils together.

In each situation, the combination of mechanisms that might be involved must be carefully evaluated. Blaming a subsidence on a single factor may be an oversimplification and lead to misdirected corrective action.

Local Thinning of Formation

Settlement, as a process (in contrast with a sudden event), is sometimes caused by a local thinning of a formation that has been overstressed adjacent to one of the types of openings described in the previous section (4). In some cases, these openings are of primary or enlarged primary porosity; in others, large openings are involved. This process is often confused with subsidence due to large openings.

Of course, the classic consolidation produced by that reduction of the primary voids of soils and similar materials is the most frequent cause of thinning. This process is not related to large openings.

One of the more mysterious of the thinning phenomena is the crushing of highly porous rock. For example, in south Florida and the humid tropical areas surrrounding the Caribbean, the poorly consolidated limestones have been reduced to a skeleton of their former mass by continued solution. This has been aggravated by water drainage, groundwater use, and changing sea levels. If the effective stress on these limestones is increased, as by a highway embankment, their porous skeleton locally fractures, which produces a phenomenon analogous to the consolidation of clean sand (Figure 2a). This mechanism has been responsible for the settlement of several structures in the Miami area and could be responsible for some of the solution depressions found in central and south Florida (5, 6). Similar crushing consolidation is observed in scoriaceous lava and shale-sandstone fills.

The collapse of a loose cemented soil due to deterioration of interparticle bonding is a major mechanism of

thinning subsidence in loess soils and the valley fill deposits of arid regions. This is not related to openings although it has sometimes been blamed on caves.

The plastic flow of soft rocks such as shale and mudstones under high stress can similarly cause a local thinning of formations and subsidence above. Concentrations of stress adjacent to excavations, as shown in Figure 2b, are responsible for the subsidence of steep cliffs of sandstone underlain by shale. If the shale deteriorates and weakens upon exposure, the subsidence can become a landslide with shear failure across the shale and through the sandstone joints. Again, openings are sometimes blamed.

In mines in which the roof support is provided by coal pillars resting on soft underclays, the pillars may punch downward and extrude the clay into the mine opening. This results in a reduction of the mine opening and continuing subsidence of the ground surface. The mine pillars themselves may also bulge plastically. This is seen in coal and salt formations.

Plastic flow can also occur at the heading of a tunnel that is inadequately supported in soft clays. If the rate of excavation at the tunnel face exceeds the rate of forward progress of the tunnel lining and bracing, there will be a trough above the tunnel at the ground surface. Similarly, the upward squeezing of soft clay on the bottom of an open excavation, even if the sides are supported by bracing, can cause subsidence outside the excavation. This is frequently unseen because the soil movement occurs while excavation is taking place. Local squeezing also occurs at the trailing edge of a tunnel shield. It is impossible to measure the volume of soil excavated accurately enough to compare it with the theoretical volume of an excavation unless the discrepancy exceeds 10 percent. These forms of subsidence are sometimes termed lost ground.

Chemical and biochemical action, including decay, chemical attack of groundwater on soil and rock minerals, and the burning of coal, bituminous shale, and certain waste fills, is a third mechanism of local thinning of formations (Figure 2c). For example, either as the result of spontaneous combustion or lightning, certain soft coals of Ohio, Pennsylvania, and the Dakotas have burned for years, and from time to time both slow surface settlement and sudden collapse occur.

Mine wastes consisting of carboniferous shale and coal frequently ignite by spontaneous combustion and burn slowly, converting the shale to bricklike fragments of soft rock, and producing large voids. Eventually, those voids collapse, causing localized subsidence. The burning of waste materials in fills, either by spontaneous combustion or by fires intentionally set to reduce the waste volume, has been responsible for localized settlement of roadways and light structures. Similarly, chemical interaction between minerals within waste fills has caused subsidence. For example, the acids from cinders have produced galvanic reactions, accelerating the corrosion and collapse of open metallic bodies such as refrigerators and automobile bodies.

Extrusion of soft soils (Figure 2d) is a fourth possible mechanism. It does not appear to occur often.

Lateral Strain

A certain amount of strain (Figure 3a) accompanies any excavation, whether it is man-made or is a natural development of an underground opening. The increase in stress caused by the reduction in the amount of solid material present produces a readjustment of the solid mass involved. Frequently, the extent of the mass involved is far greater than might be suspected from simple theories of earth pressure involving shear of the soil. For example, the lateral strain and vertical subsidence adjacent to an excavation sometimes extend from the face of the excavation as much as five times the excavation depth. This strain occurs even though the structural supports for the excavation are capable of resisting shear failure within the soil mass. In fact, excavation support designed on the basis of active earth pressure inherently requires sufficient strain to mobilize a significant part of the shear strength of the soil supported. Thus, movement within the mass is inherent in most excavation bracing designs.

Loss of Support

Still larger subsidences are produced when the excavation supports in mines, tunnels, or open excavations are not adequate to prevent continuing shear failure (Figure 3b). The soil or rock moves downward and inward, producing large lateral and vertical strains, and sharp discontinuities along surfaces of shear. This occurs because the load is greater than had been anticipated or because the supports are inadequate.

There are three major factors in the support loading. First, the rigidity and strength of the soil and rock determine what part of the ambient stress field must be provided by the support system. Any structural defects in the soil and rock, such as joints and faults, play a major part in reducing the mass rigidity and strength compared to that of intact rock. Design loads based on tests of small intact laboratory specimens can be misleading.

Second, the design and installation of the support determine the degree of load transfer as well as the ability of the support to carry the load safely. A rigid (as compared to the soil or rock) support may receive more load than one that deforms readily. On the other hand, a support that permits excessive deformation can allow disruption of the mass that will be followed by even greater loads on the support.

Third, the excavation produces reductions of the effective confining stress on the soil or rock and of its strength. The design of supports should initially be based on the undrained strength, which represents the strength as it exists under ambient conditions—generally the maximum. After excavation and reduction of the effective stresses, the effective strength is necessarily lower. Many an excavation failure, mine collapse, or tunnel blow-in has been caused by neglect of the drained strength of the material.

Two factors may be responsible for a decrease in support strength. An unforeseen load from localized movements in the mass can produce overstress and excessive bending or buckling, and damage from impact or deterioration of the material can reduce its ability to carry the load for which it was designed. For example, coal pillars in mines (Figure 3c) deteriorate from the exposure of shale seams or pyrite inclusions.

The failure of a man-made support or a portion of the intact soil or rock produces a transfer of load to the remainder of the support system. If this is already stressed to levels approaching its strength, adjoining supports may also fail, and failure propagates outward, generating extensive subsidence. On the other hand, if the initial support stresses are low, the failure of one part of the system may not cause subsidence.

Overexcavation in advance of support is also a major cause of subsidence (Figure 3d). As with bracing, designers and builders are often lulled into a false sense of security by the undrained strength of intact samples of material, but an unsupported excavation face in soil or soft rock that is stable one day may become unstable the next, due to reduction in the effective stress or to

Figure 2. Mechanisms of stratum thinning.

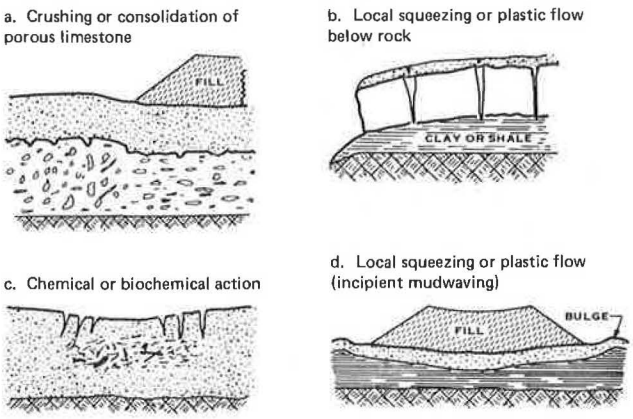

Figure 3. Loss of support.

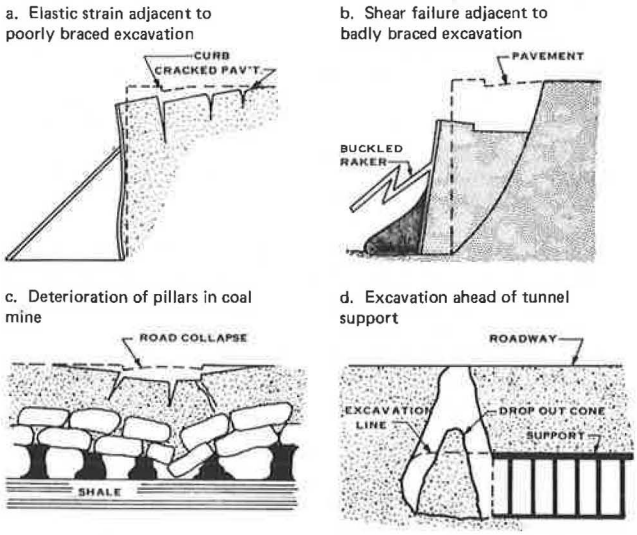

Figure 4. Collapse of opening.

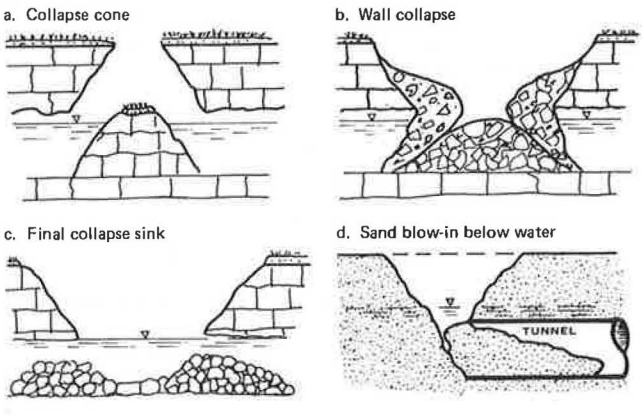

Figure 5. Raveling or soil erosion into openings.

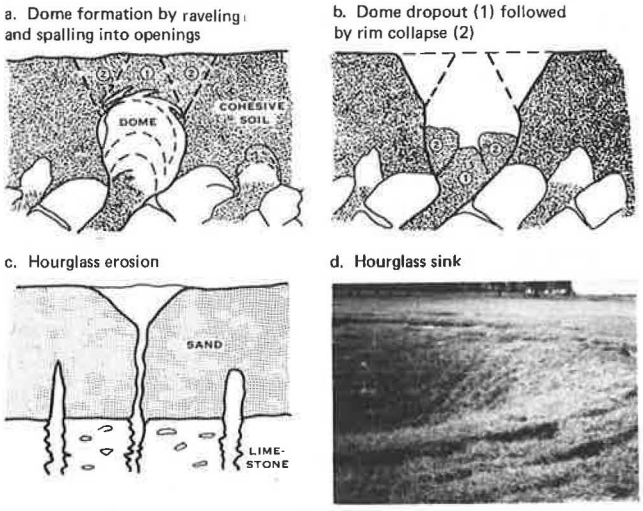

deterioration of cementing agents. Localized zones of weakness, such as faults, can also aggravate the problem.

Failures due to lack of lateral support ordinarily can be evaluated in advance by a thorough understanding of the stress-strain and shear strength properties of the materials. Both must be considered: (a) as they exist at the time of excavation, and (b) as altered by the excavation. In most instances, environmental changes brought on by excavation, such as biochemical deterioration, altered seepage patterns, or loss of strength due to loss of effective confining stress, are responsible for ultimate failure. Finite element analyses of elastic strain and limited analyses of shear failure can provide some indication of the possibility of subsidence due to loss of support.

Collapse of Unsupported Openings

The sudden collapse of an unsupported opening is the most dramatic of the subsidence mechanisms. Regardless of the chain of events leading to collapse, such failures are the result of the enlargement of the opening beyond the ability of the materials above to bridge it. A truncated cone or trapezoid of material above drops into the opening below, as shown in Figure 4. Immediately after the failure, it is possible to see the intact mass of soil or rock below, with trees and grass continuing to grow. (This is dangerous; the face of the opening slopes inward so that viewing the collapse from its rim involves standing on an overhang.) Eventually, the overhanging face sloughs or subsides, and the final opening is a truncated cone with its side slopes reversed from the initial direction (Figure 4b). If there is then erosion of the dropout cone due to surface water entering the hole from above or seepage from below, an open hole will eventually develop, sometimes with water at the bottom as shown in Figure 4c.

Collapse can be triggered by the blow-in of the unsupported heading of a tunnel or an unbraced cut. The unsupported soil caves, frequently impelled by unbalanced groundwater pressure. In low-cohesion soils, the sudden in-rush leaves a gaping hole in the soil mass immediately adjacent to the underground opening. This is followed by successive small collapses or raveling as described in the next section, and eventually there is a dropout at the ground surface. These successive conditions are shown in Figures 4d and 5.

Raveling or Erosion of Soil Into Openings

The most insidious form of failure is the raveling or erosion of soil into an underground opening. The opening can be as small as a joint in sandstone or as large

as a cave in limestone. The only requirement is sufficient seepage that erosion of the overburden can continue. Typically, the condition develops over a sewer or culvert with open joints, above solution-enlarged slots and chimney openings in limestone, or in porous lavas overlain by soils that are easily eroded. Continuing seepage washes the soil into the underground openings, as shown in Figure 5a. The small dome formed in the soil then acts as a focal point for further seepage. The continuing seepage toward the open surface of the dome causes small slabs to peel off its inner surface (ravel) so that the dome enlarges. The sloughed, softened material falls to the bottom of the dome and is carried by the downward seepage into the opening below. Eventually, the dome becomes far larger than the opening into which the soil is carried. There is evidence of domes as large as 15 m (50 ft) in diameter and 9 m (30 ft) high above sewer pipes 5 m (16 ft) in diameter, and similar domes in residual soils above small caves in limestones. The opening through which the soil was eroded, in most cases, was less than a meter (1 or 2 ft) wide.

Eventually, the dome becomes sufficiently wide that the soil above cannot bridge the opening. Collapse (Figure 5b) similar to that illustrated in Figure 4a, b, and c follows. In fact, in examining such collapsed domes it is difficult to determine whether failure was precipitated by doming in the soil or by collapse of the deeper original opening below.

Undersized sewers and culverts are particularly dangerous because the water is under pressure during periods of high flow. If they leak (through fractures or bad joints), water is forced into the soil, weakening it. Then when the flow recedes, the water drains back, carrying with it the softened soil. Numerous failures of this type occur below highways and railroads.

An unusual form of raveling develops in completely cohesionless sands in which the capillary tension is small. This occurs in fine sands during periods of drought or in coarse sands under conditions of downward seepage. The sand flows through relatively small openings, such as the solution chimneys in limestone or small raveling holes in clay, into larger underground openings in the same way that sand runs through the narrow throat of an hourglass. A cone-shaped zone of subsidence develops at the ground surface (Figure 5c and d). Three of these have been observed adjacent to the highway between Bartow and Lakeland, Florida, during the past 8 years (6).

Erosion and doming can also develop as a result of horizontal seepage between confining strata. Generally, its rate is lower than that in the vertical direction because the gradients are lower. Such horizontal seepage erosion is termed piping. Piping failures occur behind braced excavations that have a higher groundwater table outside and inadequate filtering at the face of the excavation. Similar failures occur through weep holes in retaining walls having inadequate filters between the backfill and the wall. Others are caused by poorly filtered subsurface drains adjacent to highways.

Raveling frequently occurs into the large voids between boulders or fragments of debris in fills. Downward seepage or traffic vibration above causes soil to filter into the voids below. The initial filtering is followed by more rapid raveling, eventually producing dome-like openings that collapse. A parking lot that had been constructed on top of 6 m (20 ft) of 9000-kg (10-ton) boulders blanketed with silty sand developed sinkholes 1 m (3 ft) in diameter and ½ to 1 m (1.5 to 3 ft) deep within 10 years.

Raveling and seepage erosion failures take so many forms that it is difficult to fully diagnose them. However, many of the subsidences that have been blamed on the collapse of deep caves, mines, or tunnels may have been the collapse of soil domes generated by raveling into the deep openings.

INITIATING MECHANISMS

Although there are many forms of openings, and many mechanisms leading to subsidence, the sequence of events involved is frequently initiated by some significant change in the total environment affecting the soil and rock mass. In some cases, that event is not necessarily related to the opening. This event or the environmental change is termed the triggering mechanism by engineers or the proximate cause by lawyers.

Groundwater Flow

Movement of water through the ground, in one way or another, is the most significant triggering mechanism. The seepage can be vertically downward or horizontally toward the opening. Erosion induced by seepage and the gradients producing seepage form the localized stress system inducing failure.

Among the sources of underground flow are (a) increased rainfall and surface runoff that infiltrates the soil or small openings present in the ground, (b) broken water lines, (c) broken drain pipes, (d) flow of groundwater toward wells, and (e) flow of groundwater toward improperly filtered drainage systems.

Groundwater Lowering

Lowering the water table has two effects. First, although the weight of the soil mass is reduced somewhat, the effect of this is more than offset by the increase in effective stress within the soil or rock. Lowering the water table 0.3 m (1 ft) increases the effective weight by 600 to 800 kg/m^3 (40 to 50 lb/ft^3).

A second effect of groundwater lowering is a reduction of capillary tension and temporary cohesion in cohesionless soils. For example, in damp, fine sands, large, open raveling domes can be supported by capillary cohesion, but if the sand should become thoroughly dry, the dome will collapse because the cohesion is lost. Similarly, sewer trenches in damp, fine sand sometimes can be excavated with steep slopes because of capillary tension. If the sand dries out, the apparent cohesion is lost, and the soil slope slumps inward to its angle of repose.

Groundwater lowering can be produced by excessive use of water from wells, localized drainage for construction projects, and periods of prolonged drought.

Increased Loading

Increased loading of the mass increases the stresses in the soil and rock surrounding the underground opening and produces increased strain, plastic flow, or, eventually, shear failure. In addition, there is some evidence that increased stress produces increased solubility in carbonate rocks analogous to stress cohesion in metals.

There are a number of factors responsible for increased surface loading—embankments and fills, new structures, and reduction of lateral support by deep excavations.

Dynamic load, such as shock and vibration induced by earthquakes, vibrating machinery, and blasting, can trigger failure in two ways. First, shock and vibration directly produce strains and stress increases. Second, in loose, cohesionless soils and possibly also in ultrasensitive clays, shock and vibration may induce struc-

tural collapse that is followed by surface settlement and sometimes a flow in the form of temporary quicksand. For example, saucer-shaped depressions in the ground surface, with small sand boils within them, frequently accompany earthquakes.

Deterioration

The deterioration of soil and rock materials, including the man-made supports for underground openings, is another form of triggering. Fire can destroy wood bracing systems or weaken steel supports. Burning of coal or waste materials produces new openings or enlarges old ones. Three mechanisms can be triggered: (a) gradual surface subsidence that keeps pace with the combustion; (b) sudden collapse of the opening, sometimes long after; or (c) raveling, doming, and a shallow collapse.

The gradual deterioration of rocks, such as coal, shale, and some poorly cemented sandstones, by physical, chemical, and biologic processes in the presence of air and water, can lead to collapse. Because such formations are often initially quite strong, engineers may be led into a false sense of security by forgetting the loss in strength from long-term exposure.

Deterioration of man-made supports in the moist environment is a cause of failure in old mines, poorly maintained tunnels, or even in braced excavations that have been left open longer than had been anticipated. The resulting subsidences can proceed as slowly as the rate of deterioration or may develop suddenly when the strength has degenerated to the point that rupture takes place.

CONCLUSIONS

Subsidences produced by underground openings, including the thinning of underground strata, are major maintenance problems for highways, railroads, airfields, and the foundations of engineered structures. There are many types of openings, any one of which can be a source of trouble that is far out of proportion to the size of the opening or even its proximity to the site. There are a number of mechanisms that produce subsidence, some unrelated but many interrelated. Ultimately, failure develops because of some change in the total environment—groundwater, stress, or a change in the materials involved.

Because of the complexity of the phenomena, many subsidences have been mistakenly diagnosed and considerable amounts of money spent for remedial measures that were of little or no benefit. Sometimes the subsidence has stopped because the movement that took place inhibits the mechanism or closes the opening. Thus, some remedial measures have been judged successful because the subsidence had already stopped itself.

The evaluation of the causes of subsidence requires a clear understanding of the geology of the soil and rock formations involved, a knowledge of the character of the openings, both natural and man-made, and an awareness of the different mechanisms that can lead to subsidence. Many subsidences could be predicted and their serious effects alleviated: Most can be temporarily or permanently stopped or their rate of movement materially reduced.

REFERENCES

1. D. F. Coates. Rock Mechanics Principles. Mines Branch, Canadian Department of Energy, Mines, and Resources, Ottawa, Monograph 874, 1970.
2. Subsidence Engineers Handbook. Mining Department, National Coal Board, 1975, p. 111.
3. L. Obert and W. I. Duvall. Rock Mechanics and the Design of Structures in Rocks. John Wiley and Sons, Inc., New York, 1967, pp. 554-579.
4. Proc., Tokyo Conference on Land Subsidence, International Association of Scientific Hydrology, UNESCO, Belgium, 1970.
5. G. F. Sowers. Failures in Limestones in Humid Subtropics. Journal of Geotechnical Engineering Division, Proc., ASCE, Vol. 101, No. GT8, Aug. 1975, pp. 771-787.
6. G. F. Sowers. Foundation Subsidence in Soft Limestones in Tropical and Subtropical Environments. Law Engineering Testing Co., Bulletin G-7, 1975.
7. G. F. Sowers. Settlement of Terranes of Well-Indurated Limestones. Proc., Conference on Analysis and Design of Foundations for Tall Buildings, Lehigh Univ., Aug. 1975.
8. V. T. Stringfield. Karst. American Elsevier Publishing Co.

Induced and Natural Sinkholes in Alabama–A Continuing Problem Along Highway Corridors

J. G. Newton, Geological Survey, U.S. Department of the Interior

Sinkholes are divided into two categories, induced (man-related) and natural. Since 1900, an estimated 4000 induced sinkholes or related features have formed in Alabama; fewer than 50 natural sinkholes have been reported. Most induced sinkholes are caused by water-level declines due to pumpage; others result from factors associated with construction. Almost all occur where cavities develop in unconsolidated deposits overlying openings in bedrock. The downward migration of the deposits and the development of the cavities are caused or accelerated by a water-level decline that results in the loss of buoyant support and increases the velocity of water movement, the magnitude of water-level fluctuations, and the induced recharge. Most sinkholes caused by construction are due to the diversion of drainage over openings in bedrock. Many natural sinkholes are caused by the collapse or downward migration of unconsolidated deposits into openings in bedrock. The downward migration that sometimes creates cavities in the deposits results from natural declines in the water table, progressive enlargement by solution of openings in the top of bedrock, or a combination of both. The failure of bedrock roofs over solutionally enlarged openings is a rare occurrence. The time required for the development of natural sinkholes is far greater than that associated with induced sinkholes.

Sinkholes formed by collapse of the land surface have caused a variety of problems related to the maintenance and safety of structures and the pollution of existing and potential water supplies. In Alabama there have been costly damage and numerous accidents as a result of collapses beneath highways, streets, railroads, buildings, sewers, gas pipelines, vehicles, animals, and people.

This report is an attempt to provide engineers with a description of the forces involved in the development of sinkholes so as to aid them in construction over problem areas or in repairing damage resulting from sinkholes. The description of these forces will also aid in the identification of active and potential areas of sinkhole development, which would allow planners to avoid these areas as routes for new highway corridors.

GEOLOGIC AND HYDROLOGIC SETTING

The terrane used here to illustrate sinkhole development is a youthful basin underlain by carbonate rocks such as limestone and dolomite (Figure 1). The basin contains a perennial or near-perennial stream. This particular terrane is used because it is similar to that of 10 active areas of sinkhole development in Alabama. Factors related to the development of sinkholes that have been observed in these areas are generally applicable to other carbonate terranes. The terrane differs from those examined only in the inclination of the beds, which is shown as horizontal for ease of illustration.

The development of sinkholes is primarily dependent on past and present relations between carbonate rocks and water, climatic conditions, vegetation, and topography, and the presence or absence of residual or other unconsolidated deposits overlying the bedrock. The source of water associated with the development of sinkholes is precipitation, which, in Alabama, generally exceeds 1300 mm (50 in) annually. Part of the water runs off directly into streams, part replenishes soil moisture but is then returned to the atmosphere by evaporation and transpiration, and the remainder percolates downward below the soil zone to groundwater reservoirs.

Water is stored in and moves through interconnected openings in carbonate rocks. Most of the openings were created, or existing openings along bedding planes, joints, fractures, and faults were enlarged, by the solvent action of slightly acidic water in contact with the rocks. The water in the interconnected openings moves in response to gravity, generally toward a stream channel where it discharges and becomes a part of the streamflow.

Water in openings in carbonate rocks occurs under both water-table and artesian conditions; however, this study is concerned primarily with that occurring under water-table conditions. The water table is the unconfined upper surface of a zone in which all openings are filled with water. The configuration of the water table conforms somewhat to that of the overlying topography but is influenced by geologic structure, withdrawal of water, and variations in rainfall. The lowest altitude of the water level in a drainage basin containing a perennial stream occurs where the water level intersects the stream channel (Figure 1). Openings in the bedrock underlying the lower parts of the basin are water filled. This con-

Publication of this paper sponsored by Committee on Engineering Geology.

dition is maintained by recharge from precipitation in the basin. The water table underlying adjacent highland areas within the basin occurs at higher altitudes than the water table near the perennial stream. Openings in the bedrock between the land surface and the underlying water table in highland areas are air filled. The progressive enlargement of these openings by solution has resulted in the formation of the caves that are common in some parts of Alabama.

The general movement of water through openings in the bedrock underlying the basin, even though the route may be circuitous, is toward the stream channel and downstream under a gentle gradient approximating that of the stream. Some water moving from higher to lower altitudes is discharged through springs along flanks of the basin at intersections of the land surface and the water table. The velocity of movement of water in openings underlying most of the lowland area is probably sluggish when compared to that in openings at higher altitudes.

A mantle of unconsolidated deposits consisting chiefly of residual clay (residuum), which has resulted from the solution of the underlying carbonate rocks, generally covers most of the bedrock in the typical basin described. Alluvial or other unconsolidated deposits often overlie the residual clay. The residuum commonly contains varying amounts of chert debris that are insoluble remnants of the underlying bedrock. Some of the unconsolidated deposits are carried by water into openings in the bedrock. These deposits commonly fill solutionally enlarged joints, fractures, or other openings underlying the lowland areas. The buried contact between the residuum and the underlying bedrock, because of differential solution, can be highly irregular.

SINKHOLES

Sinkholes can be separated into two categories, in relation to their occurrence, even though most of the factors involved in their development are the same. These categories are defined here as induced and natural. Induced sinkholes are those that can be related to man's activities; natural ones are those that cannot. These categories can generally be separated on the basis of their physical characteristics and environmental setting. The development of all sinkholes, regardless of their category, is dependent on some degree of solution of the underlying bedrock.

This paper is devoted almost entirely to the description of the initial stage of development of both induced and natural sinkholes. New sinkholes of either type are similar in size. Recent collapses forming sinkholes in Alabama generally range from 1 to 90 m (3 to 300 ft) in diameter and from 0.3 to 30 m (1 to 100 ft) in depth. The largest known collapse (Figure 2) occurred in a wooded area in Shelby County in December 1972, apparently in a matter of seconds, and was about 90 m (300 ft) in diameter and 30 m (100 ft) deep.

Induced Sinkholes

It is estimated that more than 4000 induced sinkholes, areas of subsidence, or other related features have occurred in Alabama since 1900. Most of them have occurred since 1950. These sinkholes are divided into two types: those related to a decline in the water table, and those related to construction.

Decline of the Water Table

The relation between the formation of sinkholes and high pumpage of water from new wells was recognized in Alabama as early as 1933 (1). Subsequent studies (2, 3, 4, 5) have verified this relation. Collapses have occurred in the immediate vicinities of 36 wells tapping limestone and dolomite formations in Alabama. The actual number of wells related to collapses probably exceeds this figure, but no inventory has been attempted. Three collapses that occurred during a pumping test of a new well in Birmingham in 1959 are excellent examples of sinkholes resulting from man-created forces (4).

Dewatering or the continuous withdrawal of large quantities of water from carbonate rocks by wells, quarries, and mines in numerous other areas in Alabama is associated with extremely active sinkhole development. The numerous collapses in these areas contrast sharply with their rarity in adjacent geologically and hydrologically similar areas where withdrawals of water are minimal. For example, in five active sinkhole areas, there are an estimated 1700 collapses, areas of subsidence, or other associated features, which have a total combined area of about 36 km^2 (14 $miles^2$). There are few recent collapses in adjacent areas underlain by the same geologic forms. This phenomenon is not unusual; the relation of this type of sinkhole occurrence to cones of depression created by water withdrawals in Pennsylvania and Africa has been well established (6, 7).

Two areas in Alabama in which intensive sinkhole development has occurred and is occurring have been studied in detail. Both areas became prone to the development of sinkholes by major declines of the water table due to the withdrawal of groundwater. The formation of sinkholes in both areas resulted from the creation and collapse of cavities in unconsolidated deposits (4, 5).

Cavities in unconsolidated deposits overlying carbonate rocks in areas of Africa and Pennsylvania where there have been water-table declines have also been described and explored (7, 8, 9). The growth of one such cavity in Birmingham has been photographed through a small adjoining opening (10). The growth of this cavity resulted from the downward migration of clay into two small openings in the top of the bedrock.

Previous reports have associated the development of sinkholes and subsidence with subsurface erosion caused by pumpage, the position of the water table, or lowering of the water table due to withdrawals of groundwater. Johnston (1) has noted that sinkholes appear to be caused by the removal by moving groundwater from the residual clay filling in fissures of the limestone. He described the stoping action and surmised that the water would have to be moving fast enough to erode the clay and that, because of this, there appeared to be a causal relationship between this type of sinkhole and high pumpage from new wells. Robinson and others (2) have attributed the development of sinkholes in a cone of depression to the increased velocity of groundwater, which caused the collapse of clay and rock-filled cavities in bedrock.

Foose (6) associated the occurrence of recent sinkhole activity with pumping and the subsequent decline of the water table. He determined that formation of sinkholes was confined to areas where a drastic lowering of the water table had occurred, that their occurrence ceased when the water table recovered, and that the shape of recent collapses indicated a lowering of the water table and the withdrawal of its support.

Jennings and others (9) have associated development of sinkholes with pumpage and the creation of cones of depression. They found that sinkhole and subsidence problems increased where the water table was lowered, and described the formation, enlargement, and collapse of cavities in unconsolidated deposits that had migrated downward. They also described the geologic conditions necessary for the formation of the cavities. Foose (7), in addition to his previous findings (6), has described

the development of cavities in unconsolidated deposits in Africa and attributed it to the shrinkage of desiccated debris and the downward migration of the debris into bedrock openings. He has also outlined geologic conditions related to cavity development and found that a lowering of the water table initiated their formation.

Previous reports have described only indirectly or in part the hydrologic forces that result from a decline in the water table and create or accelerate the growth of cavities that collapse and form sinkholes. These forces are (a) loss of support to roofs of cavities in bedrock that had been previously filled with water and to residual clay or other unconsolidated deposits overlying openings in the bedrock, (b) an increase in the velocity of movement of the groundwater, (c) an increase in the amplitude of water-table fluctuations, and (d) the movement of water from the land surface to openings in the underlying bedrock where recharge had previously been rejected because the openings were water filled.

The same forces that create cavities and subsequent collapses also cause subsidence. The movement of unconsolidated deposits into bedrock, where the overlying material is not sufficiently strong to maintain a cavity roof, will result in subsidence at the surface (8). Subsidence can also result from consolidation or compaction due to the draining of water from deposits previously located beneath the water table (11). Recognizable subsidence sometimes precedes a collapse (4). This occurrence, if the unconsolidated deposits are thin and consist chiefly of clay, indicates that the subsidence is due to a downward migration of the deposits rather than to compaction.

The forces that result in the development of cavities and their eventual collapse are shown in a schematic diagram (Figure 3) that illustrates the changes in natural geologic and hydrologic conditions previously described and shown in Figure 1.

The effects of the forces triggered by a lowering of the water table are basic and can often be observed, measured, estimated, or computed in hydrologic work.

The loss of buoyant support that follows a decline in the water table can result in an immediate collapse of the roofs of openings in the bedrock or can cause a downward migration of unconsolidated deposits overlying openings in the bedrock. The buoyant support exerted by water on a solid (and hypothetically) unsaturated clay overlying an opening in bedrock, for instance, would be equal to about 40 percent of its weight, based on the specific gravities of the constituents involved. Site 1 of Figure 1 shows an unconsolidated deposit overlying a water-filled opening in bedrock; site 1 of Figure 3 shows the decline in the water table, and the resulting cavity in the deposit after the downward migration of the unconsolidated deposit that was caused by the loss of support. The cavity may then remain stable or it may enlarge upward by the spalling of the overlying deposit until the roof collapses.

The creation of a cone of depression in an area of water withdrawal results in an increased hydraulic gradient (slope of the water table) toward the point of discharge and a corresponding increase in the velocity of the movement of water. This force can result in the flushing out of the finer grained unconsolidated sediments that have accumulated in the interconnected solutionally enlarged openings. It also transports to the point of discharge or to a point of storage in openings at lower altitudes the unconsolidated deposits migrating downward into bedrock openings.

The increase in the velocity of groundwater movement also plays an important role in the development of cavities in unconsolidated deposits. Erosion caused by the movement of water through unobstructed openings and against joints, fractures, faults, or other openings filled with clay or other unconsolidated sediments results in the creation of cavities that enlarge and eventually collapse (1, 2). Collapses and subsidence due to erosion of clay-filled, solutionally enlarged openings are occurring beneath and near Interstate 59 in Birmingham.

Pumpage results in fluctuations in groundwater levels that are of greater magnitude than those occurring under natural conditions. The magnitude of these fluctuations depends principally on variations in water withdrawal and in natural recharge (precipitation). The repeated movement of water through openings in bedrock against overlying residuum or other unconsolidated sediments causes a repeated addition and subtraction of support to the sediments and repeated saturation and drying. This might be best termed erosion from below because it results in the creation of cavities in unconsolidated deposits, and their enlargement and eventual collapse. Fluctuations of the water table against the roof of a cavity in unconsolidated deposits near Greenwood, Alabama, have been observed and photographed through a small collapse in the center of the roof. These fluctuations, in conjunction with the movement of surface water into openings in the ground, created the cavity and have caused its collapse (5).

A drastic decline of the water table in a lowland area (Figure 3) in which all openings in the underlying carbonate rock were previously water filled (Figure 1) commonly results in induced recharge from surface water. This recharge would have been rejected prior to the decline because the underlying openings were water filled. The quantity of surface water available as recharge to such an area is generally large because of the runoff moving to and through it from areas at higher altitudes.

The inducement of surface water infiltration through openings in the unconsolidated deposits interconnected with openings in the underlying bedrock results in the creation of cavities where the material overlying the openings in the bedrock is eroded to lower altitudes. Repeated rains result in the progressive enlargement of this type of cavity, and a corresponding thinning of the cavity roof due to this enlargement eventually results in a collapse. The position of the water table below unconsolidated deposits and openings in bedrock that is favorable to induced recharge is illustrated in Figure 3. Sites 2, 3, and 4 illustrate a collapse and cavities in unconsolidated deposits that were formed primarily or in part by induced recharge. The creation and eventual collapse of cavities in unconsolidated deposits by induced recharge are the process described by many authors as piping or subsurface mechanical erosion; the term has been applied mainly to collapses occurring in noncarbonate rocks (12).

In an area of sinkhole development where a cone of depression is maintained by constant pumpage (Figure 3), all of the forces described are in operation even though one may be principally responsible for the creation of a cavity and its collapse. For instance, the inducement of recharge from the surface (site 2 in Figure 3), where the water table is maintained at depths well below the base of unconsolidated deposits, can be solely responsible for the development of cavities and their collapse. In contrast, a cavity resulting from a loss of support (site 1 in Figure 3) can be enlarged and collapsed by induced recharge if it has intersected openings interconnected with the surface. In an area near the outer margin of the cone (site 4 in Figure 3), the creation of a cavity and its collapse can be the result of several forces. The cavity can originate from a loss of support; could be enlarged by continuous addition and subtraction of support and the alternate wetting and drying resulting from water-level fluctuations; could be enlarged by the increased velocity of movement of water; or could be enlarged and

collapsed by water induced from the surface.

Construction

Collapses resulting from construction are far less numerous than those due to a decline in the water table; however, they have resulted in extensive damage. In this paper, the term construction applies not only to the erection of a structure, but also to any diversion of natural drainage, and includes the clearing of timber in rural areas.

The simplest cause of sinkholes or subsidence resulting from construction is loading. The emplacement of weight on unconsolidated deposits alone can result in compaction. The compaction can be irregular if the deposits overlie an uneven bedrock surface or openings in the bedrock, and the differential compaction and accompanying subsidence can result in foundation problems. The presence of natural or induced cavities in bedrock or unconsolidated deposits may result in a collapse when the overlying roof is subjected to loading.

Construction on unconsolidated deposits that overlie air-filled openings in bedrock (site 5 in Figure 1) can result in the formation of a sinkhole (site 5 in Figure 3). In highway or other construction, grading and the removal of trees create new openings that connect the land surface with openings in bedrock. The concentration of surface runoff in drains or impoundments increases the downward movement of water. This downward movement sometimes erodes and transports unconsolidated deposits into underlying openings in bedrock, forming a cavity in the deposits that eventually enlarges and collapses. This process is the same as that described under induced recharge (piping) where the water table has been lowered by pumping. It has also been described and illustrated in a carbonate terrane in Alabama where collapses have resulted in retention-basin failures (13).

The diversion of drainage, followed by the development of cavities and a tunnel in sand overlying carbonate rocks near Centerville, Alabama, illustrates the piping process well. The grading of a timber trail caused the diversion and discharge of water into an opening at the surface (Figure 4) that interconnected with an opening in the underlying bedrock. The water moved downward about 9 m (30 ft) and laterally about 15 m (50 ft), and then discharged downward. A cavity developed at this point, and, with continued subsurface erosion, the route along which the water moved enlarged backward toward the surface forming a tunnel. A second cavity then formed as the erosion approached the surface and the collapse of its roof enlarged the opening into which water discharged.

Piping action can also be the mechanism for the development of sinkholes in places where water has been impounded on unconsolidated deposits that overlie carbonate rocks containing water-filled openings. On the floor of the impoundment, water moving through openings in the unconsolidated deposits to openings in the carbonate rocks can form and collapse cavities in the deposits. This process generally occurs where there is a considerable head or pressure exerted by the impounded water and where openings in the carbonate rocks have a discharge point outside of the impoundment at a lower altitude. The increase in the velocity of the impounded water moving through unconsolidated deposits to underlying openings in the bedrock will have an erosive capacity similar to that described previously in a cone of depression caused by pumpage. The saturation of previously unsaturated unconsolidated deposits by the impoundment will also enhance the downward transport of the deposits. This action is probably responsible for the formation of sinkholes in the impoundment behind Logan Martin Dam on the Coosa River, which reportedly resulted in the discharge of muddy water from an opening in the stream channel outside of the impoundment.

A damaging collapse due to construction involved Interstate 59 near Attalla, Alabama. A collapse about 3 m (10 ft) in diameter in a drainage ditch along the highway allowed surface drainage to enter the ground. The drainage discharged at a lower altitude beneath the fill of a lower lane, and the lubrication of residual clay underlying the lane by this discharge and some additional water from an unidentified source resulted in a landslide and subsequent highway failure.

Natural Sinkholes

Topographic maps of areas in Alabama show thousands of natural sinkholes. None of these are at the earliest stage of their development. The occurrence of new natural sinkholes is rare. Fewer than 50 of the collapses that were observed resulted in new natural sinkholes, and it is probable that a significant number of these were related in part to man's activities. (This number does not include the collapses that commonly occur inside of or along rims of existing mature sinkholes.)

The development of a new natural sinkhole may reflect displacement of the bedrock, or of the unconsolidated deposits overlying it, or both. The displacement of either or both is generally triggered by progressive solution of bedrock, by a natural decline in the water table, or by a combination of the two. The relations among progressive solution, a decline in the water table, and the accompanying failures of bedrock and unconsolidated roofing is illustrated in Figure 5. The role of solution in the development of natural sinkholes is recognized by all investigators. The effect that solution of bedrock or a decline in the water table has on unconsolidated deposits is not nearly as well defined.

Cavities in unconsolidated deposits overlying carbonate rocks in areas remote from groundwater withdrawals are identical to those resulting in induced sinkholes. This type of cavity eventually results in a natural sinkhole. These cavities have been drilled or augered near Piedmont in Calhoun County, west of Talladega in Talledega County, and near Stevenson in Jackson County. The development of natural sinkholes caused by temporary natural declines in the water table is similar to the occurrence of induced sinkholes caused by pumpage, as shown by the sudden appearance of natural sinkholes during prolonged periods of drought. The most recent prolonged drought in Alabama occurred during the early and middle 1950s, and during this period, notable natural sinkhole development occurred in Limestone, Talladega, and Shelby Counties.

Decline of the Water Table

A major factor responsible for the degradation of a carbonate terrane by solution is the lowering of the base level of a perennial stream as it affects the water table and groundwater discharge (14). Recent natural sinkhole activity along the Flint River in southwest Georgia has been related to the entrenchment of the stream that resulted in a lowering of base level (14). The downward migration of unconsolidated deposits due to the declines in the water table that accompanied a lowering of the base level is considered here to be closely related to the solution process. Major differences between the formation of natural sinkholes resulting from collapses in bedrock and from collapses in unconsolidated deposits are the times required for each to develop and the size and

type of opening required for their formation. The time required for a cavity to form in unconsolidated deposits due to changes in the hydrologic regimen in the carbonate terrane described here (Figure 1) could be extremely short as compared to that required for the enlargement by solution of a cavity in bedrock to the point where its roof becomes incompetent. A relatively large cavity in the unconsolidated deposits can also form over a small opening in underlying bedrock.

Natural declines in the water table in Alabama, with the exception of temporary ones caused by prolonged droughts, are chiefly attributable to a lowering of the base level of perennial streams. The lowering of the water table in a stream basin occurs when the stream entrenches or erodes to a lower altitude or when the basin is captured by an adjacent stream having a lower base level. The water table in the basin can also be lowered by an increase in permeability resulting from solution of bedrock (15) or by a permanent climatic change.

Many natural sinkholes in Alabama have resulted from the same kinds of forces that cause induced sinkholes. These forces result from loss of support, increase in velocity of movement of water, water-level fluctuations, and induced recharge. The role that each

Figure 1. Schematic cross-sectional diagram of basin showing geologic and hydrologic conditions.

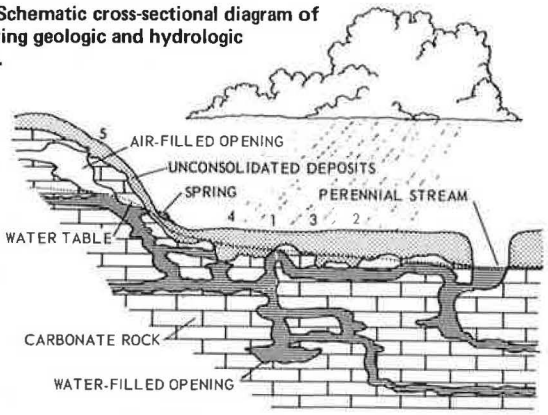

Figure 2. Sinkhole resulting from collapse near Calera in Shelby County.

Figure 3. Schematic cross-sectional diagram of basin showing changes in geologic and hydrologic conditions resulting from water withdrawal.

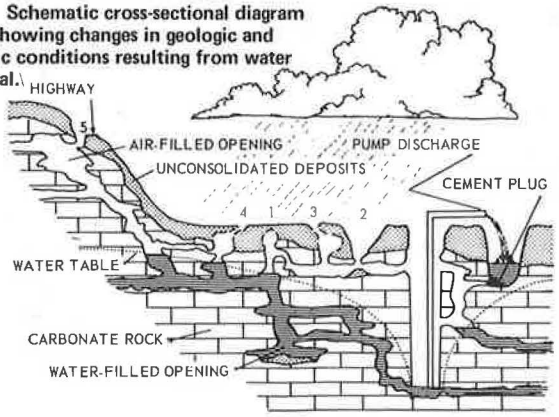

Figure 4. Opening into which water discharges.

Figure 5. Natural sinkhole development.

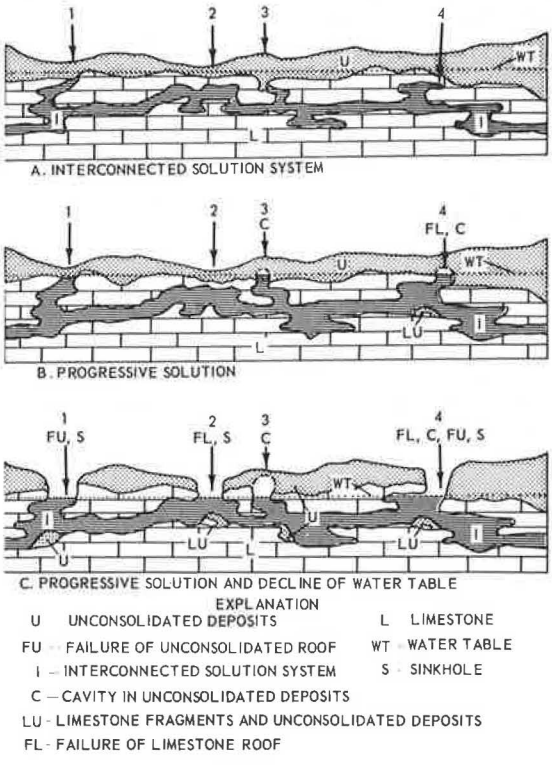

plays in the development of a sinkhole has been described in detail, and to avoid repetition, only general comments on the relation of these forces to natural sinkhole development are given here. The major difference in the development of induced and natural sinkholes resulting from these forces is the much greater time span involved in a natural lowering of the water table and the formation of natural sinkholes. Forces resulting from natural declines in the water table are much more subtle than those resulting from man-created declines.

A decline in the water table due to the entrenchment of a stream results in an increase in the hydraulic gradient toward the stream and a corresponding increase in the velocity of movement of the water. This increase in velocity would generally be much less than that resulting from most man-related declines because the hydraulic gradient would be more gentle than that resulting from pumpage. The increase would, however, actuate the same processes that cause induced sinkholes.

Water-level fluctuations that cause or contribute to the development of natural sinkholes can occur where openings in bedrock were previously water filled (Figure 1). When the rate of water-level decline exceeds the rate of deepening of the residuum-bedrock contact, the physical situation becomes more conducive to cyclic wetting and drying and the continued addition and subtraction of buoyant support to the residuum.

A natural decline in the water table in lowland areas of the type described (Figure 1) also results in induced recharge. Locally, the quantity of water moving to openings in the bedrock exceeds the recharge prior to the decline, and the water moving through openings at the surface to openings in the bedrock would no longer have its direction of movement affected or its velocity impeded by a water table located above bedrock.

Solution

The solution of carbonate rocks in the terrane shown in Figure 1 precedes the occurrence of sinkholes and is ultimately responsible for their development. The description here is oriented toward the initial stage of development of a natural sinkhole that results from solution alone. The time required for the development of such a sinkhole far exceeds that required for those resulting from other causes. Determining the rate of solution of the bedrock involved in this process is beyond the scope of this report; however, a summary of estimates by previous workers, described by Sweeting (16), indicates that rates of solution for most terranes are considerably less than 100 mm (4 in)/1000 years.

Solution of near-surface bedrock in the basin of a perennial stream is continuous. The overlying soil zone is a principal source of carbon dioxide and minerals from which the water percolating downward derives most of its acidic properties. In lowland areas the upper surface of the carbonate rocks is being degraded by solution, and openings in the bedrock beneath it are being progressively enlarged. Openings connecting the upper surface of the bedrock to the deeper solution system are being created or enlarged by groundwater from below and by surface water moving into the system through the overlying soil zone.

A well-established generalization is that solution action tends to enlarge the moderately large openings in the path of the bulk flow of groundwater at a faster rate than the small openings not in the path of bulk flow (17). This preferential solution will also apply to the upper surface of bedrock. In the terrane described here, the contact between bedrock and unconsolidated deposits is irregular; consequently, the water table may be above bedrock in some places and below it in others (Figure 1). Water percolating through unconsolidated deposits that comes in temporary contact with bedrock on highs above the water table would move toward the lows below the water table where solution is continuous.

Where highland areas bounding a basin are underlain by air-filled cavities in bedrock, a similar enlargement of openings is occurring at a slower rate than that in the lowlands because of the smaller volume of water coming in contact with bedrock after percolating downward through the soil zone. Most large openings beneath the highlands are older than are those underlying lowland areas in the basin. Most of their enlargement probably occurred when they were located in closer proximity to the water table.

Roofs over openings in bedrock can consist of bedrock or of residuum and other unconsolidated deposits, and solution enlargement of them may result in their collapse. Many openings in bedrock, which have been observed from exposures in quarries and data for wells, are filled with residuum or other sediments, but others are not. Openings in the top of bedrock in the type of basin described (Figure 1) are numerous although natural sinkholes are uncommon. More than 50 such openings were exposed in a 1.5-ha (3.7-acre) tract in Shelby County where unconsolidated deposits were removed to permit the bedrock to be washed clean by precipitation. It is apparent from the scarcity of natural sinkholes or recognizable subsidence prior to pumpage in areas such as that shown in Figure 1 that either many bedrock openings have been filled with sediments or the deposits overlying the openings are capable of supporting themselves.

Natural subsidence that has occurred over openings in bedrock in the basin described and shown in Figure 1 may have been leveled by the infill of sediments eroded from higher adjacent areas or by deposition of sediments by floods in low areas adjacent to streams. The collapse of unconsolidated deposits forming a roof over an opening in bedrock will occur when the opening is progressively enlarged by solution until the overlying deposits cannot support their weight. The enlargement of an opening that precedes the collapse is illustrated at site 1 in Figure 5. If an opening is filled with clay or other sediments, subsidence or a collapse will occur where solution progresses at a rate greater than the deposition required to maintain a level land surface.

The collapse of the bedrock roof of an opening that has been progressively enlarged by solution occurs when the roof can no longer maintain its integrity. The progressive enlargement of such an opening and the resulting roof failure are illustrated at site 2 in Figure 5. This occurrence is generally considered to be rare (18, 19). However, it may be more common than has been indicated because cavities similar to those in unconsolidated deposits associated with induced and natural declines in the water table undoubtedly result also from the collapse of bedrock roofs. A collapse of a thin but small part of a bedrock roof over an opening would, in many instances, result in a cavity in the overlying unconsolidated deposits due to their downward migration into the bedrock. Enlargement of the cavity would eventually result in a collapse at the surface that might not be interpreted as bedrock failure. The enlargement of an opening by solution, a failure in its roof resulting in a cavity in overlying unconsolidated deposits, and the resulting sinkhole are shown at site 4 in Figure 5.

In areas underlain by air-filled openings (caves), the enlargement of cavities by downward-percolating water would be expected to cause the eventual collapse of bedrock roofs. Sinkholes attributable to this mode of occurrence have been identified by Howard (19). Collapses resulting from enlargement of openings in carbonate

rocks overlain by sandstone and thin-bedded limestone have also been identified (18, 20).

Where air-filled openings in bedrock are overlain by unconsolidated deposits, the initial development of some sinkholes can be attributed to downward migration caused by inflow and infiltration of surface water; a cavity then forms in the deposits. This mode of development is the same as that resulting from the downward movement of surface water where it is responsible for induced sinkholes. These collapses generally occur in intermittent streambeds but can occur elsewhere.

Solution of the upper surface of the bedrock has long been recognized as a mode of development of sinkholes. In this case, the topography reflects the upper surface of the bedrock. In relating the probability of this mode of development to some broad and shallow sinkholes in Kentucky, Walker (21) has described the process as follows:

> When the surface of bedrock dissolves, the insoluble residue occupies only about one-tenth of the space the rock did; open space would develop except that the soil mass slumps downward and the surface with it. Solution proceeds faster at some places than at others because the rock is more soluble or joints are more closely spaced, and slight depressions appear. Once formed, the depressions tend to grow larger because local surface runoff collects in them, and more water then seeps down to attack the bedrock under them than elsewhere in the vicinity. Solution concentrated at the center finally brings about the infall of soil blocks and the development of a swallow hole.

Solution of the upper surface of carbonate rocks will result in the development of sinkholes in the terrane described here. Most sinkholes, however, will result from the solution enlargement of existing openings in the top of the bedrock surface to eventually cause displacement of overlying unconsolidated deposits. This process of enlargement and displacement is also illustrated at sites 1 and 3 of Figure 5. Surface depressions resulting from solution of bedrock where it contains no openings would probably be rare in this terrane as deposition of sediments eroded from flanks of the basin (Figure 1) or from flooding would tend to level depressions of this type. This process is indicated by the lack of surface expression over many irregularities in the top of the bedrock in basins in Jefferson County, and is similar to effects described by Coleman and Balchin (22) and Howard (19). In the terrane described here (Figure 1), it would be difficult to distinguish sinkholes resulting from solution of the upper surface of bedrock from others resulting from the progressive solution of openings in the top of bedrock that are interconnected with other openings in the subsurface. Solution of the upper surface of carbonate rocks, however, plays an integral part in the development of large, shallow sinkholes in the more mature carbonate terranes in Alabama.

ACKNOWLEDGMENTS

This report represents a summary of some findings resulting from an investigation by the U.S. Geological Survey in cooperation with the Bureau of Research and Development, Alabama Highway Department. Personnel of the Alabama Highway Department due acknowledgment for their interest and contributions include Randolph Rowe, E. N. Eiland, C. P. White, Larry Lockett, and D. Pettus. Special recognition is due Philip E. LaMoreaux of the Geological Survey of Alabama, who, over a long period of time, has given repeated assistance and encouragement. William M. Warren of the Geological Survey of Alabama has also provided valuable assistance and information. The photograph in Figure 2 is by Curtis Frizzell, and the one in Figure 4 is by L. Lockett.

REFERENCES

1. W. D. Johnston, Jr. Ground Water in the Paleozoic Rocks of Northern Alabama. Alabama Geological Survey Special Rept. 16, 1933.
2. W. H. Robinson, J. B. Ivey, and G. A. Billingsley. Water Supply of the Birmingham Area. U.S. Geological Survey Circular 254, 1953.
3. W. J. Powell and P. E. LaMoreaux. A Problem of Subsidence in a Limestone Terrane at Columbiana, Alabama. Alabama Geological Survey Circular 56, 1969.
4. J. G. Newton and L. W. Hyde. Sinkhole Problem in and Near Roberts Industrial Subdivision, Birmingham, Alabama: A Reconnaissance. Alabama Geological Survey Circular 68, 1971.
5. J. G. Newton, C. W. Copeland, and L. W. Scarbrough. Sinkhole Problem Along Proposed Route of Interstate 459 Near Greenwood, Alabama. Alabama Geological Survey Circular 83, 1973.
6. R. M. Foose. Groundwater Behavior in the Hershey Valley, Pennsylvania. Bulletin of the Geological Society of America, Vol. 64, 1953, pp. 623-645.
7. R. M. Foose. Sinkhole Formation by Groundwater Withdrawal, Far West Rand, South Africa. Science, Vol. 157, 1967, pp. 1045-1048.
8. G. W. Donaldson. Sinkholes and Subsidence Caused by Subsurface Erosion. Proc., Regional Conference for Africa on Soil Mechanics and Foundation Engineering, Salisbury, Southern Rhodesia, 1963, pp. 123-125.
9. J. E. Jennings, A. B. A. Brink, A. Louw, and G. D. Gowan. Sinkholes and Subsidences in the Transvaal Dolomites of South Africa. Proc., Sixth International Conference on Soil Mechanics, 1965, pp. 51-54.
10. J. G. Newton. Early Detection and Correction of Sinkhole Problems in Alabama, With a Preliminary Evaluation of Remote Sensing Applications. Bureau of Research and Development, Alabama Highway Department, Research Rept. HPR-76, 1976.
11. J. E. Jennings. Building on Dolomites in the Transvaal. Civil Engineer in South Africa, Vol. 8, No. 2, 1966, pp. 41-62.
12. A. S. Allen. Geologic Settings of Subsidence. In Reviews in Engineering Geology, Geological Society of America, Vol. 2, 1969, pp. 305-342.
13. W. M. Warren. Retention Basin Failures in Carbonate Terranes. Water Resources Bulletin, Vol. 10, No. 1, 1974, pp. 22-31.
14. S. M. Herrick and H. E. LeGrand. Solution of Subsidence of a Limestone Terrane in Southwest Georgia. Bulletin of the International Association of Scientific Hydrology, Vol. 9, No. 2, 1964, pp. 25-36.
15. H. E. LeGrand. Hydrological and Ecological Problems of Carbonate Regions. Science, Vol. 179, No. 4076, 1973, pp. 859-864.
16. M. M. Sweeting. Karst Landforms. Columbia Univ. Press, New York, 1973.
17. H. E. LeGrand and V. T. Stringfield. Water Levels in Carbonate Rock Terranes. Ground Water, Giannini Foundation of Agricultural Economics, Univ. of California, Berkeley, Vol. 9, No. 3, 1971, pp. 4-10.
18. A. H. Purdue. On the Origin of Limestone Sinkholes. Science, Vol. 26, No. 565, 1907, pp. 120-122.
19. A. D. Howard. The Development of Karst Features. Bulletin of the National Speleological Society, Vol. 25, Part 2, 1963, pp. 45-65.
20. V. T. Stringfield and H. E. LeGrand. Hydrology of Carbonate Rock Terranes—A Review With Special Reference to the United States. Journal of Hydrology, Vol. 8, Nos. 3 and 4, 1969, pp. 349-417.

21. E. H. Walker. Groundwater Resources of the Hopkinsville Quadrangle, Kentucky. U.S. Geological Survey Water-Supply Paper 1328, 1956.
22. A. M. Coleman and W. G. V. Balchin. The Origin and Development of Surface Depressions in the Mendip Hills. Proc., Geological Society of London, Vol. 70, Part 4, 1959, pp. 291-309.

Subsidence Control for Structures Above Abandoned Coal Mines

R. E. Gray, H. A. Salver, and J. C. Gamble, GAI Consultants, Inc., Monroeville, Pennsylvania

Subsidence of the ground surface above abandoned coal mines can cause serious damage to highways, buildings, and other facilities. Two categories of techniques used in controlling subsidence are selective support for structures and filling of voids caused by past mining operations. The particular method used must be adapted to the local geologic setting and the mining methods that were employed in extracting the coal as well as the support requirements of the structure, because these factors vary within any given site and from one locality to another. This paper presents a case history of subsidence control for an electric substation. The subsurface stabilization techniques used included drilled piers and piling for support of the structures, and grout columns and dry fly ash injection for support of the roadways.

The expansion of highways, housing, commercial structures, and other facilities has required the use of many areas that are underlain by abandoned coal mines and will continue to do so. Movement of the ground surface, i.e., subsidence, often results from collapse of rock and soil strata overlying these mines into the voids remaining from the coal extraction.

This subsidence can be extremely damaging although its effects vary greatly, depending on the extent of the mining, the soil and rock conditions, and the structural design. There are cases where portions of buildings have fallen into sinkholes that have developed over large mine voids (1). In other cases, mine subsidence has caused severe cracking of structures resulting in their abandonment or need for extensive repairs. In other situations, extension or compressional strains have caused minor cracking and increased maintenance costs.

There are numerous abandoned mine workings in the anthracite fields of northeastern Pennsylvania, and in the bituminous fields of the Appalachians, the Illinois Basin, the Rock Springs, Wyoming, area, and other areas of the United States. In both the dipping anthracite seams and the nearly flat-lying bituminous seams, various room-and-pillar patterns of mining have been used, with considerable variation in the percentage of coal extracted. The progressive deterioration of pillars, mine floors, and mine roofs by exposure to air and water may later result in the collapse of strata over the mine entries, and the crushing of the remaining coal pillars or the bearing failure of the mine floor and strata beneath the coal pillars. Subsidence then results as the collapse reaches the ground surface in the form of differential strains, depressions, cracking of the ground, and sinkhole development.

A number of techniques, often referred to as subsurface stabilization, have been developed to control subsidence above mined areas (2). These vary because the geologic and mining conditions vary from one location to another, and because the support requirements vary according to the type and sensitivity of the surface structure. They may be grouped into two categories as follows:

1. Selective support of structures or areas, usually by supplementing the existing subsurface support by the remaining coal pillars. These methods include construction of piers within the mine, deep foundations such as drilled piers and piling, and grout columns.
2. Filling void spaces in and above the mine leaving little or no room for caving of the overlying strata. The filling materials also help maintain the existing coal pillar support by providing confinement for the pillar sides and protecting the pillars from spalling and weathering. Filling methods have varying effectiveness depending on the completeness of filling and the compressibility of the fill material.

This paper presents a case history describing the investigation and exploration of mine conditions, the design of a stabilization program including several subsidence control or stabilization methods, and the construction procedures used for structure and roadway stabilization. An undermined electric substation site in the Appalachians about 240 by 270 m (800 by 900 ft) that is used to transfer power from a 1950-MW coal-fired generating station to the transmission system presented an unusually difficult and challenging foundation design problem. The substation was underlain by mine workings in various stages of collapse, and elaborate and detailed methods of inspection were needed to

Publication of this paper sponsored by Committee on Engineering Geology.

thoroughly map the soil and rock conditions and the extent of undermining and subsidence. After the subsurface investigation, drilled piers and piles were used to support structure foundations, and grout columns and dry fly ash injection were used for roadway stabilization.

GEOLOGY AND MINING

The substation site is underlain by alluvial soils of variable thickness consisting of relatively poorly graded sands, silts, and clays. These soils have been modified by grading, and part of the facility is located on compacted fill. Beneath the alluvium are beds of coal and limestone interbedded with thick shale and claystone that belong to the Monongahela group of Pennsylvanian age.

Much of the mining in the area occurred early in this century. However, large-scale mining activities continued until immediately after World War II when many of the coal pillars were mined to extract the maximum amount of coal prior to collapse of the mine roof.

Investigation showed that the substation area had been extensively undermined, with only a thin rock cover remaining above the mine. Large sinkholes were present at the ground surface, and exploration indicated numerous voids that would probably result in additional subsidence of the ground surface at the mine level.

Coal mining at shallow depths results in two types of subsidence at the ground surface: subsidence over a widespread area and sinkhole development. These ground surface movements occur both during and after mining. Widespread subsidence, after mining ceases, is generally the result of pillar failure due to weathering and stress concentrations that, in turn, result in spalling and eventual reduction of coal pillar size. Failure of one pillar overloads adjacent pillars, which accelerates their spalling and final failure. The formation of sinkholes may be sudden, when an entire section of rock strata above the coal mine void fails abruptly and the soils fall into the void space, or slow, when spalling of the mine roof creates a void that slowly propagates to the ground surface. Normally, sinkholes do not develop if the thickness of the rock cover above an abandoned mine in the bituminous coal fields of the Appalachians is more than about 12 m (40 ft). However, in this area sinkholes were present up to about 23 m (75 ft) above the mine.

Although substation facilities can sustain some movement, settlement in the amount that might be caused by coal mine subsidence could not be tolerated. Accordingly, the structures were supported on foundations extending below the mine. In addition, concern for the safety of construction and operating personnel required that roadways be stabilized where there was any possibility of subsidence.

INVESTIGATION

The initial phase of the investigation consisted of evaluating the surface evidence of subsidence and collecting the available mining data. Detailed reconnaissance showed that strip-mining had proceeded to just about the northern edge of the substation, so that the entire substation was underlain by deep mine workings. In addition, there were five large sinkholes, where subsidence in excess of 2 m (6 ft) had occurred, in the central and western portions of the substation.

Mining beneath the substation between 1900 and 1910 had used the room-and-pillar system. A system of entries was driven to the limits of the property to provide access, ventilation, and haulageways, and rooms were cut from large blocks of coal between the entries until discrete blocks of coal (pillars) remained. This mining terminated in the early 1920s with a substantial number of coal pillars in place as indicated in Figure 1. The mine was then leased to other coal mine operators and the pillars mined until about 1945, when roof conditions deteriorated so as to make further operation impossible. (The cross-hatching in Figure 1 indicates pillars that are known to have been removed. As indicated, most of the pillars were removed from the northeast portion of the substation.) The mining pattern was irregular in the southwest corner probably because of poor roof conditions that created safety problems. In addition, some areas beneath the substation, which were shown as reserves to support or protect gas wells, were probably also mined. Eight gas wells that had suffered subsidence damage were located during the investigation.

To determine the accuracy of the available mine map, an extensive drilling investigation was conducted. Eighteen standard test borings, in which split-barrel samples were obtained in the soil overburden and NX cores were obtained in rock, and sixty-four 150-mm (6-in) diameter rotary-air borings were drilled. The rotary-air borings were logged from the cuttings of the soil and rock strata penetrated. All sudden drops or jerks of the drill tools, phenomena that indicate broken rock strata or other related mine subsidence features, were noted. Rotary-air borings that encountered voids at mine level, caved rock strata, or crushed coal pillars were photographed with a stereoscopic vertical borehole camera. Photographs were taken in the rock strata above the mine at depth intervals of about 0.3 m (1 ft). The use of the borehole camera permitted the accurate location of any mine voids and provided a good record of the condition of the rock strata above the mine level. Once the voids were accurately located, a borehole camera having a self-contained light source and capable of taking horizontal pictures was used. The camera was rotated between photographs to obtain 6.3-rad (360-degree) coverage of the mine void.

SUMMARY OF SUBSURFACE CONDITIONS

The substation area varies in elevation from 320 to 302 m (1050 to 990 ft). It was graded to an elevation of 308 m (1010 ft) with fill in the central portion. The fill has a maximum thickness of about 6.1 m (20 ft) and is generally stiff in consistency. Colluvial soils up to 3.7 m (12 ft) thick were encountered in the borings along the east side of the substation. This colluvium is the result of mass wasting of the soils formed from weathering of the rock strata on the hill flanking the east side of the substation. Alluvial soils that varied from silty clays to fine sands were exposed on the surface of the remainder of the area. The thickness of the alluvial soil varies from 3.7 m (12 ft) along the north central portion of the substation to 18 m (60 ft) at its southeast corner. The alluvial soils underlie the colluvium on the east side of the substation and thin toward the west side of the substation. The upper portion of the alluvium ranges from soft to stiff cohesive soil. Laboratory consolidation tests on these soils show them to be moderately to highly compressible, with compression indices of 0.165 to 0.950. Granular alluvial soils, composed predominantly of fine sand and silty sand, underlie the cohesive soils throughout the substation. These soils are generally in a medium dense state.

Underlying the soils is a thin veneer of decomposed rock that partially mantles the firm rock surface. The top of the rock, as shown in Figure 2, slopes steeply upward just east of the substation. However, in the major portion of the substation, the rock surface is relatively flat, varying between elevations of 296 to 299 m

(970 to 980 ft): It reaches its highest elevation of 306 m (1005 ft) in the northwestern corner of the substation. Thus, the depth to rock from the grade elevation of 308 m (1010 ft) varies from 1.5 to 12 m (5 to 40 ft).

Figure 3 shows the contours of the base of the mined coal seam. The coal dipped to the southeast and varied in elevation from 294 m (966 ft) at the northwest corner of the substation to 286 m (939 ft) at the southeast corner. Comparison of Figures 2 and 3 indicates that the interval between the top of the rock and the base of the mined coal varies from about 9 to 12 m (30 to 40 ft) at the southeast and northwest corners of the substation respectively. The average interval in most of the central portion is about 6 m (20 ft) but as little as 3 m (10 ft) in the southwest corner.

The rock strata within the substation from the top of rock to the lowest strata of importance with respect to foundation design and construction are (a) limestone, (b) claystone, (c) shale, (d) coal (mined seam), (e) siltstone, and (f) silty shale. Over much of the area, hard limestone, which is commonly interbedded with claystone and is a maximum of approximately 3 m (10 ft) thick, forms the rock surface. The limestone is for the most part a competent rock and frequently bridges over underlying mine voids. Where the claystone interbeds occur and the weathering is particularly advanced, the limestone is less competent and unable to span the mine voids. Underlying the limestone there is approximately 2.4 m (8 ft) of claystone, which is usually in a medium soft state. Frequently, the claystone has caved into the mine voids resulting in a soft clayey mass at mine level. The claystone is, in turn, underlain by 1 m (3 ft) of shale, which has also caved into the mine rooms and contributes to the clayey mass. Some of the borings encountered a similar soft material at mine level that could not be attributed to caving of the mine roof. This material, termed mine gob, is mine waste that was disposed of in abandoned entries and rooms.

The mined coal seam is usually about 2 m (6 ft) thick. However, in some of the borings, crushed coal pillars were encountered. In these borings, the coal was somewhat thinner and highly fractured. The conditions encountered at the level of the mined coal seam by the 82 borings are summarized below:

Condition	Percent of Borings	Condition	Percent of Borings
Coal pillars	48	Caved material	35
Crushed coal pillars	5	Large voids	12

The mined coal seam is generally underlain by a siltstone stratum that ranges from 2 to 3 m (7 to 10 ft) thick and varies from medium soft to medium hard. Frequent interbeds of claystone occur in the siltstone. Interbedded shale, silty shale, and siltstone underlie the siltstone stratum and extend to approximately 6.7 m (22 ft) below the base of the mined coal seam. Figure 4, a typical cross section through the substation, shows the thickness of the soil and rock cover above the mined coal seam.

The water levels measured in the borings show the water table to occur at or slightly above the base of the mined coal seam. In a few cases, local ponding of water has occurred in the mine workings because of roof falls or the presence of mine bulkheads, and in one large area along the northwestern side of the substation, the mine is flooded.

Figure 1. Map of abandoned coal mine beneath substation.

Figure 2. Contours of the top of the rock.

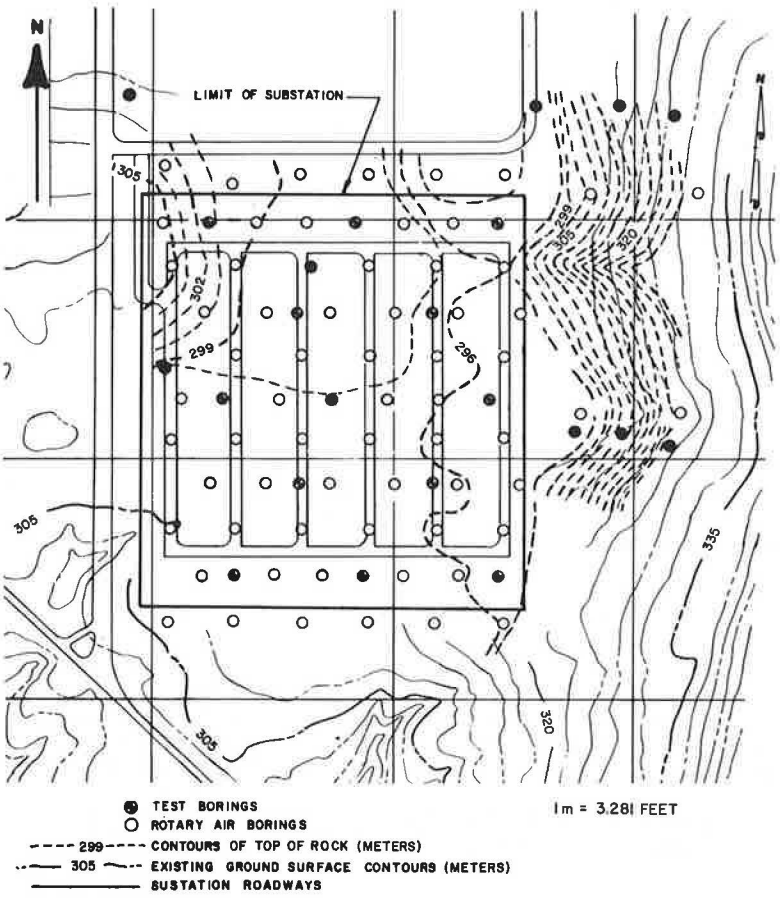

Figure 3. Contours of the base of the mined coal seam.

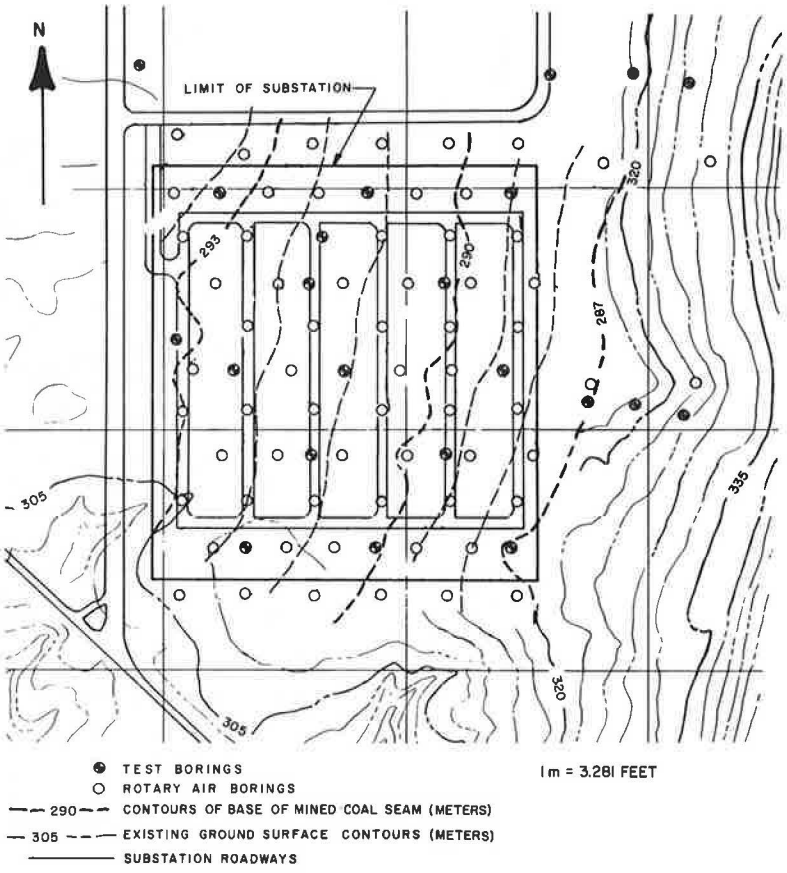

Often, the borings did not encounter conditions anticipated from the mine map. However, study of the horizontal borehole photographs indicated that the mine map should be shifted somewhat in relation to ground surface features. Once this was done, the map was quite accurate.

The substation was divided into three areas, based on the extent of mining indicated by the map and the conditions at mine level shown by the borings and photographs. In area 1, the southwestern portion of the site where the amount of rock cover above the coal was minimal, mining had not been extensive. Large coal pillars were shown on the mine map and all but a few of the borings encountered in-place coal. The voids that were encountered were the full height of the seam and contained little caved material. In area 2, the eastern half of the substation where the rock cover above the base of the coal varied from about 6 to 9 m (20 to 30 ft), removal of most of the coal pillars had resulted in almost complete subsidence. Most of the borings drilled in this area encountered caved material and a few moderate-sized voids and coal pillars. Area 3, the northwestern portion of the substation, was underlain by a fairly well-developed system of mine entries and rooms. No retreat mining involving coal pillar extraction had been conducted in this area, and the mine rooms were large and the coal pillars relatively small. The borings usually encountered either large voids or in-place coal. The rock cover above the base of the coal varied from 6.7 to more than 12 m (22 to 40 ft) in this area.

FOUNDATION DESIGN

As shown in Figure 5, the substation contains 10 circuit breakers, and the associated disconnect switches, lighting arresters, and metering and control equipment interconnected by rigid aluminum tube bus ducts with dead end towers for connections to the generating units and the 500-kV transmission lines. The control and communication cables are placed in precast concrete enclosed trenches. Because of the rigid bus duct connections, very little settlement or movement of the equipment can be tolerated.

The transmission and dead end towers exert relatively heavy lateral and vertical loads on their foundations. Therefore, because of the compressible soils overlying the rock surface and the abandoned coal mine, 0.76 and 1.22-m (30 and 48-in) diameter reinforced-concrete piers drilled in place were selected as the most suitable type of foundation for them. All of the drilled piers were socketed into rock below the base of the mined coal seam. The minimum diameter of 0.76 m (30 in) for the drilled pier construction was due to the necessity of hand cleaning the sides and bottom of the pier rock sockets. Permanent steel casing with a wall thickness of 8 mm ($^5/_{16}$ in) was securely seated into the rock at the base of the mined coal seam and extended to the ground surface to provide a form for the concrete in the abandoned mine workings. The casing also prevented bonding of the drilled pier to the rock strata above the mine, which might, at a later date, subside. In addition, the casing served as a protective liner for men working at the bottom of the drilled shaft.

Drilled piers bearing on medium hard or hard rock strata were designed for a maximum allowable end-bearing pressure of 960 kPa (10 tsf) for dead, live, and wind loadings. Rock sockets extending into medium hard rock strata were designed for load transfer between the drilled pier and the rock socket using a shear value of 350 kPa (50 psi). Where the strata at the base of a drilled pier were composed of soft to medium soft rock, drilled piers were designed for a maximum end bearing pressure of 380 kPa (4 tsf) for dead, live, and wind loadings. If the rock strata were medium soft, a design shear value of 140 kPa (20 psi) was used for load transfer between the drilled pier and the rock socket, and if the rock was soft, shear value of zero was assigned.

In places where medium soft rock was known to underlie the base of the drilled piers by less than 0.6 m (2 ft), a maximum bearing pressure of 380 kPa (4 tsf) was used. On completion of the rock socket, a 3-m (10-ft) deep test hole was drilled using percussion drilling equipment to evaluate the quality of the rock below the base of the socket.

Due to the difficulties in penetrating the hard limestone above the mined coal seam, the drilled piers were allowed to deviate from plumbness a maximum of 1 percent (6.4 mm/m, $^1/_8$ in/ft). A maximum eccentricity radius of 25 mm (1 in) from the plan location was permitted. Figure 5 shows the area of the substation in which fill was placed. In this area, because of the settlement of the alluvium under the weight of the fill, all of the drilled piers were designed for a negative skin friction load of up to 68 Mg (75 tons) per pier. All of the drilled piers were designed assuming concrete with a minimum unconfined compressive strength of 24.5 MPa (3500 psi).

The circuit breakers, disconnect switches, lighting arresters, and metering and control equipment are relatively light and exert small loads on foundations. Therefore, this equipment was supported on less costly predrilled closed-end steel pipe piling extending to the base of the mined coal seam. The piles, which are designed for a maximum vertical load of 68 Mg (75 tons), were tied together by a grade beam system at the ground surface to provide lateral resistance. Evaluation of the reduction in strength of steel piling that would result from corrosion by the acid mine water (pH approximately 3.5) showed that use of conventional steel piling was not feasible. Therefore, relatively corrosion-resistant Yoloy (a copper-zinc-manganese alloy steel) pipe was selected for use. Study showed that extra strong, 0.2-m (8-in) nominal diameter Yoloy pipe filled with concrete would safely sustain the design load over a 30-year period, and to provide an additional safety factor the piling was filled with 24.5 MPa (3500 psi) concrete. The negative skin friction loads on piling installed in the filled area amounted to approximately 4.5 Mg (5 tons)/pile. Out-of-plumb variation was limited to 2 percent of the pile length. All piles were driven within 50 mm (2 in) of the indicated plan location.

Roadway safety was carefully evaluated to provide an economical stabilization treatment; Figure 6 shows the various stabilization methods used. No treatment was required beneath the sections of the roads that were underlain by solid coal or where nearly complete subsidence had occurred. At the few locations where isolated mine entries underlaid the roads, grout columns (Figure 7) were formed by placing a cone of gravel in the mine void and then grouting the cone to stabilize the mine roof. The remaining sections of roads were stabilized by injecting dry fly ash from tanker trucks into the mine voids.

CONSTRUCTION PROCEDURES

Foundation construction and subsurface stabilization were conducted during the winter of 1971. Due to the special nature of the foundation and stabilization work, three contracts were let: one for the drilled piers, one for the closed-end pipe piles, and one for the fly ash and grout column stabilization.

Drilled pier construction totaled sixty-four 0.76-m (30-in) diameter piers and twelve 1.22-m (48-in) diameter piers. These were drilled with Williams LLDH truck-mounted diggers using 0.91 and 1.37-m (36 and 54-in)

diameter soil and rock augers to depths up to 23 m (75 ft). The holes were drilled somewhat oversized in the soil and rock strata above the mined coal seam to avoid problems in placing the casing within plumbness tolerance. However, in some cases, deviations in plumbness necessitated lowering a man into the shaft to jackhammer the obstructions so that the vertical shaft would meet the specified tolerances upon placement of casing. Where the overlying limestone was relatively thick and hard, Calweld crane-mounted rigs using roller cone bits were used until the limestone was penetrated. Permanent steel casing was then inserted to the base of the mine and a 0.76 or 1.22-m (30 or 48-in) nominal diameter socket drilled into the underlying strata using rock augers. The annulus between the oversized hole and the casing was backfilled with gravel.

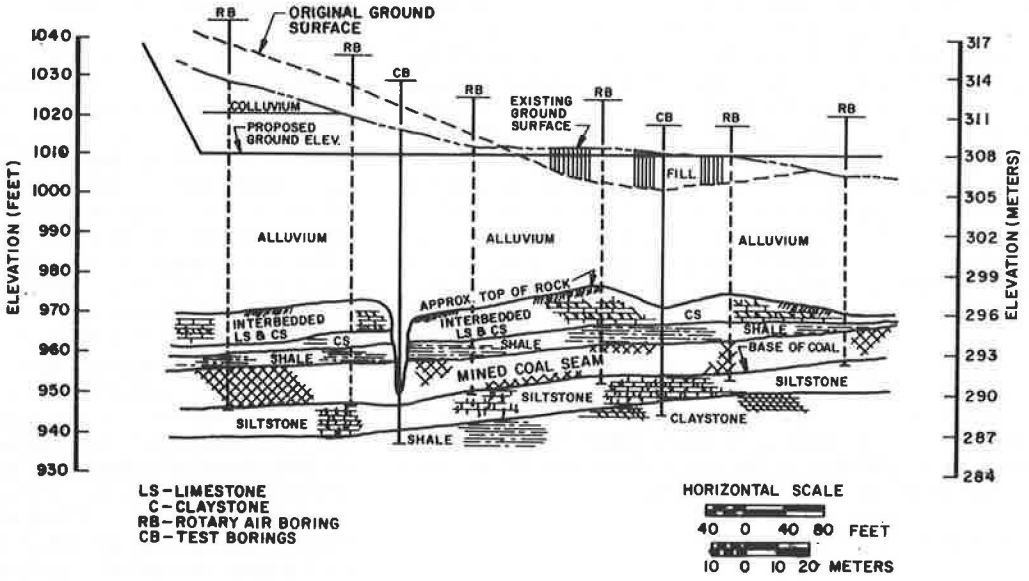

Figure 4. Typical east-west oriented cross section.

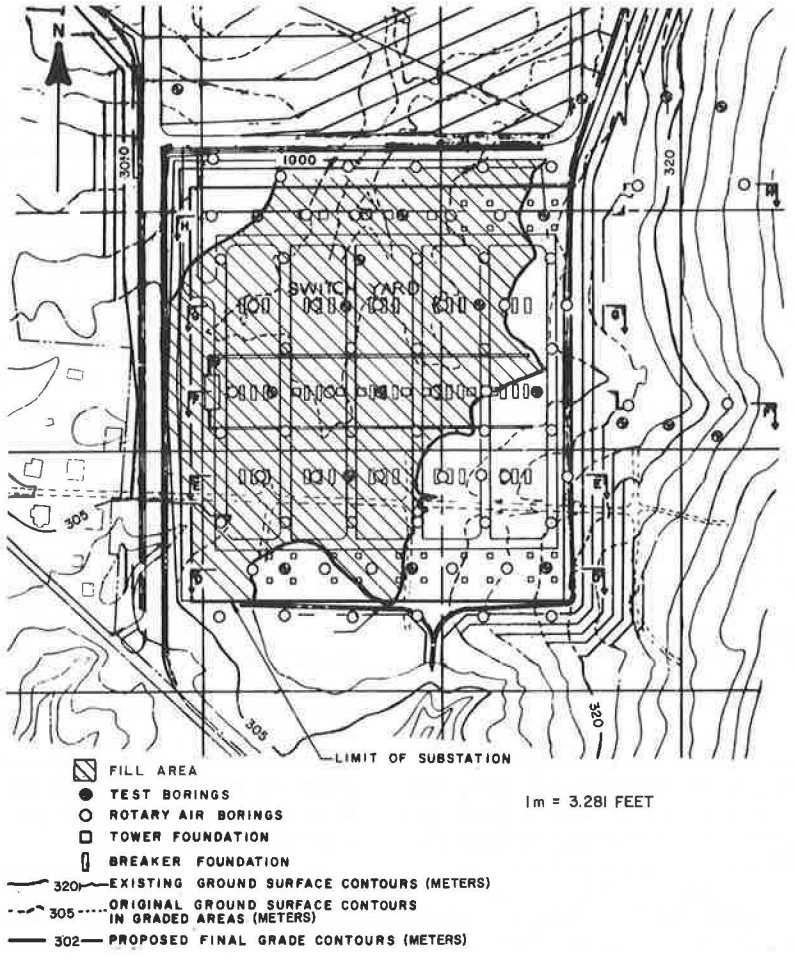

Figure 5. Fill area in substation.

Figure 6. Roadway stabilization treatment areas in the substation.

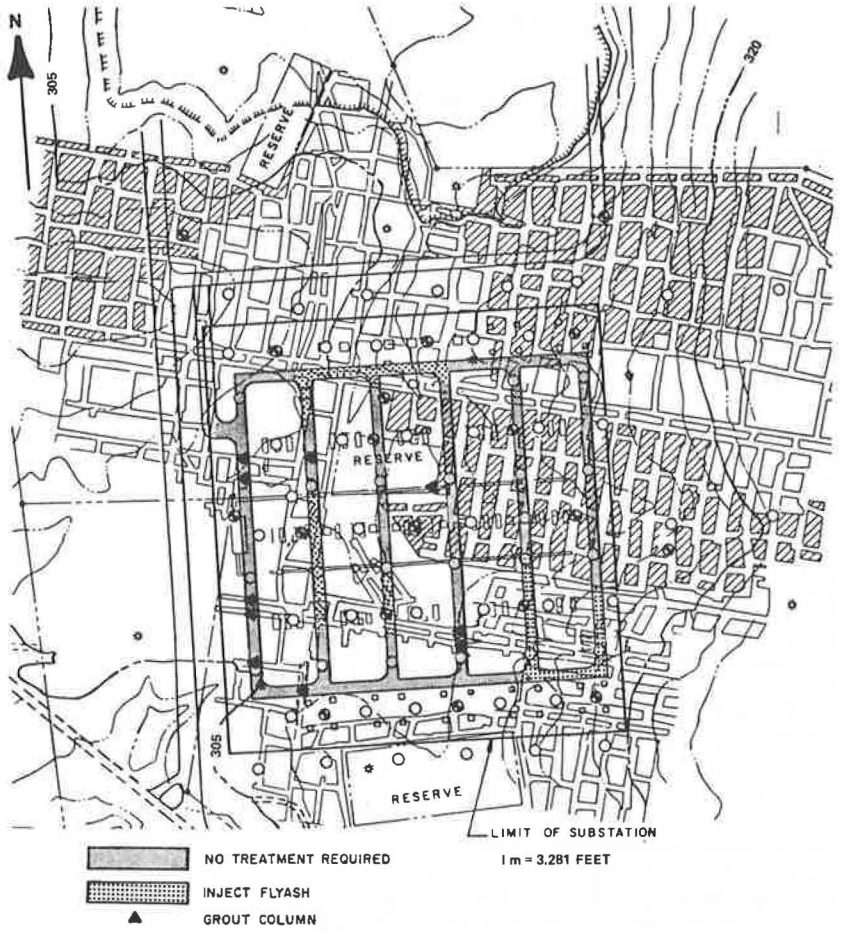

Figure 7. Typical grout column construction.

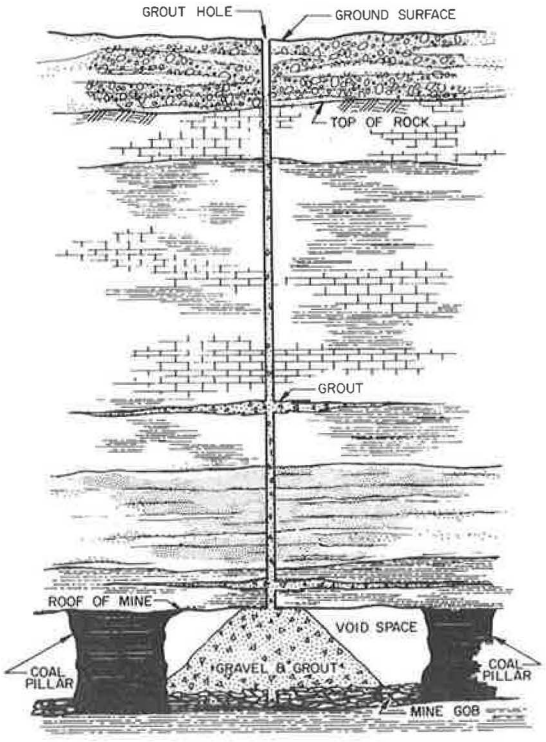

The rock sockets extended 0.5 to 2.7 m (1.5 to 9.0 ft) below the base of the mined coal seam. Their sides were thoroughly scraped clean, and loose material was removed from the base of the drilled pier shaft prior to concrete placement. In most cases the rock sockets had only small inflows of water and presented few problems in placing the concrete. Where water was encountered, a pump was placed in the shaft bottom for cleaning and dewatering, and withdrawn immediately prior to placement of the concrete, which was placed from the top of the hole using a chute to prevent it from ricocheting against the casing. Anchor bolts or steel stub angles or both were placed at the cutoff elevation.

Piling was initially installed in holes drilled to the base of the mined coal seam using a crane-mounted auger to drill soil and an air-rotary drill to extend the hole through rock. About midway through the project the use of the auger was abandoned and the remainder of the holes were drilled solely by the air-rotary rig. (Problems had been encountered in the use of two drilling rigs to complete a hole as the soil and rock portions of the hole were frequently not co-axial.) A total of 393 piles were installed. The holes were a minimum of 0.24 m ($9\frac{5}{8}$ in) in diameter. The piles were seated at the bottom of the hole using a Vulcan 08 hammer rated at 35 kJ (26 000 ft-lb) at 50 blows per minute. In all cases, the pile penetrated to the mine floor and then reached a final penetration resistance of 10 blows/25 mm (1 in). Most piles were driven from 0.3 to 0.6 m (1 to 2 ft) into the rock strata below the base of the mined coal seam. Backfilling around the piles was done in a manner similar to that used for the drilled piers. The piles were checked for plumb tolerance and then concreted to increase their

structural strength and provide an added safety factor against corrosion. They were then cut off at the design elevation and completed with anchor straps. Field splices were not permitted; all piles were brought to the site at predetermined shop fabricated lengths and then cut off as required.

Subsurface stabilization was conducted through 150-mm (6-in) diameter holes drilled with air-rotary equipment. All holes were cased to the top of rock. In the northwest portion of the substation, a dewatering well was installed to draw down the water in a portion of the mine that was flooded. The bulk fly ash stabilization was performed first. The fly ash was transported to the site in 18-Mg (20-ton) pneumatic tank trucks. A connection to the casing was made and the fly ash blown into the mine through the casing inserted in the borehole at a maximum pressure of 100 kPa (15 psi) until refusal. Some holes refused fly ash, but as much as 180 Mg (200 tons) was injected into other holes; the total amount of fly ash placed in the 180 injection holes was 3500 Mg (3800 tons).

Grout columns (Figure 7) were constructed at 15 selected locations. The columns were constructed by placing gravel down the hole, spreading the aggregate with compressed air injected through a perforated pipe at the hole bottom, and then injecting grout into the aggregate pile. The aggregate used consisted of clean gravel 6 to 19 mm (¼ to ¾ in) in diameter. The grout consisted of a fluid mix, 3 fly ash to 1 cement to 3 to 4 water, which was delivered to the grout pumping stations in agitator trucks from a local batch plant. A roof contact diameter of about 1.8 m (6 ft) for a grout column is adequate to support the mine roof.

During construction, a few small sinkholes formed at the ground surface, indicating the serious subsidence potential. Since the construction has been completed, no additional sinkholes have formed in the stabilized area.

REFERENCES

1. Underground Disposal of Coal Mine Wastes. National Academy of Sciences, Washington, D.C., 1975.
2. State of the Art of Subsidence Control. General Analytics, Inc., Appalachian Regional Commission, Rept. ARC-73-111-2550, 1974; NTIS, Springfield, Va., PB 242 465 AS.

Ground Subsidence Associated With Dewatering of a Depressed Highway Section

Joseph B. Hannon and Barry E. McGee, Structures and Engineering Services Division, California Department of Transportation

Subsidence of land areas adjacent to construction of an Interstate highway is reported. Foundation settlements of structures adjacent to a depressed section occurred as a result of pumping groundwater during construction dewatering operations. Preliminary recommendations and actual construction dewatering operations are discussed. The stability of the Sacramento River levee and the possibility of piping during high water were significant factors in planning the dewatering operation. Records of groundwater drawdown for various pumping rates are presented with data from a Ranney well pumping system located in downtown Sacramento; foundation settlement studies for buildings in the adjacent area and specifications for dewatering of the depressed highway section are described. The need for comprehensive laboratory and field tests is discussed. Unforeseen circumstances that developed during the dewatering process required deviation from the scheduled construction operations and continuous monitoring of groundwater and ground surface elevations. It is concluded that the settlement problem could have been minimized had its probability been more fully realized. Goundwater levels should have been more closely monitored during the initial stages of dewatering. Valuable information could have been developed early in the planning stages of this project from drawdown studies using deep wells pumping from a lower, more permeable stratum.

Land subsidence is a normal occurrence in many areas of California. For example, in the Santa Clara and San Joaquin Valleys, deep subsidence has resulted largely from the compaction of soil deposits caused by accelerated pumping of groundwater for agricultural purposes (1).

The general lowering of the groundwater table by dewatering to provide dry conditions during work in large open excavations can also induce land subsidence or soil settlement, which is detrimental to structures above the affected water table. Even when appropriate precautions are taken during dewatering operations, unforeseen events or conditions sometimes occur. When the water table is lowered, the effective load on the subsoil is increased by an amount equal to the difference between the drained and submerged weights of the entire soil mass between the original and the lowered water table. This increased overburden pressure causes additional compression and produces settlement (2). Settlement can occur rapidly in sands, but in clays and silt soils a much longer period of time is involved.

This report presents a case history of a ground subsidence that occurred during dewatering for construction of a depressed highway section in Sacramento.

BACKGROUND INFORMATION

During 1968 a section of Interstate 5 was constructed as a depressed freeway through the old historic area of Sacramento (Figure 1). This portion of freeway is adjacent to the Sacramento River, which traverses the westerly edge of downtown Sacramento. The design planned for construction of a 1220-m (4000-ft) depressed roadway, approaching, at one point, within 37 m (120 ft) of the river.

The city of Sacramento is protected from flooding by a system of levees along the Sacramento River on the west and the American River on the north. Because of the proximity of the river and the adjacent levee system, several safeguards were included in the depressed freeway design, along with stringent specifications and construction requirements. The area to be depressed was designed as a boat section to resist buoyant forces, with portland cement concrete up to 3.7 m (12 ft) in thickness. At the higher roadway elevations, the uplift was resisted by the weight of the concrete structure alone, but in the deepest excavation section, tension or hold-down piles were used to resist the main portion of the uplift forces and achieve economy with a thinner concrete section.

The river stage on the Sacramento River during periods of low runoff is 1.5 to 3 m (5 to 10 ft) above mean sea level. At times during the winter, it reaches 7.6 m (25 ft) and possibly higher. The average elevation of the ground surface in the downtown area is about 4.9 m (16 feet). The top of the levee is 9.8 m (32 ft) above sea level.

The low point of the finished grade in the depressed section was at about -0.6 m (-2 ft) below sea level, but excavation was required to -2.6 m (-8.5 ft) and slightly lower. Excavation for the pumping station to drain the completed facility extended down to -5.5 m (-18 ft).

Publication of this paper sponsored by Committee on Engineering Geology.

Soils in the area are moderately heterogeneous. In the southerly half of the depressed section above sea level and in the northerly half above -3.0 m (-10 ft) there are silty clays and clayey silts. These are interbedded with lenses and layers of sand and silt. Underlying these mixtures are sands and silty sands with gravel occurring at depths down to -12.2 m (-40 ft).

The stability of the levee and the possibility of piping during high water periods were prime concerns, and stringent specifications were proposed to prevent problems in this area during construction. Attention was also focused on the effects of dewatering and the possibility of subsequent settlement of certain designated buildings adjacent to the work. Specifications relating to the protection of these specific buildings were formulated. The contractor was also required to inspect and record the existing condition of these buildings prior to working in the vicinity, and to replace or restore any subsequent damage.

As the project proceeded to the bidding stage, a consultant hired by the California Department of Transportation reviewed the plans and specifications with respect to their adequacy in ensuring levee safety and maintaining existing flood protection. It was recommended that the excavation work be done in the dry condition, which required dewatering of the excavation and construction of a cofferdam.

The special provisions had several requirements relating to groundwater control:

1. The silt production of a pumping well after a 48-h developmental period was to be no more than 5 ppm;
2. At river stages below 3 m (10 ft) groundwater could be lowered as necessary to continue the work;
3. At river stages between 3 and 7 m (10 and 24 ft) work could continue in the dry condition as long as the bottom of the excavation stayed above an imaginary plane sloping away from the river surface on a maximum 5 percent gradient;
4. When the river stage was above 7.3 m (24 ft), all dewatering was to stop;
5. Relief wells were to be placed inside the cofferdam and were to be of sufficient capacity to raise the water level in the excavated area at a rate of 9 cm (0.3 ft)/h under a 3-m (10-ft) head; and
6. Additional means of flooding the excavation were to be provided in conjunction with the relief wells so that the water level in the excavation could be raised at the rate of 12 cm (0.4 ft)/h, which would keep pace with the expected maximum rate of rise of the Sacramento River.

THE DEWATERING OPERATION

Sheet piling was placed around the entire excavation area and the groundwater lowered by pumping from a deep, relatively pervious gravel stratum (rather than from a shallower well point system). A total of 29 pumps, each rated at about 7.6 m^3/min (2000 gpm), were used around the periphery of the excavation. The well casing extended to about -18.3 m (-60 ft) below sea level with a pump pickup of -12.2 m (-40 ft). The tip elevation for the sheet piling was about -7.6 m (-25 ft).

A cross section of the excavation is shown in Figure 2 with the location of the intake wells, the adjacent Sacramento River and levee embankment, the normal groundwater table sloping away from the river, the groundwater table during dewatering, and the soil profile. The silt production from the wells was a maximum of 2 ppm, which was less than the allowed maximum of 5 ppm. The intake wells were located on both sides of the excavation although the majority were on the easterly side.

The dewatering operations began with three pumps in operation on August 20, 1968. Other pumps were gradually put into operation until, about 20 days later, 16 pumps were producing an estimated 60 m^3/min (16 000 gpm). During this time, the water table was lowered from about 0 to -6.7 m (-22 ft). No water table observations were made during the early stages of dewatering since observation wells were not yet complete. (Existing wells were available but were not used.) It is therefore probable that the drawdown exceeded the maximum recorded low. The pumping rates and the resulting changes in groundwater levels along O Street over an 18-month period following the start of dewatering are shown in Figure 3.

About 15 days after pumping began, tenants in a building situated about 250 m (800 ft) from the nearest line of pumps noticed building distress. Reports of damage in other buildings came in rapidly, and it soon became apparent that settlement was taking place over a fairly wide area. The pumping was then reduced to an estimated rate of about 34 m^3/min (9000 gpm). As a result, the water table at the excavation rose from -6.7 m (-22 ft) to -4.9 m (-16 ft). At this same time, the California Department of Transportation began drilling a series of additional sample borings and observation wells, and level circuits were established to monitor elevations in the adjacent downtown area. This information was used to supplement the data that had been gathered during an extensive program of foundation exploration, drawdown testing, and laboratory soil testing prior to the actual design and construction.

A review of the buildings in the settlement area showed that pile-supported structures had not settled significantly and that buildings on spread footings had sustained only isolated minor damage. The damage that had occurred was due mainly to differential settlement in buildings whose structural elements were founded on piles and whose bottom story floors and walls were grade-supported on compacted earth. Damage had also occurred where peripheral sidewalks and similar appurtenant structures were in contact with pile-supported structures.

The settlement graphs (Figure 4) for benchmarks located along Second Street show that about 3.4 to 7.9 cm (0.11 to 0.26 ft) of settlement occurred during September 1968. About 1.8 cm (0.06 ft) of additional settlement occurred during the 1-year period following the initial drawdown. However, the benchmark elevations are influenced to a major degree by cyclic changes in the groundwater table due to the river stage and recharge from rainfall. Historically, they have varied ±0.9 cm (0.03 ft) annually.

ANALYSIS OF THE PROBLEM

Groundwater observations made at various locations in Sacramento over a period of years have indicated a probable historical low water table of 0.9 to -0.9 m (3 to -3 ft), depending on the distance from the river. The normal water table gradient prior to the excavation and the dewatering operation sloped away from the river as shown in Figure 2. After one month of dewatering, the water table varied from about -4.9 to -2.4 m (-16 to -8 ft) and sloped toward the excavation. In the area where settlement was first noticed, the difference in groundwater level was 4.9 m (16 ft).

Data from various sources were gathered to obtain a better picture of the foundation soils and their consolidation and permeability characteristics in the downtown area. Old boring logs and tests made by the transporta-

Figure 1. Project location map of depressed section.

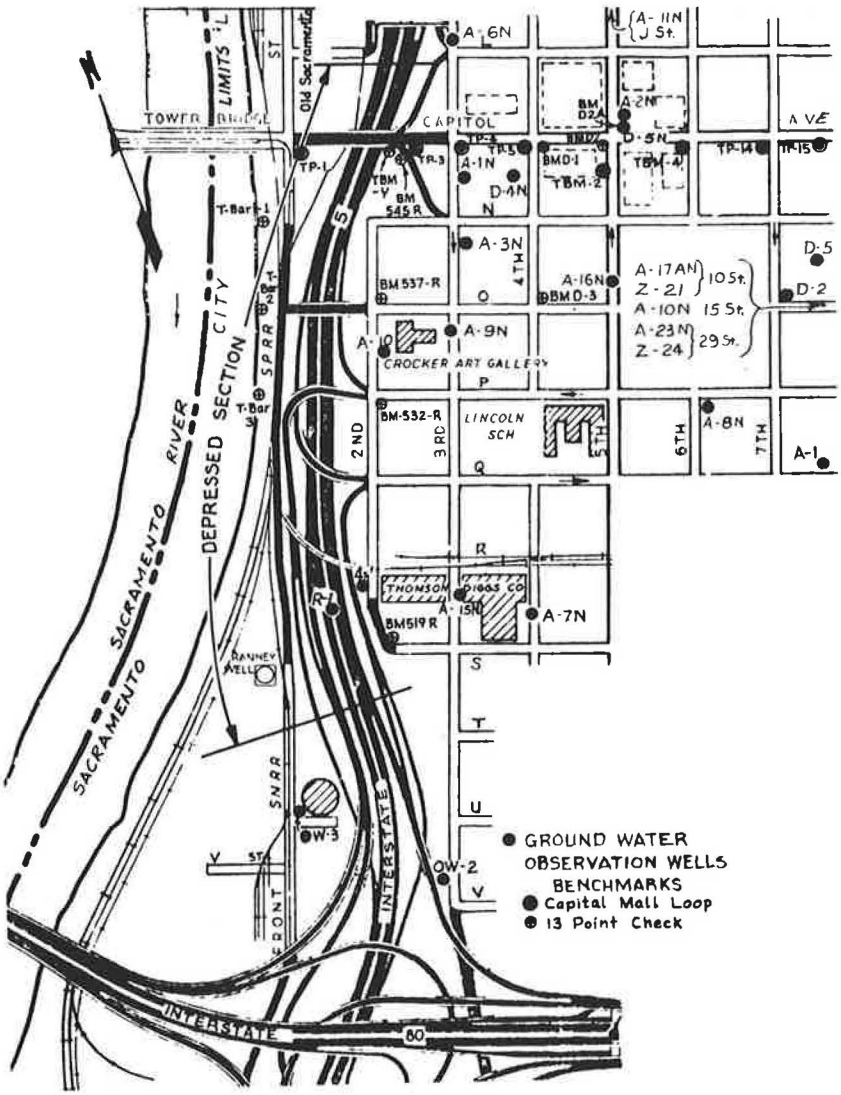

Figure 2. Cross section of excavation.

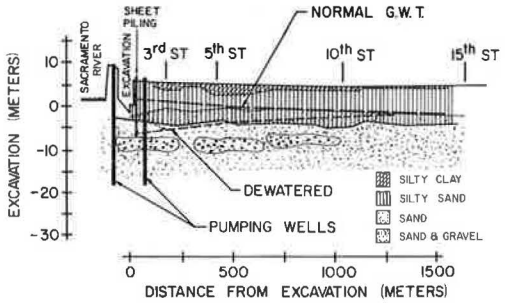

tion laboratory for state buildings in the area were examined. Foundation reports for major structures in the affected area were also obtained from the Sacramento City Engineer's Office.

The lowering of the groundwater table in the general area was complicated by the fact that several other well systems, including the new state central heating and cooling system, were also pumping from wells in the same general area. The heating and cooling system uses a Ranney well installation that went into service during the initial stages of the dewatering operation and was pumping at a rate of about 11.4 m^3/min (3000 gpm) on September 19, 1968, with rates of about 22.8 m^3/min (6000 gpm) during various 8-h periods. The main well for this collection system is located immediately west of the freeway near S Street as shown in Figure 1. Groundwater observations and pumping rates for this system are shown in Figure 5. The Ranney collector system at this location consists of a 6.1-m (20-ft) diameter caisson driven to -21.6 m (-71 ft). At -18.3 m (-60 ft), six laterals 25.6 to 36.3 m (84 to 119 ft) in length radiate outward toward the river.

Elevation measurements of benchmarks located along the Capitol Mall Loop (Figure 1) suggest some continuation of settlement after the initial drawdown in September 1968. Changes in the ground surface elevation are shown in Figure 6. The maximum drop in elevation varied from 3.1 cm (0.10 ft) nearest the excavation to about 0.3 cm (0.01 ft) near Eighth Street. This settlement occurred over a period of 1 year following the initial drawdown of the water table. The pattern of the ground surface elevation fluctuations indicated by the benchmark measurements closely follows the normal cyclic changes in groundwater levels due to changes in river stage and recharge by rainfall.

Figure 7 shows the relatively flat drawdown curve (curve C) that resulted from pumping groundwater from the deep, relatively pervious gravel stratum (Figure 2).

Figure 3. Groundwater levels (along O Street) and pumping rates.

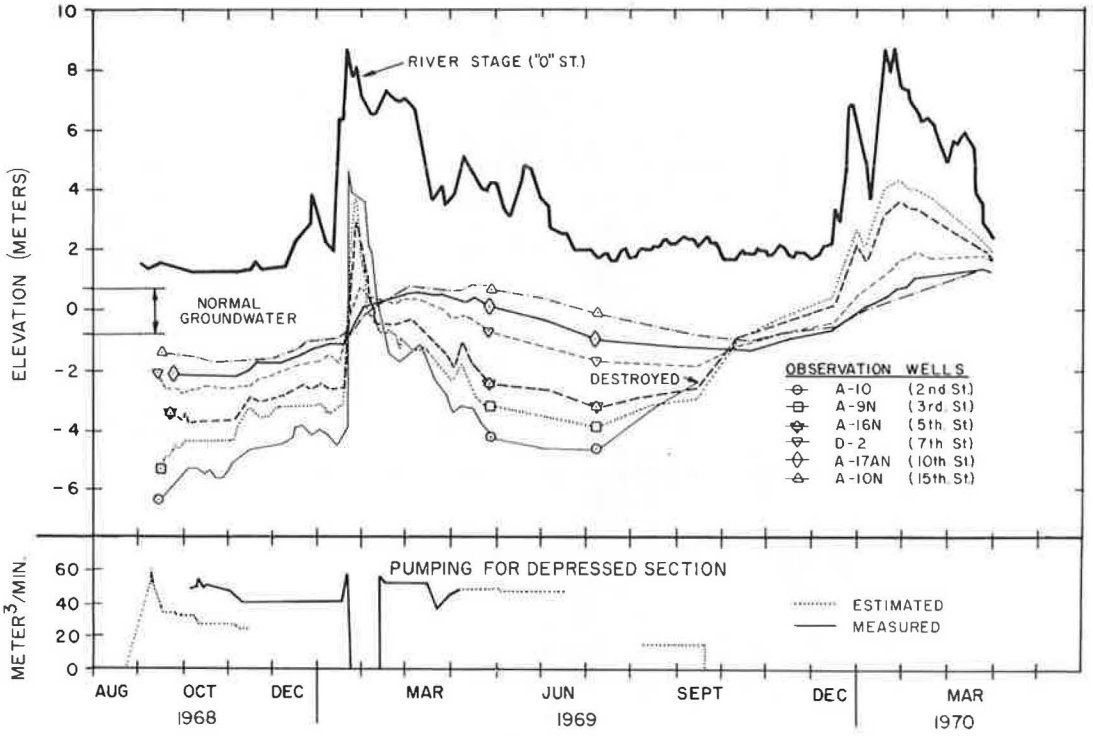

Figure 4. Change in benchmark elevations (Second Street).

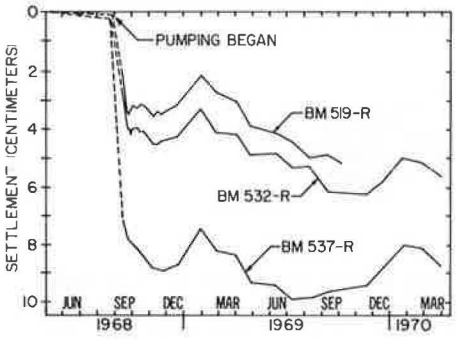

Earlier groundwater studies had been based on wells that pumped at a much shallower depth in a less permeable layer, and resulted in a much sharper drawdown curve (curve A). Curve B illustrates the drawdown curve that was developed during contract pump tests prior to construction using a single deep well founded in the underlying permeable layer with water recharge from below the drawdown cone. The pumping rates were approximately 4.6 and 6.8 m^3/min (1200 and 1800 gpm).

Supplemental consolidation tests using undisturbed soil samples of the silt and silty sands located near the area of greatest reported distress were performed to analyze the settlement problem. Settlement calculations were based on the increased effective overburden pressure resulting from the lowering of the water table. It was assumed that historically the water table had a previous low of 5.2 m (17 ft) below the ground surface and that the underlying soil had been preconsolidated by this condition. Settlement was then calculated with the water table lowered as much as 6.1 m (20 ft). The results of these calculations for various applied building loads are shown in Figure 8.

The calculated settlements are of the same relative magnitude as the reported drop in benchmark elevations in the affected area (Figure 4) and confirm that the rapid settlement had occurred in the silt and silty sand deposits.

An evaluation of the situation was made soon after the initial settlement was detected and the initial data could be analyzed. It was concluded, based on precision follow-up ground surface elevation measurements and settlement calculations, that the situation had stabilized and that no additional significant settlement would occur as a result of higher pumping rates during high river stage if the groundwater table beneath the excavation was maintained at about the same level. It was also felt that pile-supported structures would not settle as a result of downdrag or any other consequence of the dewatering activities. The contract specifications were also considered adequate to ensure protection of Sacramento during expected high river stages. It was decided to continue pumping in the dry condition as long as the river stage was between 3.0 and 7.3 m (10 and 24 ft), and to provide standby power: The excavation would be flooded when the river reached 7.3 m (24 ft). It was also recommended that the maximum differential in head between the water in the river and the water in the excavated section not exceed 2.4 m (8 ft).

During January 1969, high water stage in the Sacramento River reached 8.5 m (28 ft) and remained there for about 24 h. Dewatering was stopped and the excavation flooded by pumping directly into the excavation. The elevation of the water in the excavation stabilized at approximately 3.7 m (12 ft) shortly after the high river stage. Flooding the excavation provided the necessary counterbalance of excess hydrostatic pressures in the bottom of the excavation. The performance of the section under these conditions indicates that the specification requirements are conservative and provide adequate protection for the city.

Six days after flooding, dewatering was resumed with

Figure 5. Groundwater levels (along S Street) and pumping rate for Ranney well.

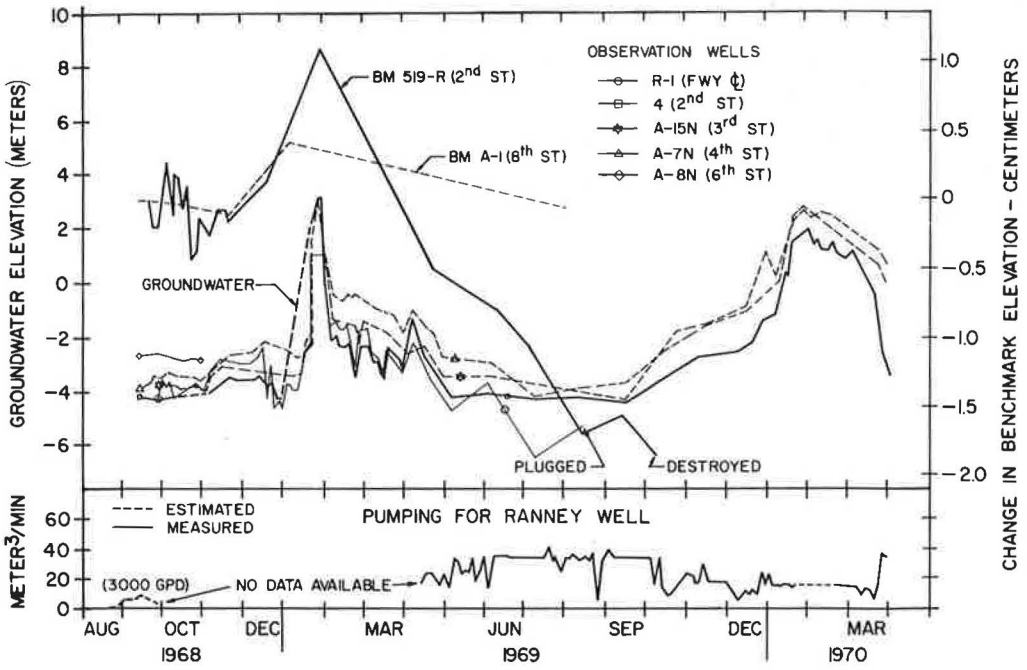

Figure 6. Settlement and groundwater elevation (Capitol Mall Loop).

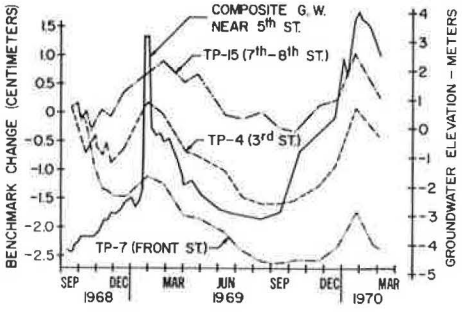

Figure 7. Drawdown test results.

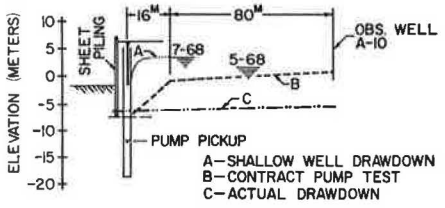

Figure 8. Settlement due to drawdown.

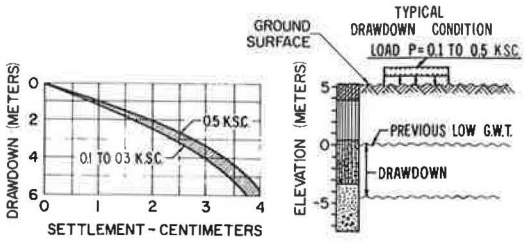

no complications, and construction continued with no further subsidence under adjacent structures.

SUMMARY AND CONCLUSIONS

1. Even when appropriate precautions are taken during construction dewatering operations, unforeseen events or conditions may occur and require deviation from planned construction.
2. Wide fluctuations in groundwater levels can result in ground subsidence.
3. Closer monitoring of groundwater during the initial stages of dewatering is recommended for future construction projects.
4. Subsidence could have been minimized on this project by pumping from closely spaced well points at a shallower depth.
5. If the original preliminary test data had not been misinterpreted, the probability of subsidence would have been more fully realized.
6. Valuable information could have been established early in the planning stages of this project from drawdown studies using deep wells pumping from a lower, more permeable stratum.
7. The specification requirements were appropriate; adequate stability of the river levee system and flood protection of Sacramento during high river stages were provided.

ACKNOWLEDGMENTS

This paper is based on data collected by the California Department of Transportation during construction of Interstate 5 in Sacramento, California. Information on the Ranney Well System was supplied by the Office of Architecture and Construction, State of California. The authors are indebted to the various persons who collected the test information and compiled the chronological data on this project. The opinions expressed in this report are those of the authors and not necessarily those of the California Department of Transportation.

REFERENCES

1. B. Lofgren. Subsidence Related to Groundwater Withdrawal. Proc., Geologic Hazards Conference on Landslides and Subsidence, California Resources Agency, Los Angeles, May 26 and 27, 1965.
2. K. Terzaghi and R. B. Peck. Soil Mechanics in Engineering Practice, 2nd Ed. John Wiley and Sons, Inc., New York.

Geologic Indicators of Catastrophic Collapse in Karst Terrain in Missouri

James H. Williams and Jerry D. Vineyard, Division of Geology and Land Survey, Missouri Department of Natural Resources, Rolla

Although the records of 97 catastrophic collapses in Missouri karst terrain have emphasized such man-made causes as dewatering, vibration, or water saturation, there is an underlying commonality of geologic features that offers insight into ways to avoid collapse problems in highways and other construction. Collapse events are more likely to occur in areas overlain by moderately thick residual soil, in losing valleys, and in wet seasons. Significant collapses have occurred where there was no indication of sinkholes or other typical karst landforms. Of the numerous collapses related to highway construction, most have involved upward stoping of residuum from underlying cavernous channels in carbonate bedrock, and have been triggered by constructional or operational activities that altered drainage conditions. Exploration for incipient collapses is costly and more effective in limited areas. Analysis of geologic indicators such as losing streams, relict karst landforms, and residuum type and thickness, as well as speleological data offer more cost-effective techniques to define target locales for subsequent detailed exploration. Initial exploration with a backhoe generally gives more useful near-surface data than drilling. Drilling is necessary, however, to validate evidence inferred by surface geologic indicators and geophysical methods such as fixed-depth resistivity and high-precision gravity surveys.

Both collapse and subsidence represent vertical settling of the land surface (1), but our interest is directed more to collapse. The unpredictability of collapse and its catastrophic mode of occurrence add a risk factor to all aspects of land use in karst terrain, whereas the gradualness of subsidence permits salvage or the repair of damage.

The records of collapse have emphasized man-related causes such as dewatering, vibration, or water saturation. However, there are a commonality of natural conditions and a history of surface failures involved with most collapse events. In Missouri, of the 97 catastrophic surface failures recorded since the 1930s, 46 can be attributed to some activity of man (Figure 1). Of these, water was a contributing factor to the 52 percent in which leaky utility lines and altered surface drainage conditions attributed to roads and other urban developments had weakened the overburden. Water saturation by impoundments was a primary cause of 22 percent, while 15 percent were due to dewatering, 7 percent to highway construction, and 4 percent to blasting. Most of the catastrophic failures caused by altered drainage have also involved roads and streets. Thus, road construction and use are directly or indirectly prominent contributors to collapse and subsidence in karst terrain. However, nearly all of these man-related surface failures occurred in regions where natural subsidence and collapse events were common.

Catastrophic failures are as apt to occur in broad, subsiding sinkholes as in karst terrain having closely spaced pinnacles of carbonate bedrock: The soil mechanics properties of the overburden are of more importance than the bedrock configuration in considering the likelihood of collapse versus subsidence. Catastrophic collapse in carbonate terrain can occur where there are no sinkholes. Thus, if one assumes that it will occur only in areas having well-defined sinkholes or broad areas of subsidence, some hazardous areas may be overlooked.

BACKGROUND

Through the years, general features have been given to aid in the identification of areas subject to subsidence and collapse. Foose (2) listed seven conditions that are common in areas of karst topography subject to collapse. He pointed out that there are few sinkholes where the overburden is less than 10 m (33 ft) thick, that the water table is usually below the overburden and the bedrock weathering irregular or pinnacled, and that there are often extensive cavernous openings and major structural elements in the underlying bedrock.

Vineyard and Williams (3) have cited 11 features that may foretell of collapse or subsidence in stream valleys developed in karst terrain. Generally, losing valleys with poorly graded alluvium, angular valley cross sections, and irregular valley gradients are indicative of areas subject to collapse events.

Aley, Williams, and Massello (4) have described seven diagnostic characteristics of karst terrain where catastrophic collapses, primarily those induced by construction of impoundments such as small lakes and sewage

Publication of this paper sponsored by Committee on Engineering Geology.

lagoons, but also some caused by changes in groundwater level, have occurred.

FACTORS IN CATASTROPHIC COLLAPSE AND SUBSIDENCE

Records of sinkhole collapse in Missouri are admittedly scanty and incomplete. Our mutual interest in the topic began in the early 1960s and peaked in the spring of 1973, an unusually wet season.

Alterations of soil moisture and groundwater account for most land surface failures in karst terrain in Missouri and elsewhere. The type of failure (subsidence or collapse) is partially related to the intensity and magnitude of the changes. The mechanical properties of the soil overlying the bedrock and the hydrologic characteristics of the region also affect the type of land surface failure. For example, 13 catastrophic collapses occurred in remote timbered areas of Missouri during a 2-month period in the spring of 1973. This was a period of sustained, abnormally high rainfall with precipitation 3 to 6 in higher than normal for those months. These failures were typical catastrophic collapses in karst terrain. The sinkholes were cylindrical, 12 to 18 m (36 to 60 ft) deep, and 6 to 7 m (20 to 25 ft) in diameter (Figure 2). They occurred on uplands and ridges, and in floodplains.

Although collapse or subsidence as a result of highway construction is not a principal cause of surface failure in karst terrain, when such failures occur the results can be serious in both monetary loss and danger to human life. The most notable collapse in Missouri that could be attributed directly to highway construction occurred in February 1966, in Pulaski County (3). While the surface collapse that permitted entry into an active cave system beneath the highway was caused by water discharge on the downstream end of a box culvert, there was an additional active collapse occurring in another part of the cave beneath the shoulder of westbound I-44. This part of the cave, mostly in residual soil, was enlarging upward as chert boulders and soil fragments fell from the roof. Other dome roofs in the cave system were inactive, but this one showed active roof failure; here traffic vibrations could be felt.

The most tragic of such incidents occurred in 1967 in Hannibal, Missouri. Small depressions formed during highway construction through a limestone formation that has a maze of caves had resulted in several small collapses. Three boys entered one of these openings and were never found. Several similar examples have occurred throughout Missouri. Of all the dangers in construction through karst terrain, these small and easily overlooked openings are the most lethal and yet the most subtle.

Such variables as loading, vibration, excavation, and fill changes of the landscape are not the primary causes of subsidence or collapse in highway construction. Rather, the important factors involve a number of minor alterations that culminate in changing the water regimen. The most serious example of the effects of the combination of many minor factors exists in the eastern Missouri Ozarks at Farmington. Here, at least 22 large catastrophic failures have occurred during the past 40 years within an 0.8-km (0.5-mile) radius. The failures have occurred under city streets, buildings, lawns, and in open grounds. These collapses are predominantly in the built-up portion of the city, and their rate has increased during the last 10 to 15 years.

The collapses are vertical-walled sinks, some 6 to 7 m (20 to 25 ft) in diameter and 9 to 12 m (30 to 40 ft) in depth. Dolomite bedrock, which underlies the region, may be exposed as pinnacles, and some water may be present. Exploration drilling has shown that the bedrock ranges from 3 to 4 m (10 to 20 ft) to more than 22 m (70 ft) beneath the surface. Areas of excessively thick soil cover and sink occurrences have developed along major joint trends. Collapse has been attributed to traffic vibrations, to rainfall, and to the concentrated water sources typical of a city with poor housekeeping procedures.

Mining and mine dewatering have extended to within 2 km (1.5 miles) of Farmington. However, collapses were recorded at least 30 years prior to the mining and have continued for 10 years subsequent to the completion of mining activities. Although deep mines exist in Missouri in areas subject to catastrophic collapse and continuous dewatering is required for mining, only minor surface effects have resulted. In other portions of the United States and in Africa mine dewatering has been a major cause of massive catastrophic collapse (5, 6, 7).

The description of collapses by Aley, Williams, and Massello (4) deals primarily with alteration of the landscape by man, especially changes of groundwater levels or variations in soil moisture. For the most part, these involved water impoundments and sewage lagoons. Some were attributed to drainage alterations caused by construction of early logging railroads.

Vineyard and Williams (8) have described a sinkhole near Lebanon, Missouri, in the western Ozarks as possibly being triggered by the Alaskan earthquake of March 27, 1964. A previously existing sink filled with loess was exposed on one edge of this sink. Recent work (9) has shown that loess of Yarmouth and Sangamon ages filled or partially filled sinks within this area. Thus, the intermittent collapse of sinks for more than 30 000 years emphasizes the persistence of construction problems in karst terrain. At least one catastrophic collapse in paleokarst in Mississippian limestone capped by Pennsylvanian and Pleistocene sediments has been recorded.

REGIONAL CHARACTERISTICS OF KARST SUBJECT TO SUBSIDENCE AND COLLAPSE

As described by Davies and LeGrand (10), karst provinces in the United States are numerous and diverse. Karst develops in bedrock of all ages. It can be found on the plains or in mountains and in rocks ranging from limestone to gypsum. Well-known karst areas include the Appalachians from Pennsylvania to Alabama; Kentucky; Indiana; Tennessee; the Ozarks of Missouri and Arkansas; the plateaus of Texas and eastern New Mexico; and the coastal plain of Florida. The most common cause of subsidence and collapse in these regions is the changing of water regimens.

The most common bedrock type in which karst develops is limestone or dolomite, but collapses have occurred in areas underlain by sandstone, such as those in the St. Peter Sandstone in Warren and Perry Counties, Missouri. Karst phenomena have been reported in many kinds of rock (11). Allen (12) has pointed out that collapse and subsidence can occur in materials ranging from loess to frozen gravel. Spectacular failures have been recorded in places where gypsum deposits are widespread, particularly in areas of Texas and Oklahoma (13, 14).

Although local karst features can be diagnostic in pinpointing areas having a greater likelihood of collapse and subsidence, these indicators may have limited regional usefulness since the various physical properties of karst are the result of local conditions.

Although cavern roof collapse in bedrock has been cited as a cause of catastrophic sinkhole formation (15, 16), no contemporary event that could be attributed directly

to this cause has been observed. While bedrock cavern roof collapse (breakdown) is a normal and regular occurrence in the cycle of cave development, when viewed in the perspective of time such events are rare. When dealing with caves in bedrock, it is more useful to determine the stability of cavern roofs (17) and perform necessary corrective measures.

The downward weathering of bedrock is a more common cause of collapse and subsidence than the upward mechanical failure of cave roofs. Most collapses have occurred where there is a moderately thick mantle of soil. In Missouri few collapses occur where the soil cover is less than 18 m (60 ft) thick (Figure 3). Collapses are rare where the soil thickness is less than 12 m (40 ft). A thick soil cover provides a setting that accelerates the chemical weathering of bedrock: Soil pH readings range from 4 to 5 in areas of thick soil cover but are near 7 in thin soil areas. Water can be produced

Figure 1. Causes of sinkhole collapse in Missouri, based on partial records gathered since 1930.

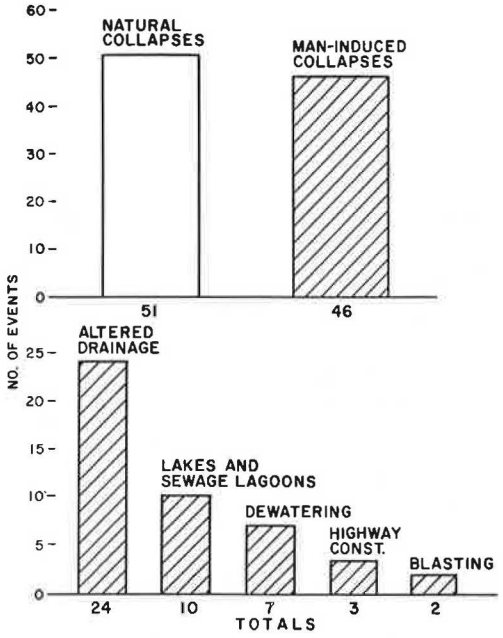

Figure 2. Typical sinkhole collapse common to uplands or valleys in Missouri.

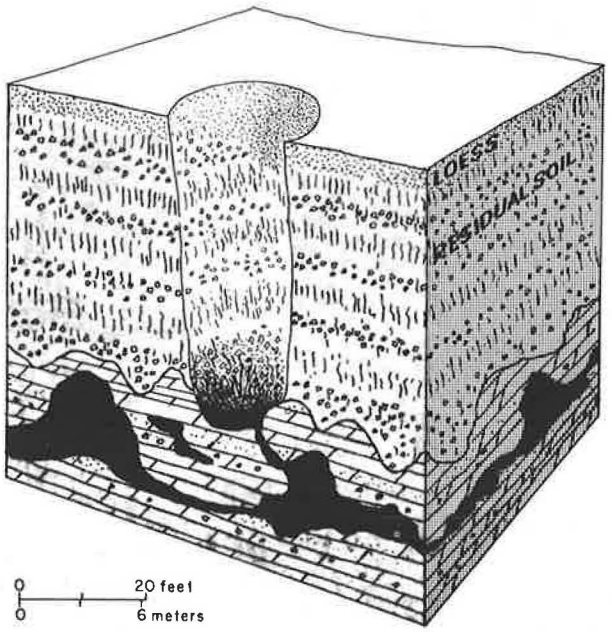

Figure 3. Locations of sinkhole collapses as related to thickness of residual soil.

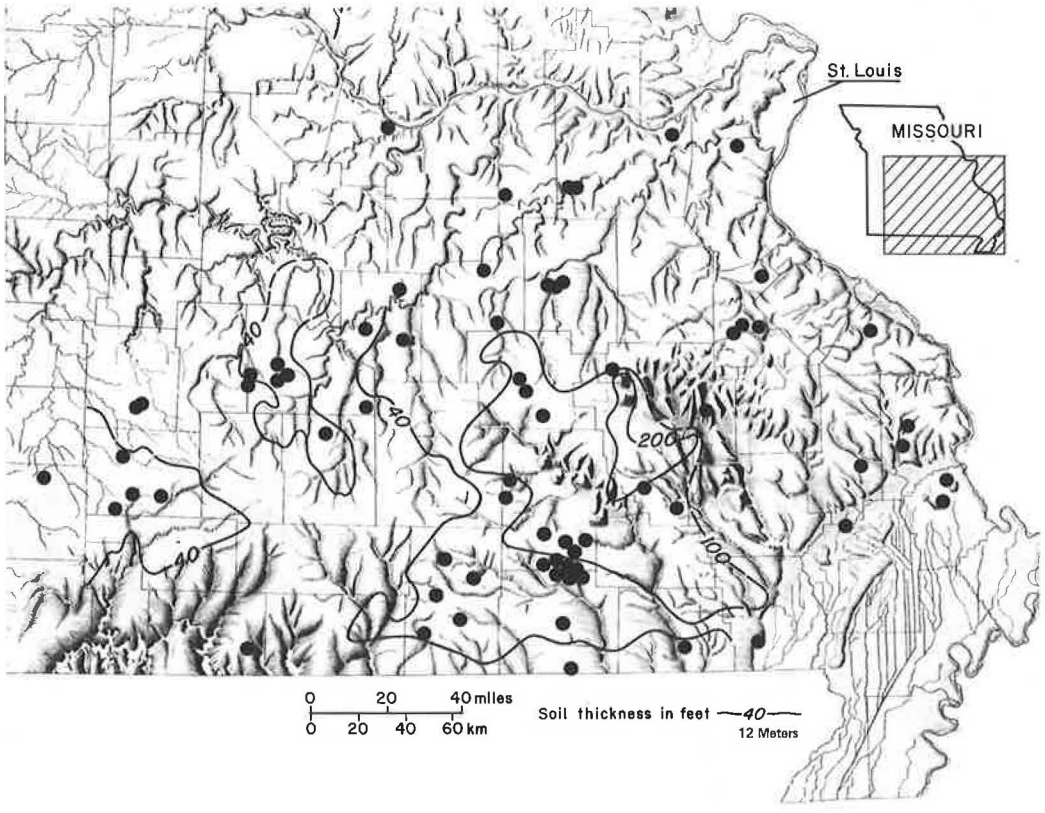

in minor quantities from wells drilled in thick soil deposits of the Ozarks. Thus, the initial phase leading to collapse is downward, not upward, weathering even though the actual collapse is triggered by mechanical upward stoping.

To understand the mechanics of such events it was necessary to study several sites where catastrophic collapses were imminent. A typical example is at the construction site for a theater at Fort Leonard Wood in the central Missouri Ozarks. Excavations for footings and utility lines were being made at the site, on an upland plateau setting, in soil derived from weathering of the Roubidoux formation, a sandstone, chert, and dolomite sequence. Investigation of a small hole exposed in a backhoe trench showed a vertical shaft 23 m (75 ft) deep, beneath the excavated trench, that was entirely in residual soil. The shaft had developed by gravity stoping from below until the roof was within 2 m (7 ft) of ground level. There was no evidence of sinkholes at the site or in the immediate area. Given favorable conditions of soil moisture, vibration, or other triggering mechanism, a catastrophic collapse would have occurred by the failure of the 2-m (7-ft) residual soil section. The resulting sinkhole would have had vertical sides. There was no access to underlying cave passages through which the soil material had been previously transported. Numerous collapses with the same characteristics (vertical walls in residual soil and the final remains of collapse material blocking access to cavern passages) have shown little evidence of the large volume of material that has been removed. Thus, a long period of time must be involved in the development of conditions that lead to a catastrophic collapse.

As examples of the variations in karst, and indicators of karst-related failures, consider three manifestations in Missouri. Well-defined sinkholes occur in some areas where 3 to 14 m (10 to 45 ft) of transported and residual soil cover slight to moderately weathered limestone and dolomite. In southern Missouri, solution and surface erosion have formed a pattern of coalesced sinks in an area of thick residual soil and deeply weathered bedrock. A third type of karst described as losing watershed terrain has thick residual soil over cavernous bedrock. Losing watersheds and streams are widespread, but few sinkholes exist in this region.

WELL-DEFINED SINKHOLE TERRAIN

Much of the limestone and dolomite countryside in the central, eastern, and southwestern portions of Missouri has karst development expressed as classical, well-defined sinkholes that drain into solution-enlarged cavities developed along joints and bedding planes. Cave passageways, while extensive in length, are not cathedral in size. Consequently, during periods of excess rain, the maximum storage capacity of the subsurface cavities is reached relatively quickly. Surface water flow can then be observed in stream channels flowing across limestone and dolomite terrain pockmarked with sinkholes. Soil cover averages 8 m (25 ft) in thickness.

The only area of well-defined sinkhole terrain in Missouri having a history of catastrophic collapse is in the southwest. Here, the soil cover ranges from 8 to 14 m (25 to 45 ft) in thickness. It is a residual clay having low plasticity (MH; A-7-5), and is characterized by retaining the relict fabric of the parent bedrock, a cherty limestone. The clay minerals have been classified as kaolinite (18), halloysite (19), and dehydrated halloysite (20). The structure of the soil is medium to coarse angular blocky: Individual soil peds have high dry strength and break with a brittle fracture when struck. Although the clay fraction commonly exceeds 60 percent, the soil is well drained. Macroscopic fractures and the relict bedrock patterns facilitate subsoil seepage (water movement).

The residual soil indicative of an area subject to land surface failure by catastrophic collapse has low in-place dry unit weight [1 to 1.2 g/cm^3 (65 to 75 lb/ft^3)]. While the strength of the individual peds is due to capillary forces and cohesion, the strength of a cave roof in the residual soil is due more to frictional forces between dry fragments of soil and angular chert gravel. Collapse of an upward-stoping dome is preceded by fall of these angular fragments from the roof. Surface failure usually does not occur, even under wetted conditions, until roof thickness is less than 2 m (7 ft). Catastrophic collapses are not common where transported or residual soils having mechanical properties described as CL to CH (A-6 to A-7-6) cover the bedrock.

The most common problems caused by construction are those that involve interference with surface runoff into sinkholes. The changing of spring discharges, usually on property owned by others, is a frequent result of this. Early recognition of these conditions in eastern Missouri prompted the relocation of Interstate 55 so that the highway would lie outside a karst area drained internally by sinkholes.

COALESCED SINKHOLE TERRAIN

A second type of karst development in Missouri is that of a moderately rolling landform of coalesced relict sinkholes, but few active, well-defined sinks. In this type of area preexisting, well-defined sinkholes have been destroyed by subsequent surface erosion and subsurface solution and subsidence. The soil cover averages 18 m (60 ft) in thickness.

The lack of obvious sinkhole development in these areas has led to unfortunate choices of location for several projects. Numerous dry lakes exist in the area. Garbage dumps have been placed in relict sinkholes. Several collapses have been caused by works such as sewage lagoon operation. Although these areas have not had many failures, where failures do occur they are catastrophic rather than gradual.

For the most part, the soil material preserves the fabric of the parent bedrock, a dolomite. It is predominantly a residual clay with properties similar to those previously described. Collapses have occurred on the uplands and in floodplains. Bedrock is exposed in some, but caves also exist entirely in the residual soil.

The most widespread area of karst in Missouri is in the central Ozarks. However, few classic karst landforms are found there. Rather, the region consists of deeply weathered, highly permeable residual soil, underlain by massive cavernous dolomite and dolomite-sandstone bedrock. Some of the larger springs in the United States are here but there are few sinkholes. Nevertheless, this area has had the greatest number of catastrophic sink collapses in Missouri. Some watersheds draining several hundred square kilometers may have flow only once every 2 years. These losing watersheds and streams are a type of landform in which numerous catastrophic failures have occurred. While attempts to delineate points of potential collapse have been unsuccessful, attempts to describe areas of greater likelihood of collapse have been successful. For example, no collapses have been recorded where soil thicknesses are greater than 65 m (200 ft). Collapses more frequently occur where soil thickness ranges from 12 to 30 m (40 to 100 ft).

Catastrophic collapses seldom occur on gaining watersheds or streams. They occur in losing watersheds or streams, and more commonly in the stream valleys of

Figure 4. Typical collapse sinkhole with relict bedrock structure in residuum.

these watersheds. It is rare for a natural collapse to occur where the groundwater level is below the level of the cave passageways in a floodplain.

The collapses are large, at least 6 m (20 ft) in diameter and usually 15 to 18 m (50 to 60 ft) in depth. They are sudden, and nearby residents usually describe the event as a thunderous, ground-shaking occurrence. Some occur only in residual soil, but the larger ones usually involve lower cave passageways in bedrock. Some activity by man is responsible for almost 50 percent of the catastrophic collapses we have documented. Usually, the soil of the sidewalls of the collapse has retained the fabric of the relict bedrock structure (Figure 4).

EXPLORATION PROCEDURES

Surface examination prior to the use of costly or time-consuming investigative tools is an important exploration procedure, as is the recorded history of collapse in local areas. Speleological investigations are becoming an increasingly important part of project site evaluations in Missouri. Data gathered during the past 10 to 20 years in the form of cave descriptions and maps are now sufficient in many areas to give considerable insight into the types and dimensions of subsurface karst features that may be expected. For example, caves in massively bedded cherty Mississippian limestone are prone to develop joint-controlled, vertical shafts in bedrock. Thin roofs of cherty residual soil are hazardous to construction activity, but few large natural collapses have been recorded in this setting. In contrast, caves in massively bedded Cambrian and Ordovician dolomites do not develop as many bedrock shafts, but vertical shafts are formed in the overlying thick mantle of residual soil. These shafts are enlarged upward by stoping, which is accelerated by vertical drainage through the permeable residual soil.

Topographic maps are the most cost-efficient method for initial evaluation of karst terrain. Losing watersheds and streams, sinkholes, and areas with only relict karst features have distinctive landform features. These may be local in character, but are nonetheless useful.

Close attention should be given to the surface and groundwater conditions of the area. The examination should not be limited to the right-of-way, but should include areas several kilometers distant. Hayes and Vineyard (21) have described procedures used to avoid changing shallow groundwater conditions as the result of US-65 construction near Springfield, Missouri. Undue changes of groundwater in this karst setting would have affected the highway as well as an important spring 5 km (3 miles) to the southeast.

Exploration tools that best reveal the fabric of the soil materials should be used. For example, some 1.3 km (4000 ft) of exploration backhoe trenches were dug in an area of proposed tailings ponds in karst terrain in southwestern Missouri. The local area had a history of collapses resulting from man-induced changes, particularly water impoundments. Backhoe exploration exposed the tops of several caverns that were being formed by upward stoping in the residual soil. Trench exploration should also be considered, particularly for construction projects that cross valleys known to be affected by karst conditions. The void diameter of cave domes that collapse is usually no more than 3 to 4 m (10 to 15 ft). Thus, numerous drillholes would be needed to locate such openings, and backhoe exploration may be less costly and permit a more precise evaluation of in-place soil materials.

Love (22) has found that fixed-depth resistivity traversing is a useful exploration technique to outline buried solution cavities. Shallow refraction seismic or expanding resistivity methods were less successful, due to problems of erratic time arrivals, particularly sudden increases in time of travel. Similar results have been in karst areas subject to collapse. Unfortunately, the data usually are insufficient to locate individual cavities. Refraction seismic data have been used to locate caves in massive dolomite bedrock in the foundation exploration of an Army Engineers dam site in eastern Missouri.

Bates (23), in a thorough study of techniques used for detection of subsurface cavities, concluded that airborne or remote sensing methods and seismic methods have limited possibilities of success. He concluded, however, that various electrical resistivity procedures usually have useful results, although their interpretation has been questioned. He recommends the modified Bristow method of electrical resistivity surveying for subsurface cavity exploration.

Several investigators have discussed the use of microwave radio studies in delineation of buried karst topography. This is based on the relation of soil moisture change to the cavity. Kennedy (24) concluded that detection was possible in most cases.

Gravity surveys (25) have been reported as useful in identification of near-surface cavities at Anchor Reservoir, Wyoming. An investigation using seismic methods at this same location by Godson and Watkins (26) has established that seismic data also provide a useful means of cavity delineation. Recently Omnes (27) has used high-precision gravity surveys to aid in the location of cavities. Applied gravity surveys have also been used.

The variations of soil moisture and groundwater conditions in areas of karst are frequently cited as common features. Thus, it would appear that use of thermal imagery could be an aid in delineation of sinkholes. Coker and others (28) have been successful in predicting a sinkhole collapse along a highway near Bartow, Florida, by this method. However, Harvey and others (29) were unsuccessful in attempting to outline potential collapse sites in a karst terrain of central and southwestern Missouri in this way. These investigators have been successful in locating losing watersheds and geologic fea-

tures that characterize areas subject to collapse. Stohr and West (30) also failed in their efforts to outline sinkholes by the use of thermal infrared imagery. They concluded that imagery was best used as a supplement to stereophoto interpretation rather than as a primary exploration tool. Their test area was in a karst region in the Valley and Ridge province of Virginia. Rinker (31) was able to locate active sinkholes in Puerto Rico with thermal infrared scanning equipment. However, these sinks were creating thermal anomalies by discharge of air from caves.

CONCLUSIONS

Geologic indicators such as we have described can be used to outline areas where sudden failure of the land surface by collapse may occur. However, experience has shown that current exploration techniques used to locate individual potential collapses are not cost-effective over large areas, and can be justified only for high-cost applications such as bridge foundations or buildings. For construction projects involving large areas such as highways, reasonable efforts should be made to reduce drainage modifications of both surface and groundwater regimens, because such changes are a major cause of catastrophic collapse. In some circumstances, even a minor route realignment would avoid an area or watershed subject to collapse events.

While a potentially serious threat to travel safety does exist in karst terrain subject to catastrophic collapse, the likelihood of such occurrences under a highway is rare. Thus, it may be difficult to justify detailed and costly subsurface exploration over large areas. Rather, geologic indicators such as those enumerated below and discussed elsewhere in this paper are more useful and cost-effective for engineering projects involving large areas. These indicators can be used to justify some route realignment and additional expenses in drainage control facilities, and also more detailed subsurface explorations for foundations of costly structures.

1. Collapses are more likely to occur in residual soil ranging in thickness from 12 to 30 m (40 to 100 ft).
2. Collapses are more apt to occur in residual soil retaining the fabric of the parent material; they are uncommon in colluvial deposits or in alluvium deposited by gaining streams.
3. Collapses are more likely to occur where the clay fraction has the low plasticity (MH; A-7-5), common to kaolinitic and halloysitic clays.
4. Collapses are not common in poorly drained surface soils even if this surface soil is underlain by other features typical of collapse indicators.
5. Collapses are more apt to occur in losing streams and watersheds than in gaining ones, and they are as common in the uplands or slopes as in the floodplains.
6. Sinkholes per se are not necessarily indicative of land surface failure by catastrophic collapse.
7. Collapses are more frequent in areas underlain by limestone, dolomite, and gypsum, but have been reported in other types of bedrock.
8. Cave systems developed along the soil-bedrock contact are common in areas having a history of land surface failure by collapse.
9. Cave passageways are periodically or continuously drained by cave streams.

REFERENCES

1. N. P. Prokopovich. Land Subsidence and Population Growth. Proc., 24th International Geological Congress, Montreal, Sec. 13, 1972, pp. 44-54.
2. R. M. Foose. Surface Subsidence and Collapse Caused by Groundwater Withdrawal in Carbonate Rock Areas. Proc., 23rd International Geological Congress, Prague, Vol. 12, 1968, pp. 155-166.
3. J. D. Vineyard and J. H. Williams. A Foundation Problem in Cavernous Dolomite Terrain, Pulaski County, Missouri. Proc., 18th Annual Highway Geology Symposium, Purdue Univ. Engineering Bulletin, Engineering Extracts Series 127, Vol. 51, No. 4, 1967, pp. 49-59.
4. T. J. Aley, J. H. Williams, and J. W. Massello. Groundwater Contamination and Sinkhole Collapse Induced by Leaky Impoundments in Soluble Rock Terrain. Engineering Geology, Series 5, 1972.
5. R. M. Foose. Sinkhole Formation by Groundwater Withdrawal, Far West Rand, South Africa. Science, Vol. 157, No. 3792, 1967, pp. 1048-1054.
6. R. M. Foose. Mine Dewatering and Recharge in Carbonate Rocks Near Hershey, Pennsylvania. Engineering Geology Case Histories, No. 7, 1969, pp. 45-60.
7. W. J. Powell and P. E. LaMoreaux. A Problem of Subsidence in a Limestone Terrain at Columbiana, Alabama. Alabama Geological Survey Circular 56, 1969.
8. J. D. Vineyard and J. H. Williams. A New Sink in Laclede County, Missouri. Missouri Mineral Industry News, Vol. 5, No. 7, 1965, pp. 69-71.
9. D. L. Rath. A Study of Middle to Late Quaternary Sediments in a Karst Trap. MS thesis, Univ. of Missouri—Rolla, 1975.
10. W. E. Davis and H. E. LeGrand. Karst of the United States. In Karst (M. Herak and V. T. Stringfield, eds.), Elsevier, New York, 1972, pp. 467-505.
11. J. Avias and L. Dubertret. Karstic Phenomena in Noncarbonate Rocks. In Hydrogeology of Karstic Terrains (A. Burger and L. Dubertret, eds.), International Association of Hydrogeologists, Series B, No. 3, 1975, pp. 31-40.
12. A. S. Allen. Geologic Settings of Subsidence. In Reviews in Engineering Geology (D. J. Varnes and L. Kiersch, eds.), Vol. 11, 1969, pp. 305-342.
13. G. Brune. Anhydrite and Gypsum Problems in Engineering Geology (abstract). Association of Engineering Geologists, Sacramento, 1964, p. 11.
14. W. E. Jameson and J. B. Schiel. Possible Man-Made Sinkholes at Southard, West-Central Oklahoma: A Case Study in Landscape Modification. Oklahoma Geology Notes, Vol. 35, No. 5, 1975, pp. 187-193.
15. W. E. Davies. Mechanics of Cavern Breakdown. Bulletin of the National Speleological Society, Vol. 13, 1951, pp. 36-43.
16. E. L. White and W. B. White. Processes of Cavern Breakdown. Bulletin of the National Speleological Society, Vol. 31, No. 4, 1969, pp. 83-95.
17. J. D. Landrum. A Foundation Investigation of Cherokee Cave Under I-55, City of St. Louis. Proc., 15th Annual Highway Geology Symposium, Rolla, Mo., 1964, pp. 81-89.
18. A. N. Alcott. Clay Mineralogy and Compaction Characteristics of Residual Clay Soils Used in Earthen Dam Construction in the Ozark Province of Missouri. MS thesis, Univ. of Missouri—Rolla, 1970.
19. W. J. Graham. The Effects of Structure on the Consolidation of Compacted Unsaturated Clay Soils. MS thesis, Univ. of Missouri—Rolla, 1969.
20. J. H. Williams. Classification of Surficial Materials. PhD thesis, Univ. of Missouri—Rolla, 1975.
21. W. C. Hayes and J. D. Vineyard. Environmental Geology in Town and Country. Missouri Geological Survey and Water Resources, Ed. Series 2, 1969.
22. C. L. Love. A Geophysical Study of a Highway Problem in Limestone Terrain. Materials and Research Department, California Division of Highways,

Sacramento, Research Rept. M.R. 642730.
23. E. R. Bates. Detection of Subsurface Cavities. Soils and Pavement Laboratory, U.S. Army Engineer Waterways Experiment Station, Vicksburg, Miss., 1973.
24. J. M. Kennedy. A Microwave Radiometric Study of Buried Karst Topography. Bulletin of the American Geological Society, Vol. 79, 1968, pp. 735-742.
25. G. P. Eaton. Extended Gravity Survey of Near-Surface Cavities in the Anchor Reservoir, Wyoming (abstract). Association of Engineering Geologists, Anaheim, California, 1968.
26. R. H. Godson and J. S. Watkins. Seismic Resonance Investigation of a Near-Surface Cavity in Anchor Reservoir, Wyoming. Bulletin of the Association of Engineering Geologists, Vol. 5, No. 1, 1968, pp. 27-36.
27. G. Omnes. Microgravity and Its Applications to Civil Engineering. TRB, Transportation Research Record 581, 1975, pp. 42-51.
28. A. E. Coker, R. Marshall, and N. S. Thomson. Application of Computer-Processed Multispectral Data to the Discrimination of Land Collapse (Sinkhole) Prone Areas in Florida. Proc., 6th International Symposium, Remote Sensing of the Environment, Willow Run Laboratory, Univ. of Michigan, Ann Arbor, 1969.
29. E. J. Harvey, J. H. Williams, and T. Denkel. Role of Remote Sensing in Studies of Groundwater-Surface Water Relationships in Missouri. U.S. Geological Survey (in press).
30. C. J. Stohr and T. R. West. Delineation of Sinkholes Using Thermal Infrared Imagery. Laboratory for Application of Remote Sensing, Purdue Univ., West Lafayette, Ind., 1974.
31. J. N. Rinker. Airborne Infrared Thermal Detection of Caves and Cave Crevasses. Photogrammetric Engineering, Vol. 41, No. 11, 1975, pp. 1391-1400.

Subsurface Cavity Detection: Field Evaluation of Radar, Gravity, and Earth Resistivity Methods

Lewis S. Fountain, Southwest Research Institute, San Antonio

Gravity, ground-penetrating radar, and earth resistivity profiling as subsurface cavity detection methods were experimentally evaluated and compared in three geological environments. Verification tests showed that the gravity measurements located large cavernous areas but did not detect mud-filled troughs; the radar detected air-filled cavities at depths up to 4.6 m (15 ft) at one site, but only penetrated 3 m (10 ft) with inconclusive results at a second site, and could not resolve 0.6-m (2-ft) diameter vertical cylindrical cavities at another. Earth resistivity measurements using a pole-dipole electrode arrangement located cavities at all sites, indicating targets at depths up to 25 m (80 ft). Both air-filled cavities, including vertical cylinders, and mud-filled troughs were detected by using the resistivity technique, which gave accurate depth and size resolution. A large mud-filled trough was detected at a 9-m (30-ft) depth that extended below 30.5 m (100 ft). The earth resistivity technique was capable of delineating the irregularities of the bedrock at the soil-rock interface.

Sudden collapse or subsidence above unknown cavities results in extensive damage and property loss; corrective action costs are very high and are not always positive cures. Public costs for damages, property losses, and accidents would be greatly reduced if subsurface earth structural conditions along transportation routes and at building construction sites were known prior to final planning and construction.

At present, the only reliable method for locating underground cavities is by direct drilling. However, the time and cost of this method, because of the close spacings required between borings in order to reliably detect and delineate all possible underground cavities, generally restrict its use.

The subsurface cavities of most concern for highway stability and construction are those located within 15 m (50 ft) of the surface. They may be of various sizes and shapes and may contain various amounts of air, water, or soil. Conventional geophysical exploration techniques have been of limited success in detecting these cavities because of size resolution difficulties and the low contrast between the various observable cavity manifestations and the typical background conditions.

The presence of possible underground cavities may sometimes be noted from subtle indirect surface anomalies by using airborne sensing techniques. According to Warren and Wielchowsky (1), who used infrared photography, thermography, and side-looking airborne radar to study subsidence and collapse problems in several carbonate terrains, the results of aerial surveys can be a good starting point for further geologic and hydrologic studies. Newton (2) also has found remote sensing (multispectral photography and infrared imagery) useful in delineating features such as water loss in streams, geologic structures, and vegetative stress related to sinkhole formation.

Lakshmanan (3) and Colley (4) have both reported successful cavity detection using gravity measurements. Neumann (5) has also successfully demonstrated that detection of solution cavities is possible by gravity measurements if extreme care is taken to make the measurements on a very tight grid and to carefully account for topographic features.

Ground penetrating impulse radar is one of the most recent methods to show promise for subsurface cavity detection (6, 7, 8, 9). Results have shown detection capability, although only to depths of about 2.4 m (8 ft) in moist clay-rich soils; possibilities appear to be good if instrumentation is improved.

A third detection method worth evaluating is earth resistivity measurements. Bristow (10) has described a search method using a pole-dipole electrode array that can resolve small underground cavities. He used a graphical data display technique that allowed a bearing to be obtained on the location of the cavity, as well as a prediction of its size and shape. Bates (11) has reported successfully detecting cavities using Bristow's method and modified the search procedure to allow more redundant data to be collected. Shallow voids have been detected by using a mobile equatorial dipole electrode array (12). The Federal Highway Administration has also evaluated subsurface cavity detection methods (13).

The three search methods selected for evaluation

Publication of this paper sponsored by Committee on Engineering Geology.

Notice: The Transportation Research Board does not endorse products or manufacturers. Trade (and manufacturers') names appear in this report because they are considered essential to its object.

(gravity surveys, ground penetrating radar mapping, and earth resistivity surveys) were tested at sites in Alabama and Florida. All sites were in areas where sinkhole formation is known to be active. At each site all surveys were made over a common base grid pattern composed of a rectilinear array of traverse lines equally spaced at a distance of 3 m (10 ft).

INSTRUMENTS USED AND SURVEY METHODS

Gravity Survey

A Lacoste model G gravity meter was used in the evaluation tests. It had a vernier scale permitting gravity readings to 10^{-8} m/s^2 (0.001 milligal). Repeatability is within 10^{-7} m/s^2 (0.01 milligal).

At the test sites the elevation of each grid point was measured to the nearest 30 mm (0.1 ft) so that elevation variations could be compensated for in the gravity readings. In the gravity survey a minimum of two measurements were made at each station, and the measured values then averaged. Gravity data analysis and display were in the form of a Bouguer gravity map compiled for each test site. Gravity values to 10^{-8} m/s^2 (0.001 milligal) and contour intervals of 2×10^{-7} m/s^2 (0.02 milligals) were plotted on these maps.

Radar Survey

A van-mounted radar system manufactured by Geophysical Survey Systems, Inc., that transmits a base-band voltage pulse of approximately 3 ns was used for the radar survey. The system radiates the quasi-gaussian pulse waveform into the earth by means of a broad-band antenna. The radiated signal is an electromagnetic transient having a frequency spectrum with -3 dB points at about 30 MHz and 120 MHz. The pulse peak power is 35 W with an average power of 5.2 mW. A two-way transmission loss of 110 dB, indicating the ratio of peak radiated power to the minimum detectable received signal power, is claimed for the system.

The radar field data were collected in a continuous profile by pulling the sled-mounted antenna assembly across the area of interest. Real-time profile data were displayed on an oscilloscope and on a graphic recorder, while simultaneously being recorded on a magnetic tape recorder for subsequent laboratory playback and analysis.

The data consist of signals reflected or scattered from subsurface anomalies such as voids. Depth to the target is indicated by the time delay between the pulse transmit time and the signal receive time.

Resistivity Survey

Instrument and Method

The earth resistivity surveys were made using a Keck model IC-69 earth resistivity instrument. The instrument is a dc system obtaining power for earth current from dry cell batteries having a total power of 630 V. Resistance could be measured over the range 0.001 to 1000 Ω, and the dial read to 1 part per thousand.

Porous-pot electrodes were used as the potential electrodes to eliminate problems and errors caused by galvanic action between metal electrodes and the soil. Since the contact resistance between the bottom of a porous-pot electrode and the ground can be as high as several thousand ohms, copper-clad steel electrodes were used as the current electrodes.

The main differences among the various electrical resistivity geophysical profiling methods are in the electrode array patterns used and in the manner in which the electrodes are moved or scanned over the area being surveyed. The methods of resistivity data analysis and interpretation also differ with the different electrode arrays. The pole-dipole array has had less use and shown the greatest potential for detecting underground cavities and predicting their depths and locations.

Pole-Dipole Earth Resistivity Electrode Array

Theory and Method

The pole-dipole electrical resistivity survey method is based on a four-electrode, straight-line array configuration in which the current sink electrode is located at infinity, and the potential electrodes are separated from one another by a fixed minimum distance proportional to the desired resolving power of the system. The potential electrode pair is located at various positions along the array line on both sides of the current source electrode as the means of vertically sounding the subsurface below the current source electrode. The current source electrode is moved ahead at suitable incremental distances to provide horizontal profile scanning. This array is illustrated in Figure 1.

In order that the equipotential surfaces be hemispherical and concentric about the source electrode, the sink electrode must be located at an effective infinity, which is generally 5 to 10 times the largest value of detection penetration depth of interest. The overlapping survey procedure can be described as follows for a typical 30-m (100-ft) penetration depth survey:

1. Place the current source electrode, C_1, as shown in Figure 1 at the first traverse station;
2. Place the current sink electrode, C_2, at a minimum distance of 150 m (500 ft) (5 r_2) and behind C_1 on a preestablished traverse line [having already decided that the maximum potential electrode scan distance from C_1 will be 30 m (100 ft)];
3. Place the potential electrodes, P_1 and P_2, at preestablished station markers 3 and 6 m (10 and 20 ft) respectively on the sink electrode side of C_1, and obtain the resistance reading;
4. Repeat step 3 above with the potential electrodes, P_1 and P_2, at preestablished station markers 6 and 9 m (20 and 30 ft) respectively on the sink electrode side of C_1, obtain this resistance reading, and continue the movement of the P_1 and P_2 electrodes in this manner until a final potential reading is obtained at 27 and 30 m (90 and 100 ft) from C_1;
5. Next, place the potential electrodes at preestablished 3-m (10-ft) interval station markers on the opposite side of C_1 from C_2, and obtain resistance readings at each station pair out to the 30-m (100-ft) limit, which completes the survey procedure for the first current station position for C_1;
6. Move C_1 up the traverse line a distance of 12 m (40 ft), and obtain resistance readings over the 30-m (100-ft) scan zones on each side of this current station; and
7. Repeat step 6 above until the complete traverse line is surveyed. This procedure gives four overlapping resistance readings for each 3-m (10-ft) spaced potential electrode pair station to a depth of more than 15 m (50 ft) as the survey proceeds.

Figure 1. Pole-dipole earth resistivity electrode array.

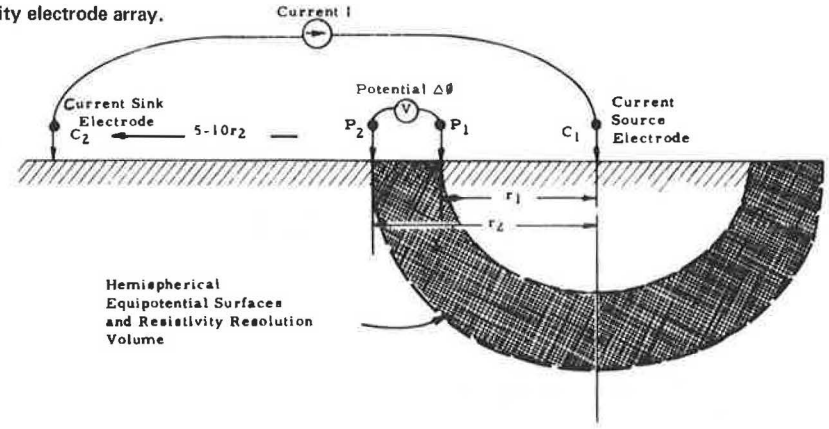

Figure 2. Sample resistivity traverse data sheet with anomalies marked.

PROJECT SwRI 14-4013 SITE 1-59 ALA
TEST NO #7 AREA 1-59, Birmingham, Alabama Grid Col. A
DATE 28 Oct. 74 Monday 12:50 to 1:05 pm CURRENT PROBE POSITIONS +280 (Std. 387+301 +1000
WEATHER CONDITIONS Fair Warm OBSERVER H&K

P-P (m)	P-P (m)	READING OHMS	FACTOR 10^3	RESISTIVITY OHM-CM x 10^3	INTERPRETATION
-3 to -6	4.5	2.67	3.83	10.23	
-6 to -9	7.5	0.969	11.49	11.11	
-9 to -12	10.5	0.550	22.98	12.64	
-12 to -15	13.5	0.386	38.30	14.78	
-15 to -18	16.5	0.394	57.45	22.64	
-18 to -21	19.5	0.365	80.43	29.36	Limestone
-21 to -24	22.5	0.138	107.25	14.80	
-24 to -27	25.5	0.048	137.89	6.62	Possibly Solution
-27 to -30	28.5	0.090	172.36	15.51	
3 to 6	4.5	3.01	3.83	11.53	
6 to 9	7.5	0.902	11.49	10.36	
9 to 12	10.5	0.511	22.98	11.74	Possibly Solution
12 to 15	13.5	0.388	38.30	14.86	
15 to 18	16.5	0.321	57.45	18.44	
18 to 21	19.5	0.275	80.43	22.12	
21 to 24	22.5	0.252	107.25	27.03	Limestone
24 to 27	25.5	0.203	137.89	27.99	
27 to 30	28.5	0.165	172.36	28.44	

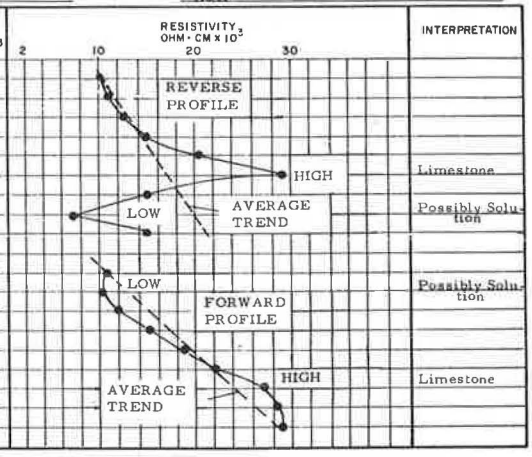

Note: 1 OHM-CM x 10^3 = 10Ω-m.

Figure 3. Graphical method of locating a resistivity anomaly.

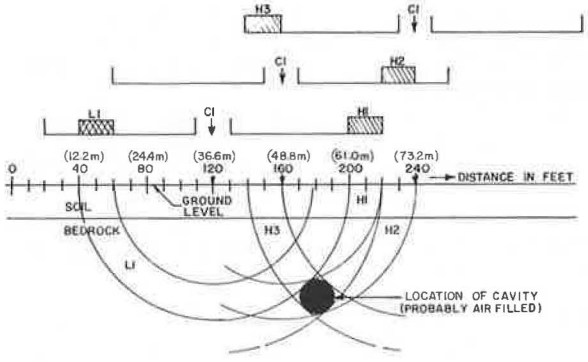

Graphical Data Analysis

The success of the graphical analysis used is largely achieved through the spatial redundancy of the field data; as a result target ambiguities and false interpretations are minimized, and improved cavity size and shape indications are derived.

It is best illustrated by examining a sample of the field data. The basic field measurements were recorded on specially prepared data forms. Figure 2 is a sample data sheet showing the recorded instrument readings and calculated resistivity values, and a graph of a derived resistivity profile. The first column on the data sheet is the potential-pair electrode distance from the current source electrode; the second column lists the distances from current electrode to the midpoint between the potential electrodes; the third column is the resistivity instrument reading in ohms; the fourth column is the geometrical factor required to calculate the apparent resistivity for the distances listed in the first column, using the resistances recorded in the third column; and the fifth column is the calculated value of the apparent resistivity.

The pole-dipole geometrical factor in column four is calculated from the relationship

$$KPD = 2\pi r_1 r_2/(r_2 - r_1) \qquad (1)$$

where r_1 and r_2 are the distances of the potential electrodes, P_1 and P_2, from the current source electrode, C_1, as illustrated in Figure 1. The basic principles on which the geometrical factor, KPD, is derived are discussed in many texts on geophysical prospecting (14).

Graphs of the forward and reverse apparent resistivity profiles are plotted on the data sheet as shown in Figure 2. Those points on the profiles that indicate resistivity perturbations above or below the average profile trends are next identified and marked for transfer to a scaled drawing used to graphically locate the anomalous underground resistivity structures.

An example of the scaled drawings used in the graphical analysis is shown in Figure 3 (this is not related to

the data of Figure 2). The distance along the ground surface representing the survey traverse is marked, and the consecutive positions of the current probe are shown by the arrows marked C_1. The perturbations interpreted from the forward and reverse resistivity profiles for each current electrode station, C_1, are denoted on the bracketed lines drawn above the ground surface line. The high resistivity anomalies in this example are labeled H1, H2, and H3. With a compass centered at each C_1 location on the ground surface line, arcs are drawn at distances representing the bounds of the high resistivity anomaly with respect to the current probe position to give the pairs of circular arcs labeled H1, H2, and H3, corresponding to the observed anomalies. The space where the three sets of arcs intersect is the graphically derived location of the underground structure responsible for the high resistivity perturbations. The single isolated low resistivity perturbation shown in the example of Figure 3 is insufficient to provide a graphical intersection with other low resistivity perturbations and is therefore ignored. A useful arbitrary guide for taking advantage of the redundancy of the overlapping field measurements is to require the intersection of a minimum of three arcs at a common location before that location is interpreted with any confidence as a probable underground anomaly. Moreover, as illustrated in Figure 3, the arcs are drawn only in the 90-deg sectors corresponding to either the forward or reverse profiles containing the perturbations being used. The reason for this is that the distortions of the equipotential lines (represented in a first order manner by the circular arcs) are very weak if the perturbing anomaly is located in the opposite 90-deg sector.

The pairs of arcs drawn for each resistivity perturbation describe not only the resistivity perturbations in the vertical plane along the ground traverse line but also apply, to some extent, to a three-dimensional spherical shell segment extending laterally on each side of the traverse line. It has been speculated by both Bristow (10) and Bates (11) that this apparent lateral field of view away from the traverse line is contained within an angle of about ±25 deg on each side of the traverse line relative to the source electrode location.

FIELD TEST RESULTS

Medford Cave Test Site, Reddick, Florida

The first test site selected is near Reddick, Florida, south of Gainesville. It has accessible air-filled underground limestone solution caverns known as Medford Cave. The underground caverns have rooms ranging in size to 12 m (40 ft) in width, and many smaller passages. These caverns are primarily in miocene Hawthorne formation limestone of the Alum Bluff group, but deeper portions are in eocene Ocala limestone. The subsurface cavities average about 3 to 9 m (10 to 30 ft) below the surface in most places, although some rooms reach depths down to 24 m (80 ft). The 0.9 to 1.8 m (3 to 6 ft) of soil on top of the limestone is sandy clay containing some phosphate and weathered limestone.

The first tests were made at this site because of its known features.

Gravity Survey

Major caverns were detected by their gravity anomalies, and a few other suspicious areas were noted. The survey consisted of gravimeter measurements at 563 stations on a 3-m (10-ft) rectilinear grid. The large near-surface joints and cracks that ran in many directions from the main rooms of the cavern caused a very high level of lithological noise that made recognition and interpretation of the gravity anomalies more difficult.

Two gravity depressions were noted near relatively large cavities. In these locations the cave was under about 6 m (20 ft) of overburden. In the vicinity of the largest of these anomalies, the roof thickness was 3 to 5 m (10 to 15 ft).

Figure 4 is an outline map of the cave with the cavity detection results of the three remote sensing methods superimposed. The principal gravity anomalies are the shaded areas designated by the symbols A through E. Anomaly A was not verified. Anomaly B was drilled, but no cavity was found. Anomaly C probably results from a composite effect of the large and small caves, with an added effect from the large sinkhole near the small cave. Anomalies D and E are over the main cave complex. A number of smaller gravity anomalies were noted but not verified. The unexplained anomalies were probably caused by cracks and fractures in the area.

Thus the gravity method detected only the largest room of the Medford Cave complex with any certainty. Negative drill verification results of gravity anomalies having magnitudes comparable to those associated with the large room tend to reinforce this uncertainty of detection.

Radar Survey

The final results of the radar survey are shown in Figure 4. There are six anomalous subsurface areas. One is located over the main room of the cave and another over one edge of it. The largest of these was verified to be the cave ceiling at a depth ranging from 3 to 4.5 m (10 to 15 ft). Another anomaly, that in the vicinity of row 16, column 24, in the lower left of Figure 4, is located near a fairly large room of the small cave section. The validity of this radar detection was not tested by drilling, but there is a fracture in the roof of this room that extends in the direction of the indicated radar anomaly. The small anomaly near row 13, column 20, is over a large fractured area, a part of which was a man-sized passage. The surveyed depth below surface in this area was about 5.5 m (18 ft). The large irregular anomaly centered on about row 12, column 15, was not drilled, but its depth below the surface as predicted by radar ranged from 2.7 to 5.2 m (9 to 17 ft). The other sensing methods showed no significant anomalies corresponding to this location. The curved radar anomaly centered at about row 16, column 12, was drilled at grid row 15.5, column 11. Rock was encountered at about 0.9 m (3 ft) and continued to a depth of 16 m (52 ft) where drilling stopped. The radar return was probably from the soil-limestone interface.

Thus the radar technique was fairly successful at the Medford Cave test site. It detected known or verified limestone cavities that were not more than about 4.6 m (15 ft) below the surface. It also detected soil-rock interfaces.

Earth Resistivity Survey

Eleven lines were traversed at the Medford Cave test site using the pole-dipole electrode array with very good results. Over 55 high resistivity anomalies were mapped and interpreted to show the depth below the surface of their tops and bottoms. A large number of these were located in the known cavernous area. There were also indications of deeper subsurface cavities in at least one location under the floor of another void. One of these was verified by the cave mapping crew, who found a deep narrow room approximately 3 m (10 ft) high located at a depth of about 17 m (55 ft) below the main room whose floor

Figure 4. Outline of Medford Cave with location of underground anomalies.

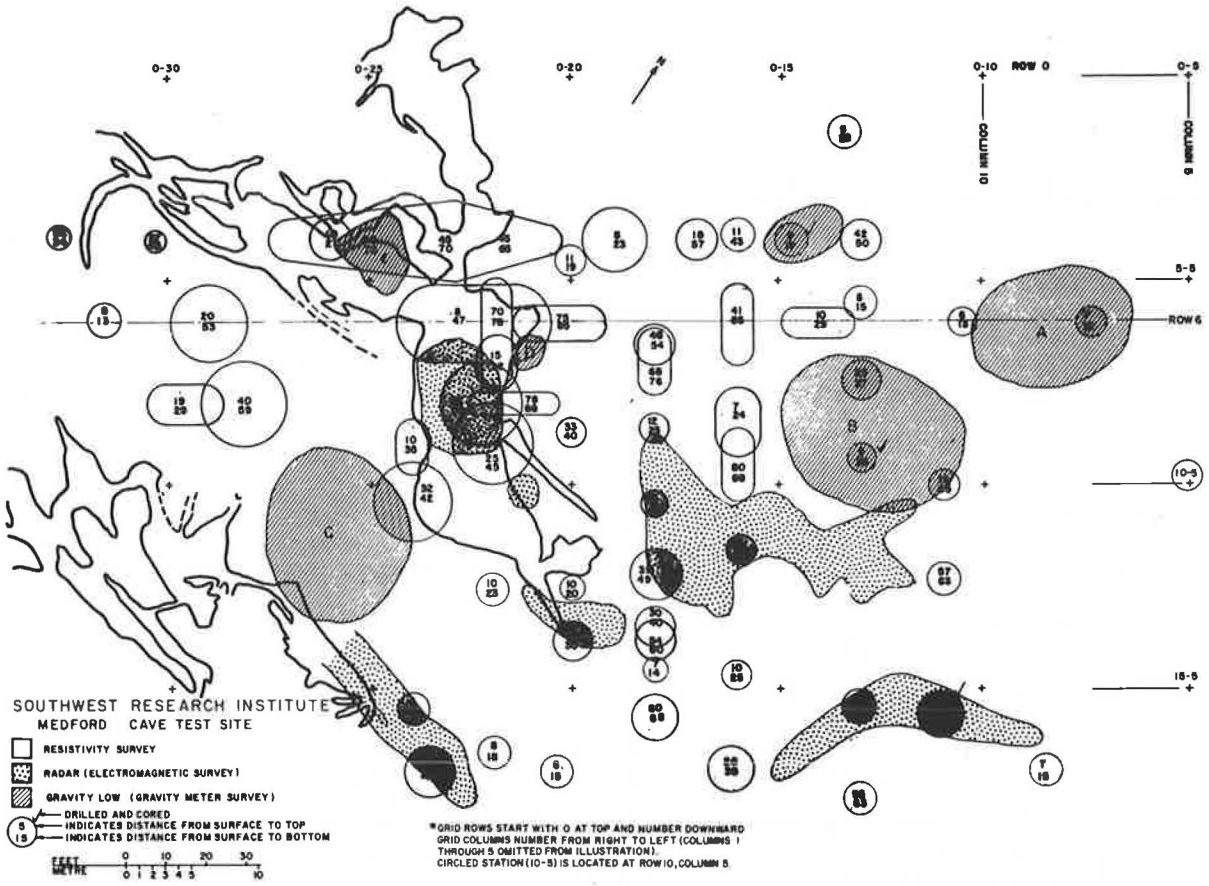

Figure 5. Pole-dipole resistivity survey results.

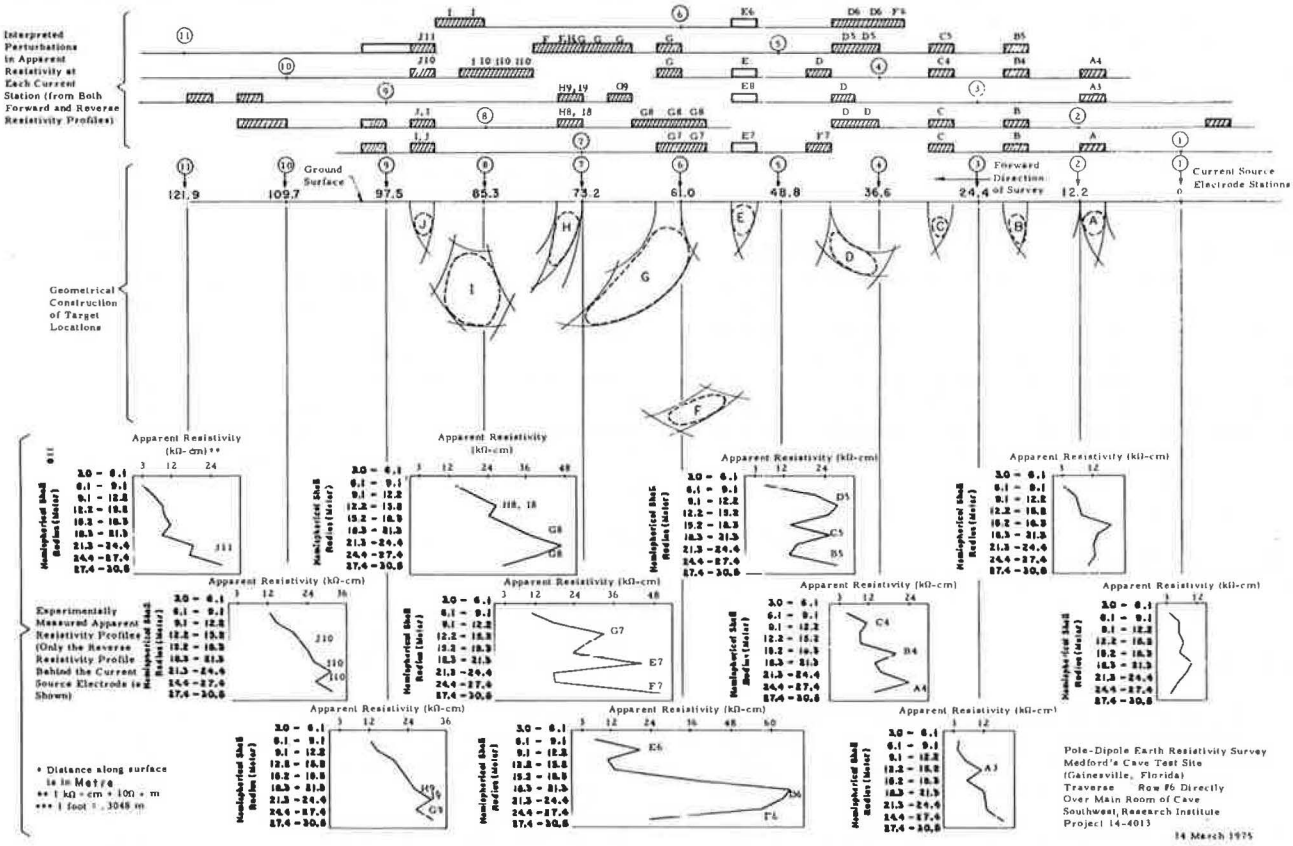

was at about 8 m (25 ft) below the surface).

The results of this survey are also indicated on the map in Figure 4. The high resistivity indications are plotted as if they were spheres or cylinders. The dimensions shown for these anomalies are the predicted top-to-bottom dimensions of the anomaly as derived from the graphical analysis. In order to determine more detailed horizontal extensions of these anomalies, it would be necessary to obtain resistivity readings on a much tighter survey grid.

Figure 5 is an example of pole-dipole resistivity results found for the Medford Cave test site. The data in this figure are from a traverse along row 6 crossing over the main room of the cave. The circled numbers along the ground surface line indicate the current source electrode positions analogous to those illustrated previously in Figure 1. The high resistivity perturbations that were interpreted for each current station are indicated by the shaded blocks in the upper section of the figure. The lower portion of the figure shows some of the measured apparent resistivity profiles from which the perturbations were derived. Only the reverse profiles are shown because of limited space.

Examples of high resistivity interpretations are identified on the lower section of the figure and labeled A3, A4, B4, etc. These high perturbations are transferred as arc radii to construct the subsurface zones of intersection as discussed earlier. The cavity labeled G in Figure 5 is the large cylindrical pattern on row 6 that extends from about column 20 to column 24 in Figure 4. The roof and floor of this cavity are interpreted to be at 2.4 and 14 m (8 and 47 ft) respectively.

Three test borings at the Medford Cave site did not encounter any additional cavities. Since an extensive verification description of most of the surveyed area could be obtained by mapping the cave, the various detection results indicated by the resistivity tests as well as by the other survey methods were verified by comparison with the cave map.

In summary, the resistivity survey was successful in detecting all of the known voids associated with the survey paths traversing the Medford Cave test site. Many more anomalies were detected away from the mapped cave area and are predicted to be inaccessible and unmapped voids in the limestone bedrock.

US-19, Chiefland, Florida

A second field test site selected in Florida was located about 3 km (2 miles) north of Chiefland, Florida, along US-19. This area is underlain by the Ocala limestone of the Jackson age in the eocene series. It is generally covered with sand from the ground surface to a depth of about 3 m (10 ft), then a fairly heavy clay-sand mixture (argillaceous sand) down to about 4.6 to 6 m (15 to 20 ft). Soft limestone is generally found below the surface soil materials, and harder limestone exists at greater depths.

Sinkhole cavities in this area are generally in the form of vertical pipes a meter or two (a few feet) in diameter, with depths of 15 m (50 ft) or greater. Some pipes are air filled, and some are filled with sand and clay mixtures.

The ground penetrating radar and earth resistivity systems were evaluated at this site.

Radar Survey

The results of the radar survey at US-19 showed good penetration depth but no verified cavity detection.

The electromagnetic attenuation constant of the earth materials for the radar signal frequency range was low enough in this area to permit two-way radar signal penetration to maximum depths of about 9 m (30 ft). The propagation velocity of the radar signals was high in the relatively dry sand, causing signal wavelengths to be too long to resolve the small diameter cavities of the area. A shorter wavelength radar system with an improved two-way transmission loss capability should find most of the piping in this Florida location.

Earth Resistivity Survey

Particularly good results were obtained from the resistivity survey. Only the high resistivity anomalies interpreted are shown on the map in Figure 6, although some low resistivity anomalies were found in the moist sandy clay at some depths. Seventy-eight high resistivity target areas were marked. Because of the limited time and availability of drilling equipment, only 13 verification holes were drilled. From these, five different air cavities were encountered. In those test borings where the predicted cavities were not found, it is possible that, because of the small diameters of the vertical-pipe voids, their localized position was missed by the drill.

The effectiveness of the pole-dipole resistivity survey technique is shown clearly by the verification tests at grid location C, 55.5. The resistivity anomaly interpreted at this location was a high perturbation having a graphically indicated depth range 2.7 to 6 m (9 to 21 ft). The drill tests showed a cavity extending from 4.3 to 8 m (14 to 25 ft). The absence of this cavity at positions of ±1.5 m (5 ft) on each side of the grid position indicated the limited lateral extent of the detected cavity. Similarly, another anomaly was interpreted as being due to a small cavity near the surface at grid location E, 28. Drill verification of this anomaly showed a 0.6-m (2-ft) diameter, 2.7-m (9-ft) deep pipe concealed under only 0.3 m (1 ft) of surface soil.

Interstate 59, Birmingham, Alabama

The third site selected is in Birmingham, Alabama. It is a portion of the highway right-of-way along Interstate 59 in the Roberts Industrial Park area located 73 m (240 ft) from a very large limestone quarry. The test area is mostly clay underlain by a light gray Ketona dolomite having an irregular surface at depths in the range 9 m (30 ft). Much of the layered limestone is badly cracked and fragmented, probably by shocks from explosive charges used in the quarry. The entire area is very active with sinkhole formations of various sizes and depths.

All three detection methods were evaluated at the I-59 test site, but only the earth resistivity method was successful in locating potential subsidence areas. The radar tests had extremely high electromagnetic attenuations in the soil, which resulted in limited depth penetration. The gravity survey was aborted because ground vibrations caused by the heavy traffic flow at close proximity to the measurement stations disturbed the instrument. (The traffic flow on I-59 at this location averages about 75 000 vehicles/d, a great many of which are large trucks.)

Earth resistivity measurements were successful at the site in spite of two problems encountered: (a) A chain link fence with ground-contacting metal parts ran parallel to the highway at distances of 3 to 21 m (10 to 70 ft) from the desired resistivity traverse lines; and (b) very strong dc earth currents, apparently caused by the various manufacturing processes in the area, such as a metal plating plant, caused occasional problems in making accurate resistivity measurements. At various times during the day these slowly varying earth currents were so strong that the survey was interrupted until after the disturbances stopped.

Although no subsurface voids were found, a total of

92 high resistivity anomalies were detected. Of this number, 33 were augered to rock and 2 were cored into the rock. All of the high anomalies except 2 were caused by the soil-bedrock interfaces, some of which were thin rock strata over mud-filled slots. The two high anomalies not caused by bedrock were interpreted as the base structures of highway light poles near the traverse path. In all of the verified subsurface anomalies, the predicted depth was correct to within 0.6 to 0.9 m (2 to 3 ft). A number of low resistivity areas were also detected, usually under a rock layer, indicating a mud- or solution-filled slot or trough.

Three areas having low resistivity anomalies beneath higher resistivity soil or rock were verified as having large mud-filled subsurface troughs. At one location a shattered rock layer about 0.6 m (2 ft) thick was encountered. The verification auger broke through the rock at about 10 m (34 ft) and hit very soft mud that extended to a depth greater than 31 m (100 ft) below the surface. A second mud-filled trough was verified in an area where clay soil was found to a depth of about 7.6 m (25 ft) and, below this very soft mud, to a depth greater than 19 m (63 ft). A third and a fourth mud-filled trough were found in the vicinity of an earlier construction fill in the 6 to 9-m (20 to 30-ft) and 9 to 15-m (30 to 50-ft) depth ranges respectively.

From the larger scale interpretations of the resistivity anomalies, there appears to be a deep mud-filled channel crossing under the highway in this area. Sinkhole activity was found on the north side of the highway where there is one sinkhole near the fence. Available drilling logs also showed soft mud to depths greater than 32.9 m (108 ft) in the median. On the south side of the highway there are a number of sinkholes at the surface along the right-of-way. These sinkholes have funnel type vents in the bottom where water enters underground, probably to feed larger underground channels extending under the highway.

With the additional knowledge of the average soil depth to bedrock, available from drilling logs of the area, the close-spaced resistivity data can be more readily interpreted and understood. Figure 7 shows the vertical

Figure 6. Underground anomalies as indicated by radar and earth resistivity survey techniques.

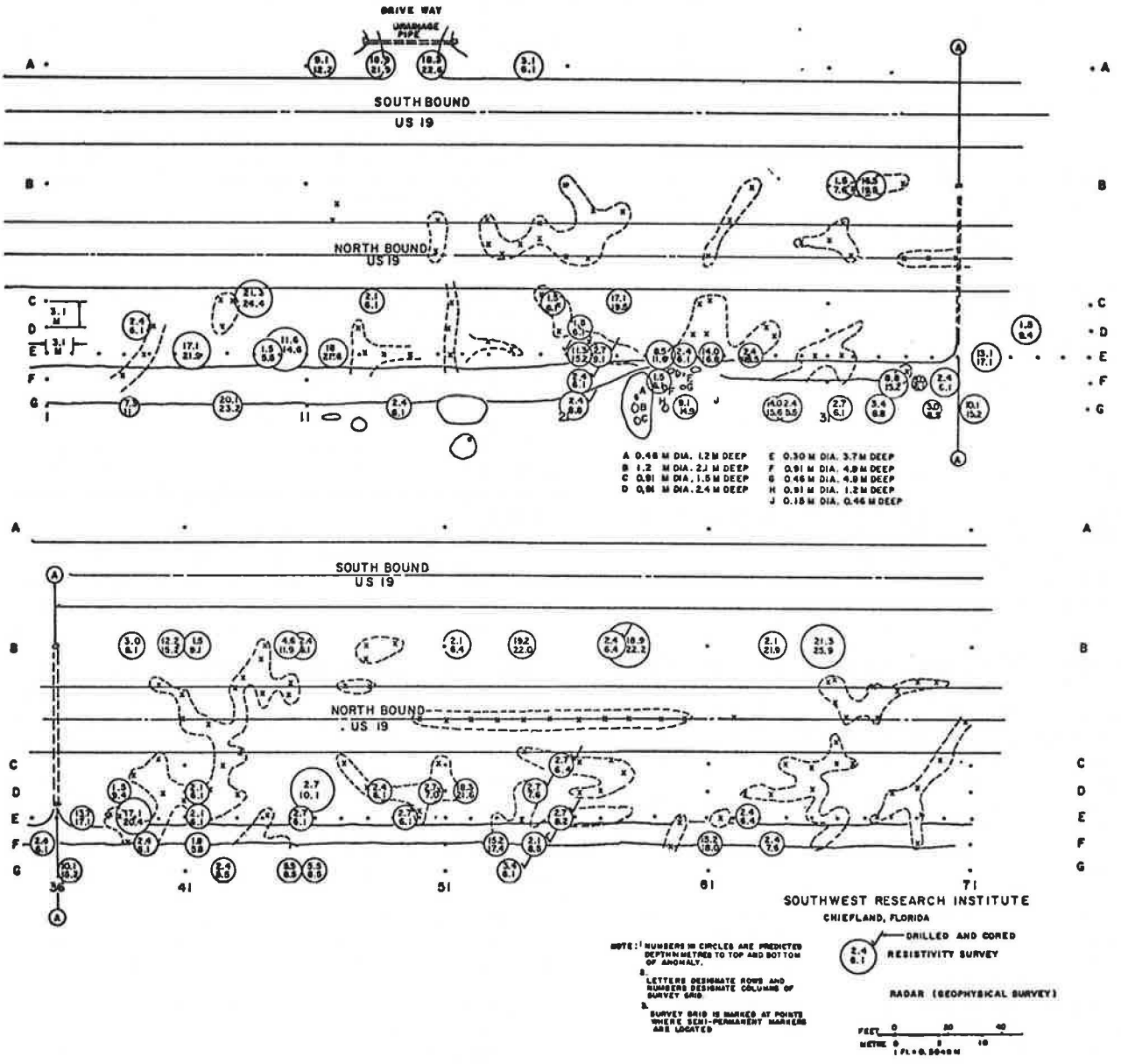

resistivity profile along one of the survey lines parallel to the highway about 3 m (10 ft) from the pavement. The results of seven of the test borings are also shown in this figure. The bars above the profile show the current electrode positions and the extent of the traverse on each side of the current electrode. The coded blocks on these lines show positions of high and low resistivity anomalies that enable geometrical constructions of the subsurface profile.

The three small air-filled cavities were very strong highs on the data graphs, but were not verified by drilling. The isolated low resistivity anomaly below the 119-m (390-ft) marker was not verified, but was a strongly indicated anomaly. The undulating bedrock surface caused resistivity highs whenever a near-surface peak, or pinnacle, was encountered during a traverse, and numerous test borings verified their presence.

In summary, the earth resistivity survey was successful at the I-59 site, revealing not only the soil-bedrock interfaces, but also the mud-filled slots, pinnacles, and overhangs that were verified by drilling. Enough information was gained from the data to allow a conceptual drawing of the complete subsurface profile structure to a depth of greater than 15 m (50 ft) along a survey line 305 m (1000 ft) long.

CONCLUSIONS

Three methods for surface detection of remote underground cavities were field tested and evaluated. These methods were: (a) gravity surveys, (b) electromagnetic subsurface profiling (ground penetrating radar), and (c) earth resistivity surveys.

The following conclusions are drawn from the results.

1. Earth resistivity surveys were the most successful of the three methods evaluated. The method was successful at three field sites having different geologic structures. Both the size and depth interpretations of the detected cavities were generally good (as verified by subsequent verification drilling). Voids were detected at depths up to 25 m (80 ft).

2. The information from close-spaced pole-dipole electrode resistivity surveys can be used with basic geological information to prepare vertical profiles of subsurface structures.

3. The currently available radar instruments can locate subsurface voids in some materials, but cannot reliably do so in all materials because of the variations in earth material electromagnetic properties. The penetration depth by the radar used in these tests ranged from a minimum of 2.4 to 3 m (8 to 10 ft) in Alabama to about 9 m (30 ft) in Florida. This radar could not detect 0.6 to 0.9-m (2 to 3-ft) diameter vertical pipe cavities in the low loss earth materials characteristic of the sinkhole environment investigated in Florida.

4. The gravity perturbations caused by many underground voids are large enough to be detected using commercially available gravimeters. These voids generally must be fairly large, and located at depths that do not exceed more than about one diameter of a roughly spherical equivalent cavity. This detection capability depends upon the density of the surrounding earth materials and their variations. In practice, a gravity anomaly of about 2×10^{-7} m/s^2 (0.02 milligal) can probably be detected, but this may be the state-of-the-art limit. Normal gravity variations caused by the variations in the subsurface structure are greater than 1×10^{-7} m/s^2 (0.01 milligal). The gravity survey had only marginal success on this program.

ACKNOWLEDGMENTS

The research covered by this report was sponsored by the Federal Highway Administration, U.S. Department of Transportation. Recognition is given to Francis X. Herzig

Figure 7. Vertical resistivity profile.

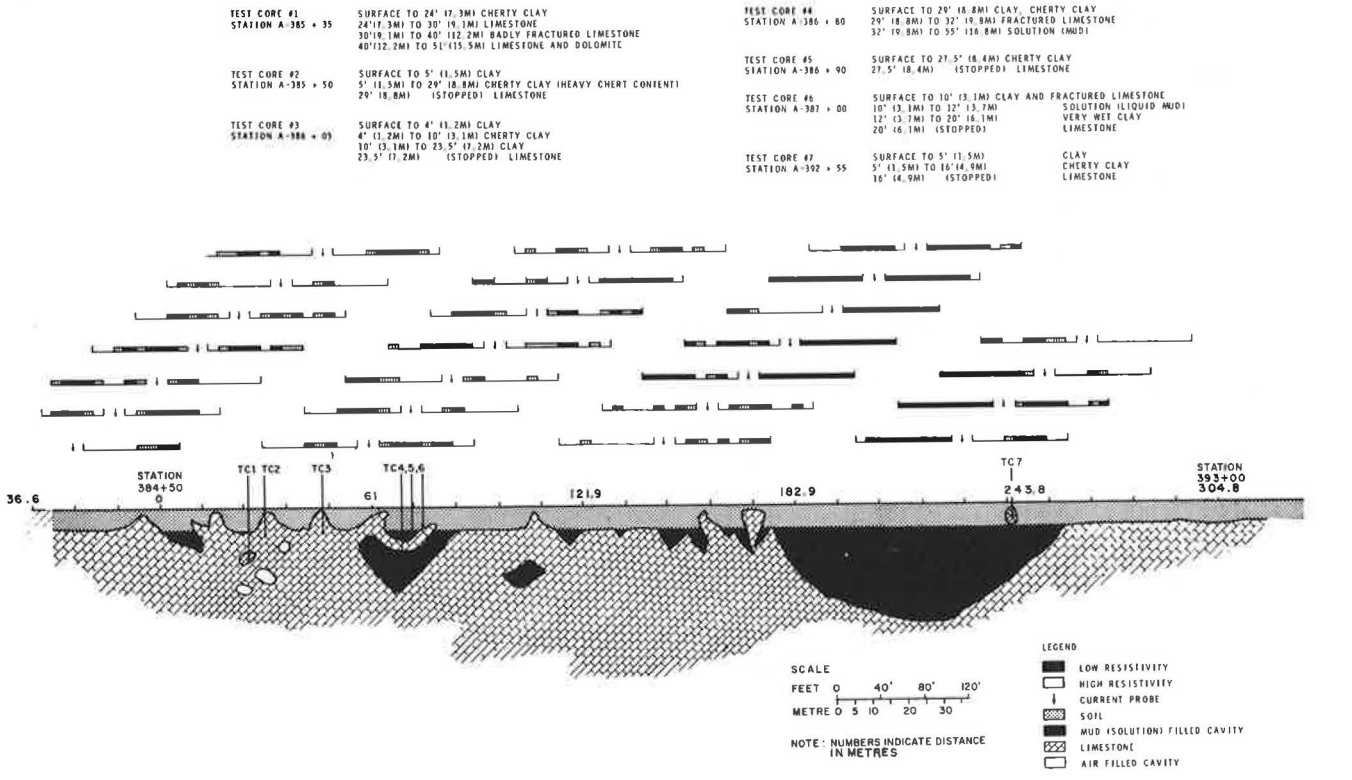

who assisted in all phases of the work and to Glenn T. Darilek who surveyed and mapped Medford Cave. Acknowledgment is given to Tidelands Geophysical Company and to L. L. Nettleton who did the gravity survey and data interpretation. Acknowledgment is also given to Geophysical Survey Systems, Inc., who made the radar surveys. The Alabama Highway Department and Florida Department of Transportation provided excellent support in field site preparation and in test verification drilling. Helpful suggestions were given by Thomas E. Owen of Southwest Research Institute and by James F. Koca of FHWA. Appreciation is expressed to Katherine W. Taylor, owner of the Medford Cave near Reddick, Florida, for allowing tests to be conducted on the property.

REFERENCES

1. W. M. Warren and C. C. Wielchowsky. Aerial Remote Sensing of Carbonate Terranes in Shelby County, Alabama. Ground Water, Vol. 11, No. 6, Nov.-Dec. 1973.
2. J. G. Newton, C. W. Copeland, and L. W. Scarbrough. Sinkhole Problem Along Proposed Route of Interstate Highway 459 Near Greenwood, Alabama. Alabama Geological Survey Circular 83, Univ. of Alabama, 1973.
3. J. Lakshmanan. Investigation of Underground Cavities With Electrical and Gravimetric Methods. Sols, March 1963.
4. G. C. Colley. The Detection of Caves by Gravity Measurements. Geophysical Prospecting, Vol. 11, No. 1, March 1963.
5. R. Neumann. High Accuracy Gravity—Recent Progress. Paper presented at the European Association of Exploration Geophysicists meeting, Paris, June 1972; abstracted in Geophysical Prospecting (Netherlands), Vol. 20, No. 3, Sept. 1972, p. 1733.
6. D. L. Moffatt and L. Peters. An Electromagnetic Pulse Hazard Detection System. Proc., North American Rapid Excavating and Tunneling Conference, June 1973, pp. 235-255.
7. L. T. Dolphin, R. L. Bollen, and G. N. Oetzel. An Underground Electromagnetic Sounder Experiment. Stanford Research Institute, Menlo Park, Calif.
8. J. C. Cook. Seeing Through Rock With Radar. Proc., North American Rapid Excavating and Tunneling Conference, June 1972, pp. 89-101.
9. Final Report on Subsurface Investigation of Mine Cavities. Geophysical Survey System, Inc.; Federal Highway Administration Purchase, June 1972.
10. C. Bristow. A New Graphical Resistivity Technique for Detecting Air-Filled Cavities. Studies in Speleology 1, Part 4, Dec. 1966, pp. 204-227.
11. E. R. Bates. Detection of Subsurface Cavities. U.S. Army Engineer Waterways Experiment Station, Vicksburg, Miss., Miscellaneous Paper S-73-40, June 1973; AD 762 538.
12. L. S. Fountain. An Exploratory Study of Soil Resistivity Measurements Using a Rolling Contact Electrode Array. Southwest Research Institute, Internal Research Project 14-9057, Final Technical Rept., April 1972.
13. L. S. Fountain, F. X. Herzig, and T. E. Owen. Detection of Subsurface Cavities by Surface Remote Sensing Techniques. Southwest Research Institute and Federal Highway Administration, Rept. FHWA-RD-80; NTIS, Springfield, Va., June 1975.
14. M. B. Dobrin. Introduction to Geophysical Prospecting, McGraw-Hill, New York, 1960.

Part 2
Moisture and Frost Actions and Classification

Mathematical Model for Predicting Moisture Movement in Pavement Systems

Barry J. Dempsey and Atef Elzeftawy, Department of Civil Engineering, University of Illinois at Urbana-Champaign

A comprehensive moisture model for predicting moisture conditions in pavement systems, based on the Philip and de Vries equations for nonisothermal moisture movement and heat conduction, was developed. By using numerical methods, the implicit finite difference approximations to the moisture movement and heat-transfer equations were programmed for computer solution. Validation studies indicated that the moisture model could be used to accurately predict isothermal moisture conditions in pavement systems. The model was also used to show the relative influence of nonisothermal conditions on pavement moisture content. The model was applicable to a wide range of boundary conditions and could be used with climatic input data to predict the moisture-temperature regime in pavement systems.

The behavior of pavement systems in response to moisture changes, especially with reference to the mechanisms of moisture movement and the consequences of such moisture changes, has been widely studied. The chief task is that of quantitatively and qualitatively predicting moisture movement and equilibria in pavement systems at any particular place, depth, and time.

The dominant factor influencing space-moisture conditions in pavement systems is climate. Other factors are permeability through the pavement profile, the type of ground cover and surrounding vegetation, the local topography, surface runoff from the pavement, drainage conditions, water table location, and pavement edge conditions. Low and Lovell (1) have presented a generalized concept of the sources of moisture in pavement systems (Figure 1).

Moisture movement and equilibria in soils have been major concerns in the field of soil science and agriculture for some time (2, 3, 4, 5, 6), but only in recent years have investigators (7, 8, 9, 10) attempted to analyze moisture conditions in pavement systems. Thus, this research has the following objectives:

1. To develop, based on climatic factors, a theoretical model for predicting moisture movement and equilibria in pavement systems; and
2. To validate the moisture model by means of available laboratory data.

Publication of this paper sponsored by Committees on Subsurface Drainage and Frost Action.

FLOW IN SOIL-WATER SYSTEMS

Darcy's Law

Analysis of soil-water flow systems is a highly empirical science based almost entirely on the universality of an empirically derived statement, known as Darcy's law, that has the following general differential form:

$$q = -K\nabla H \quad (1)$$

This law states that the rate of flow of water, q, in any direction in a porous medium is proportional to the change in the hydraulic potential H. The hydraulic conductivity, K, is the proportionality constant for flow.

The symbols used in all equations are defined as

- a = volumetric air content (cm^3/cm^3)
- C = volumetric heat capacity ($cal/cm^3/C$)
- D_Θ = isothermal moisture diffusivity (cm^2/s)
- D_T = thermal moisture diffusivity ($cm^2/s/C$)
- $D_{\Theta liq}$ = isothermal liquid diffusivity (cm^2/s)
- $D_{\Theta vap}$ = isothermal vapor diffusivity (cm^2/s)
- D_{Tliq} = thermal liquid diffusivity ($cm^2/s/C$)
- D_{Tvap} = thermal vapor diffusivity ($cm^2/s/C$)
- D_{atm} = molecular diffusion coefficient of water vapor in air (cm^2/s)
- g = acceleration due to gravity (cm/s^2)
- H = total water potential (cm)
- h = capillary potential (cm)
- h_o = relative humidity
- K and K_Θ = unsaturated hydraulic conductivity (cm/s)
- L = heat of vaporization (cal/g)
- q and Q = water flux (cm/s)
- Q_a = heat flux resulting from long-wave radiation emitted by the atmosphere ($cal/m^2/h$)
- Q_c = heat flux resulting from convection heat transfer ($cal/m^2/h$)
- Q_e = heat flux resulting from long-wave radiation emitted by the pavement surface ($cal/m^2/h$)

Q_g = heat flux into the pavement (cal/m²/h)
Q_h = heat flux from transpiration, condensation, evaporation, and sublimation (cal/m²/h)
Q_i = heat flux resulting from incident short-wave radiation (cal/m²/h)
Q_r = heat flux resulting from reflected short-wave radiation (cal/m²/h)
R = gas constant for water vapor (erg/g/C)
T = temperature (C)
t = time (s)
x and y = horizontal coordinates (cm)
z = vertical coordinate (cm)
Z = water gravity term (cm)
α = tortuosity factor for diffusion of gases in soils
β = g/cm³/C
γ = temperature coefficient (C^{-1})
Θ = volumetric water content (cm³/cm³)
λ = thermal conductivity (cal/cm/s/C)
ν = mass flow factor
ρ = density of water vapor (g/cm³)
ρ_μ = density of liquid water (g/cm³)
∇ = differential operator

In terms of the x, y, and z coordinates Darcy's law is expressed as follows:

$$q_x = -K_x(\partial H/\partial x) \quad (2)$$

$$q_y = -K_y(\partial H/\partial y) \quad (3)$$

$$q_z = -K_z(\partial H/\partial z) \quad (4)$$

The hydraulic conductivities K_x, K_y, and K_z in equations 2, 3, and 4 respectively may or may not be equal. If they are all equal, the porous medium is isotropic; if they are not, it is anisotropic. [Childs (11) has indicated that equations 2, 3, and 4 are valid for anisotropic porous media only if x, y, and z are the principle axes of the medium with respect to hydraulic conductivity.]

Darcy's law, although originally conceived for saturated flow only, has been extended by Richards (12) to unsaturated flow. This equation, in which the conductivity is a function of the matrix suction head, is expressed as follows:

$$q = -K_\Theta \nabla H \quad (5)$$

In equation 5, K_Θ is a function of the unsaturated water content and ∇H is the hydraulic head, which is a function of the suction head and the gravitational head as follows:

$$H = h + Z \quad (6)$$

Equation 5 has been found to be valid for unsaturated flow by Childs and Collis-George (13) and Kirkham and Powers (14), and for nonsteady flow by Rogers and Klute (15).

Transient Flow

The mathematical laws necessary for consideration of transient flow systems are the extension of Darcy's law to unsteady flow systems and the principle of the conservation of matter. The equation of continuity, which is a statement of the law of conservation of matter, can be written as follows:

$$\partial\Theta/\partial t = \nabla \cdot (-K_\Theta \nabla H) \quad (7)$$

Since the total head is equal to the sum of the pressure head and the gravitational head (equation 6), equation 7 can be written as follows for one-dimensional transient moisture flow in the vertical direction:

$$\partial\Theta/\partial t = \partial[K_\Theta(\partial h/\partial z)]/\partial z + (\partial K_\Theta/\partial z) \quad (8)$$

or

$$'\partial\Theta/\partial t = \partial[D_\Theta(\partial\Theta/\partial z)]/\partial z + (\partial K_\Theta/\partial z) \quad (9)$$

In equation 9, D_Θ is the soil-water diffusivity, and it is equal to $K_\Theta(\partial h/\partial\Theta)$. A detailed description of the derivation of the diffusivity and hydraulic conductivity terms is presented elsewhere in this Record.

Simultaneous Flow

The flow equations that have been considered thus far do not include the influence of solutes or temperature gradients on moisture movement. Hillel (16) has discussed simultaneous water and solute movement in soils, and this area will not be considered further. However, in pavement systems the simultaneous movement of heat and water is a common occurrence, and very important to the development of design methodologies to resist the influence of climatic effects.

The fact that temperature gradients can induce water movement in soils has been generally known for the last 50 years. Studies of the relative importance and interaction of thermal and suction gradients in transporting soil moisture have been made by Hutchinson, Dixon, and Denbigh (17), Philip and de Vries (18), Taylor and Cary (19, 20), Cassel (21), Cary (22), Hoekstra (23), and Jumikis (24). Taylor and Cary (19) applied the theories of irreversible thermodynamics to the study of the transport of water, heat, and salts through soil systems to develop a linear flow equation for each component of the soil system. This equation has the following general form:

$$J_i = \sum_{k=1}^{n} L_{ik} X_k \quad (10)$$

In equation 10, J_i represents the mutually interacting fluxes resulting from forces such as diffusion, temperature, and pressure. The term L_{ik} represents the transmission coefficients, such as the diffusion coefficient, hydraulic conductivity, and thermal conductivity, of the various fluxes and n is the number of driving forces.

From a mechanistic approach, Philip and de Vries (18) developed the following equation for water movement under combined moisture and temperature gradients:

$$Q = D_\Theta \nabla\Theta + D_T \nabla T + K_\Theta \quad (11)$$

In equation 11, Q is the net water flux, D_Θ is the isothermal moisture diffusivity, $\nabla\Theta$ is the moisture content gradient, D_T is the thermal moisture diffusivity, and ∇T is the temperature gradient. The terms D_Θ and D_T are made up of two components each, one for vapor flow and one for liquid flow. The term K_Θ is the gravity term.

Cassel (21) has compared his experimental results to the predictions made by the use of Philip and de Vries and Taylor and Cary models and, in general, obtained better results from the Philip and de Vries theory.

DEVELOPMENT OF A MATHEMATICAL MOISTURE MODEL

In studies of moisture movement and equilibria, experimental and empirical relations will often be inaccurate and impractical because of changing climatic conditions

that will affect the pavement systems. Formal mathematical procedures based on thermodynamic principles and incorporating the necessary daily environmental boundary conditions of a given geographical area are needed.

Several investigators (18, 25, 26, 27, 28, 29) have proposed mathematical formulas based on thermodynamic principles for predicting moisture movements caused by nonisothermal and isothermal conditions. In these formulas the important liquid and vapor diffusivity parameters for defining the potential that causes moisture movement are expressed quantitatively in terms of soil properties and soil suction.

Klute (25) and Selim (27) have developed reasonable models for predicting moisture movement in soils subjected to isothermal conditions. These models are based on finite difference solutions to the differential equations for one-dimensional and two-dimensional moisture movement. Richards (26) has been successful in using computer methods for predicting the time-space moisture conditions in pavement systems subjected to isothermal conditions in a two-dimensional model. Lytton and Kher (28) have developed a model to predict moisture movement in expansive clay subgrades. They analyzed only the isothermal case but used both one- and two-dimensional programs and validated the model by a field study.

However, the moisture movement theory of Philip and de Vries (18) provides the most comprehensive basis for the development of a moisture model to predict transient flow in pavement systems. By differentiating equation 11 and applying the continuity requirement, the general partial differential equation describing moisture movement in porous materials under combined temperature and moisture gradients can be stated as follows:

$$\partial\Theta/\partial t = \nabla \cdot (D_T \nabla T) + \nabla \cdot (D_\Theta \nabla\Theta) + (\partial K_\Theta/\partial z) \quad (12)$$

In equation 12 the thermal diffusivity, D_T, has two components, which can be expressed by the following equation:

$$D_T = D_{Tliq} + D_{Tvap} \quad (13)$$

Similarly, the moisture diffusivity, D_Θ, has two components as follows:

$$D_\Theta = D_{\Theta liq} + D_{\Theta vap} \quad (14)$$

The liquid diffusivities are the more important at high moisture contents, while the vapor diffusivities are the more important at low moisture contents (18).

The equation describing heat transfer is

$$C(\partial T/\partial t) = \nabla \cdot \lambda \nabla T - L\nabla \cdot D_{\Theta vap} \nabla\Theta \quad (15)$$

Equation 15 is similar to that used by Dempsey (30) and Dempsey and Thompson (31) to develop a heat-transfer model for predicting temperatures and evaluating frost action in multilayered pavement systems.

Equations 12 and 15 are the basic equations used to describe moisture movement and heat transfer in the mathematical moisture model.

Finite Difference Approximation for Water Movement and Heat-Transfer Equations

In the moisture model the water flow equation (equation 12) and the heat-transfer equation (equation 15) are nonlinear second-order parabolic partial differential equations. Since exact solutions to nonlinear equations are difficult and sometimes impossible to obtain, numerical methods were used to develop the model.

The numerical solutions to equations 12 and 15 are obtained by first expressing them as finite difference approximations. The three main types of methods commonly used to provide finite difference approximations are the fully implicit, fully explicit, and implicit-explicit methods. The moisture model was developed by using the implicit finite difference approximation (Figure 2). This method is always stable. The implicit finite difference approximation of the water flow equation (equation 12) can be expressed as follows for the one-dimensional case:

$$\begin{aligned}(\Theta_i^{n+1} - \Theta_i^n)/\Delta t = {} & [D(T_{i+\frac{1}{2}}^{n+\frac{1}{2}})(T_{i+1}^n - T_i^n)]/(\Delta z)^2 \\ & - [D(T_{i-\frac{1}{2}}^{n+\frac{1}{2}})(T_i^n - T_{i-1}^n)]/(\Delta z)^2 \\ & + [D(\Theta_{i+\frac{1}{2}}^{n+\frac{1}{2}})(\Theta_{i+1}^{n+1} - \Theta_i^{n+1})]/(\Delta z)^2 \\ & - [D(\Theta_{i-\frac{1}{2}}^{n+\frac{1}{2}})(\Theta_i^{n+1} - \Theta_{i-1}^{n+1})]/(\Delta z)^2 \\ & - [K(\Theta_{i+\frac{1}{2}}^{n+\frac{1}{2}}) - K(\Theta_{i-\frac{1}{2}}^{n+\frac{1}{2}})]/\Delta z \end{aligned} \quad (16)$$

Similarly, the finite difference approximation for the heat-flow equation (equation 15) can be expressed as follows for the one-dimensional condition:

$$\begin{aligned}[C(T_i^{n+1} - T_i^n)]/\Delta t = {} & [\lambda(T_{i+\frac{1}{2}}^{n+\frac{1}{2}})(T_{i+1}^{n+1} - T_i^{n+1})]/(\Delta z)^2 \\ & - [\lambda(T_{i-\frac{1}{2}}^{n+\frac{1}{2}})(T_i^{n+1} - T_{i-1}^{n+1})]/(\Delta z)^2 \\ & - L[D_{\Theta vap}(\Theta_{i+\frac{1}{2}}^{n+\frac{1}{2}})(\Theta_{i+1}^n - \Theta_i^n)]/(\Delta z)^2 \\ & - L[D_{\Theta vap}(\Theta_{i-\frac{1}{2}}^{n+\frac{1}{2}})(\Theta_i^n - \Theta_{i-1}^n)]/(\Delta z)^2 \end{aligned} \quad (17)$$

The numerical solution to these equations gives the water content $\Theta(z, t)$ and temperature $T(z, t)$ at incremental distances, Δz, and incremental time steps, Δt, where $z = i\Delta z$ and $t = n\Delta t$. Equation 16 can be solved for the water content, Θ_i^{n+1}, at time step $n + 1$, where Θ_i^n and T_i^n are known from the initial boundary conditions. Equation 17 can be solved for the temperature, T_i^{n+1} at time step $n + 1$ by using the water content computed from equation 16 and values of T_i^n. Repeated solutions of equations 16 and 17 give the water content and temperature distribution at any particular time desired, with the temperature computation lagging behind the moisture computation by one time step. The numerical solution to the implicit finite difference equations results in a set of simultaneous equations that can be solved by the Gauss elimination method.

In the moisture model the temperature and moisture diffusivities each has two components as described by equations 13 and 14. The procedure for obtaining the liquid moisture diffusivity, $D_{\Theta liq} = K(\partial h/\partial\Theta)$, is described by Elzeftawy and Dempsey in a paper in this Record. The vapor moisture diffusivity, $D_{\Theta vap}$, is obtained from the following equation of Philip and de Vries (18):

$$D_{\Theta vap} = D_{atm}\, \nu\alpha g\rho\, (\partial h/\partial\Theta)/(\rho_W)RT \quad (18)$$

and the thermal liquid diffusivity, D_{Tliq}, and thermal vapor diffusivity, D_{Tvap}, are computed from

$$D_{Tliq} = K\gamma h \quad (19)$$

and

$$D_{Tvap} = D_{atm}\, \nu\alpha h_o(\beta/\rho) \quad (20)$$

Computer Program

The numerical solution to the implicit finite difference equations (equations 16 and 17) was programmed on a

digital computer to provide a comprehensive and flexible moisture model. Numerous pavement geometric variables and hydrologic parameters are programmed into the model. Both one-dimensional and two-dimensional studies can be conducted. It is also possible to specify whether isothermal or nonisothermal moisture movement is to be predicted in the pavement system. Stationary or moving water table conditions can be specified in the moisture model. The data are programmed into the computerized model by using a free-form scan program that allows substantial flexibility in changing various inputs to the computer program. Climatic conditions can be put into the moisture model by using standard weather bureau data such as year and month of study, day of month, maximum and minimum daily temperature, rainfall, snowfall, wind velocity, percentage of possible daily sunshine, time of sunrise and sunset, and theoretical extraterrestrial radiation.

Most of the temperature computation procedures used in the moisture model are based on a heat-transfer model developed by Dempsey that considers meteorological parameters such as radiation and convection into or out of the pavement system (Figure 3) (30). A meteorological energy balance approach described by Berg (32) and previously used by Dempsey (30) is used to relate the climatic parameters to the pavement surface as follows:

$$Q_i - Q_r + Q_a - Q_e \pm Q_c \pm Q_h \pm Q_g = 0 \quad (21)$$

Precipitation at the pavement surface is considered either as snow or rain. The amount of rainwater that infiltrates the pavement is a function of the rainfall intensity and duration, the surface runoff, and the pavement surface permeability. Water infiltration from snow is considered only if the temperature rises above freezing.

VALIDATION OF THE MOISTURE MODEL

The validation of the moisture model using data from

Figure 1. Sources of moisture in pavement systems.

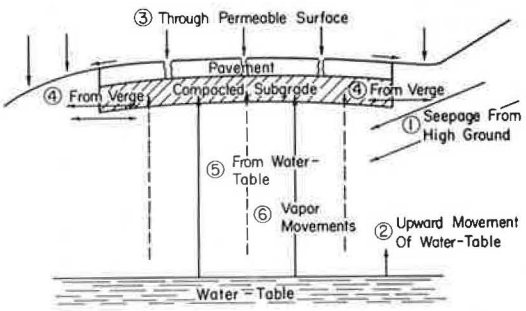

Figure 2. Implicit system for diffusion equation.

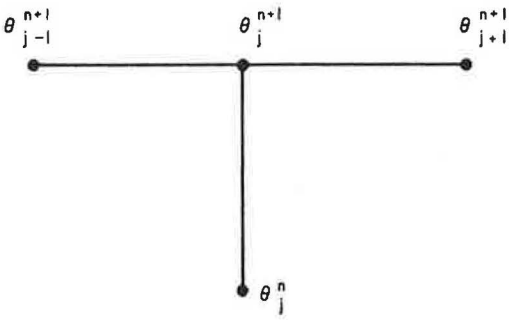

Figure 3. Heat transfer between pavement and air.

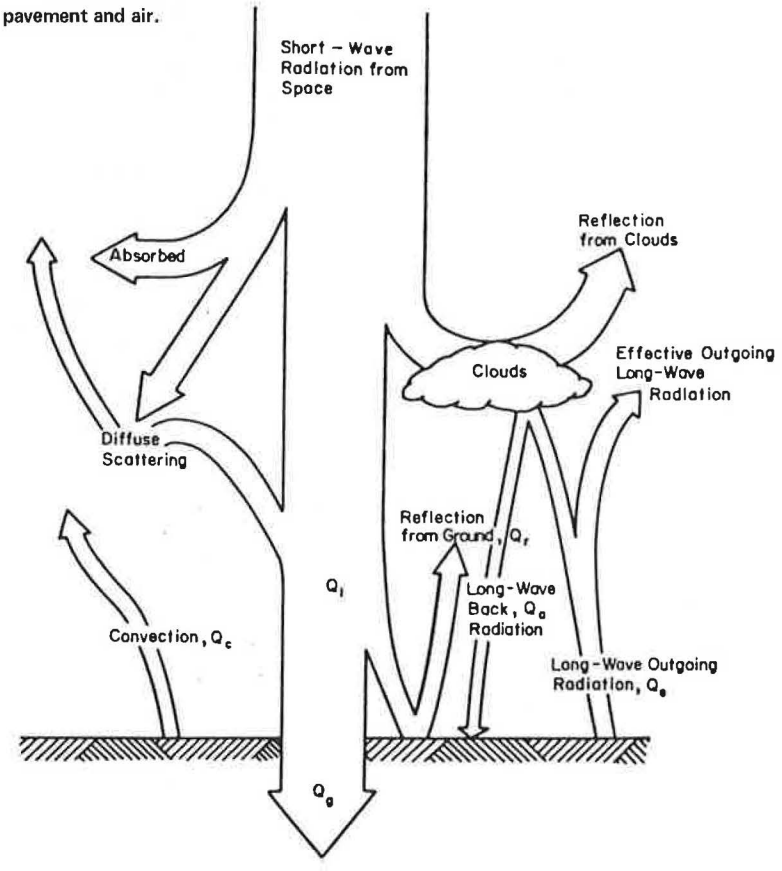

controlled laboratory and field studies is not completed at this time. However, comparisons between predicted and measured moisture contents have been made using laboratory data from one-dimensional studies.

Figure 4 shows the comparisons between the predicted and measured moisture contents at varying depths in Lakeland fine sand (AASHO Classification A-3) for one-dimensional, isothermal conditions. The composition and some physical properties of the sand are given below.

Component	Percentage
Sand	98.00
Silt	2.00
Clay	0.00
Liquid limit	Nonplastic
Plastic limit	Nonplastic
Compacted water content	0.65
HYGR	0.65

Property	Value
Compacted dry density (kg/m^3)	1560
Saturated hydraulic conductivity (cm/s)	4.11×10^{-3}

The boundary conditions for the program were

1. The moisture content at the surface remained constant at 0.26 cm^3/cm^3 (gravimetric water content = 16.6 percent) during $0 \leq t \leq t_{final}$,
2. The water table was sufficiently deep so that the moving water front did not reach to that depth, and
3. The average initial water content distribution at t = 0 was 0.109 cm^3/cm^3 (gravimetric water content = 7.0 percent).

From Figure 4 it is apparent that the isothermal moisture contents predicted by the moisture model compare favorably with the measured moisture contents.

Figure 5 shows a comparison between the predicted and measured isothermal moisture contents for an Illinoian till soil (AASHO Classification A-4) above a water table condition. The composition and some physical properties of the till are given below.

Component	Percentage
Sand	62.00
Silt	20.00
Clay	18.00
Liquid limit	22.20
Plastic limit	14.70
Compacted water content	11.70
w_{HYGR}	1.40

Property	Value
Compacted dry density (kg/m^3)	1720
Saturated hydraulic conductivity (cm/s)	8.61×10^{-5}

The boundary conditions for the program were

1. The average initial water content distribution at t = 0 was 0.21 cm^3/cm^3 (gravimetric water content = 12.2 percent),
2. An instantaneous water table moved upward to a depth of 120 cm (3.94 ft) below the surface at t = 0, and
3. The surface moisture was not allowed to evaporate during $0 \leq t \leq t_{final}$.

From Figure 5, it would appear that the moisture model was adequate in predicting moisture content changes with time in a fine-grained soil for one-dimensional, isothermal conditions. By comparing Figure 4 with Figure 5, it is possible to observe the differences in the rate of moisture movement caused by soil type and gravitational force. The downward movement of water shown in Figure 4 is assisted by gravity while the upward migration of water from the water table shown in Figure 5 must move against gravity: It appears that more than 60 days may be required for the Illinoian till soil to reach equilibrium for the given boundary conditions.

Nonisothermal moisture data are not readily available to validate the moisture model. Figure 6 shows the influence of a temperature gradient of approximately 0.2° C/cm (0.9° F/in) on the Illinoian till soil for the same initial boundary conditions as specified for Figure 5. The temperature increased from the top downward in the pavement system. Comparison of Figures 5 and 6 shows that temperature can exert substantial influence on moisture movement in a soil with time. Apparently, the model has the potential to simulate nonisothermal conditions.

DISCUSSION OF MOISTURE MODEL

The moisture model is a comprehensive and flexible method for predicting moisture conditions in pavement systems. As additional laboratory and field data become available, further validation work will be possible for both one-dimensional and two-dimensional moisture movement.

The ultimate objective of the application of moisture flow theory to field flow situations is the understanding of the soil water regime as a tool for the improvement of pavement design. In the process of developing the theoretical concepts that can model the soil-water flow system, there is an increased understanding of the system, and these concepts can be used to make predictions about the response of a soil-water flow system to the imposition of particular boundary conditions or modifications of the properties of the system. Making an adequate prediction makes it possible to manage the behavior of the soil-water system within the saturated to the unsaturated range.

In a broad way there would seem to be two purposes for the quantitative analysis and prediction of the performance of a given flow system. These are the verification of the validity of the flow theory and the practical prediction of the hydraulic performance of a given body of soil material in the pavement system.

The theory of soil-water movement is often used in a qualitative manner. As the basic concepts of flow in unsaturated soils become more generally known and understood, more use can and will be made of these concepts. For example, the recognition that the hydraulic conductivity decreases rapidly with decreasing water content can be of great use in qualitative and quantitative ways to analyze the behavior of a soil-water system.

The moisture model represents an important and necessary step in the development of a better understanding of climatic effects on pavement systems. Stating the moisture flow theory in mathematical terms as embodied in the partial differential equations of flow provides a basis for a more quantitative prediction of behavior. The classical mathematical-physical approach requires mathematical statements of the initial and boundary conditions that describe the specific flow situations and knowledge of the conductivity and water capacity functions that characterize the soil. It is then possible to obtain a solution to the flow equation and predict the behavior of the flow system by using analytical or numerical methods. The solution is in the form of the spatial and temporal distribution of the water content or the pressure head of the soil water or both. From these, such quantities as flux and cumulative flows can be derived at any point in the pavement system.

APPLICATIONS OF THE MOISTURE MODEL

Moisture is an important factor affecting the durability properties and the resilient properties of highway soils and materials, and the performance and fundamental behavior of pavement systems. Water directly governs the mechanical properties of most pavement materials and soils; therefore, any variation in water content will alter the properties of most pavement materials and soils. Methods for predicting moisture movement and equilibria in pavement systems are needed to fully describe material and pavement behavior. The increased use of subsurface drains also requires a better understanding of moisture movement and moisture equilibria in pavement systems as sound decisions concerning the

Figure 4. Comparison between predicted and measured moisture contents for Lakeland fine sand.

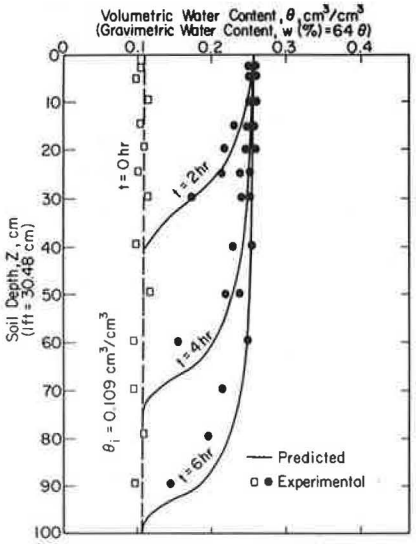

Figure 5. Comparison between predicted and measured moisture contents for Illinoian till above water table.

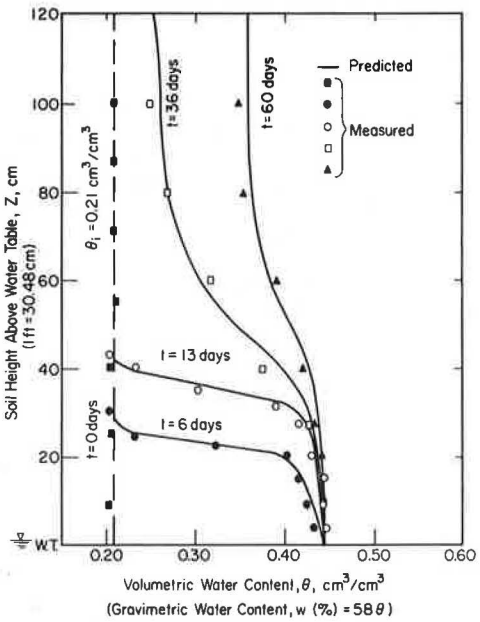

Figure 6. Predicted nonisothermal moisture movement for Illinoian till above water table.

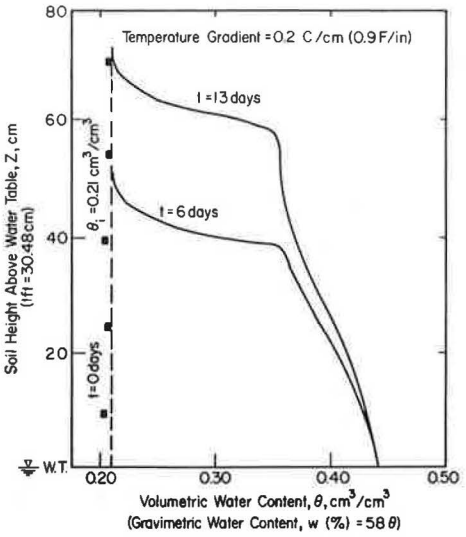

Figure 7. Changes in nonisothermal pavement moisture content as a function of depth, climate, and time.

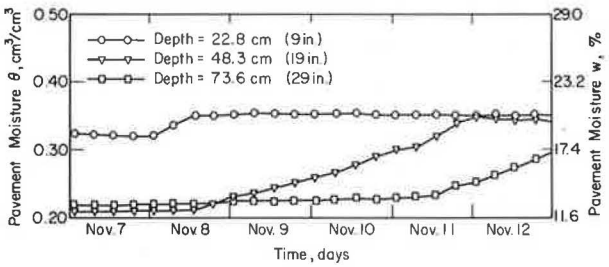

Figure 8. Changes in pavement temperature as a function of depth, climate, and time.

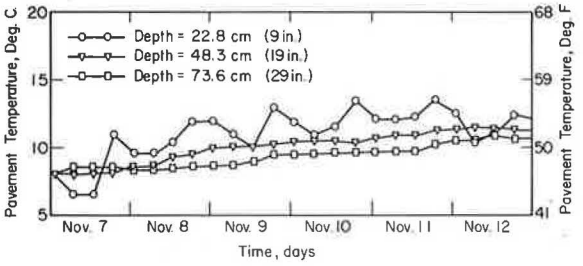

Figure 9. Air temperature and precipitation input for moisture model.

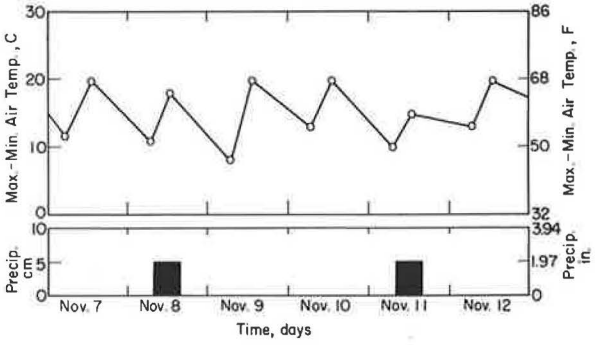

location of such drains require a thorough knowledge of the time-dependent moisture regime of the pavement system.

The moisture model can be used to study the changes in moisture content in a pavement system with time under varying climatic conditions. Figures 7 and 8 show variations in subgrade moisture content and temperature respectively for a 6-d period (the air temperatures and precipitation for the period are shown in Figure 9). The physical properties of the soil used to develop Figures 7 and 8 are the same as those for the Illinoian till in Figure 5. The subgrade moisture changes shown in Figure 7 reflect the influence of the rainfall shown in Figure 9. Although it is not readily evident, the water table position and temperature also have an effect on the moisture changes shown in Figure 7.

It is expected that the findings from this investigation will be helpful in making decisions related to moisture problems in pavement systems. The moisture model can be used to determine how various design modifications influence the moisture regime in a pavement system. It is anticipated that use of the model and related field and laboratory studies will lead to a less empirical approach for incorporating moisture effects into pavement design, construction, and behavior.

CONCLUSIONS

1. The moisture model provides a comprehensive procedure for predicting moisture conditions in pavement systems.
2. The Philip and de Vries equation for moisture movement provides a sound basis for predicting moisture conditions in pavement systems.
3. The moisture model gives valid results for predicting isothermal moisture movement.
4. Although it is not yet validated, the moisture model has the potential for predicting nonisothermal water movement.
5. The model can be used with climatic input data to predict the moisture-temperature regime in pavement systems.
6. The moisture model is potentially useful for many types of pavement research related to climatic effects.

ACKNOWLEDGMENTS

This report was prepared as part of the Illinois Cooperative Highway Research Program, by the Department of Civil Engineering in the Engineering Experiment Station, University of Illinois at Urbana-Champaign, in cooperation with the Illinois Department of Transportation and the Federal Highway Administration, U.S. Department of Transportation. The contents of this report reflect the views of the authors who are responsible for the facts and the accuracy of the data presented here. The contents do not necessarily reflect the official views or policies of the Illinois Department of Transportation or the Federal Highway Administration. This report does not constitute a standard, specification, or regulation.

REFERENCES

1. P. F. Low and C. W. Lovell, Jr. The Factor of Moisture in Frost Action. HRB, Bulletin 225, 1959, pp. 23-44.
2. R. K. Schofield. The pF of Water in Soils. Trans., Third International Congress of Soil Science, II, Oxford, 1935.
3. D. Croney and J. D. Coleman. Soil Structure in Relation to Soil Suction (pF). Journal of Soil Science, Vol. 1, 1954.
4. C. G. Gurr, T. J. Marshall, and J. T. Hutton. Movement of Water in Soil Due to a Temperature Gradient. Soil Science, Vol. 74, 1952.
5. R. Gardner. Relation of Temperature to Moisture Tension of Soil. Soil Science, Vol. 79, 1955.
6. J. W. Cary. Water Flux in Moist Soil: Thermal Versus Suction Gradients. Soil Science, Vol. 100, 1965.
7. G. Kubler. Influence of Meteorologic Factors on Frost Damage in Roads. HRB, Highway Research Record 33, 1963, pp. 217-255.
8. K. A. Turner, Jr., and A. R. Jumikis. Subsurface Temperatures and Moisture Contents in Six New Jersey Soils, 1954-1955. HRB, Bulletin 135, 1956, pp. 77-109.
9. D. Croney and J. D. Coleman. Soil Thermodynamics Applied to the Movement of Moisture in Road Foundations. Proc., Seventh International Congress for Applied Mechanics, Vol. 3, 1948.
10. M. P. O'Reilly, K. Russan, and F. H. R. Williams. Pavement Design in the Tropics. Road Research Laboratory, Ministry of Transport, Her Majesty's Stationery Office, London, 1968.
11. E. C. Childs. An Introduction to the Physical Basis of Soil Water Phenomena. Wiley, New York, 1969.
12. L. A. Richards. Capillary Conduction of Liquids in Porous Mediums. Physics, 1, 1931.
13. E. C. Childs and N. Collis-George. The Permeability of Porous Materials. Proc., Royal Society 201A, 1950, pp. 392-405.
14. D. Kirkham and W. L. Powers. Advanced Soil Physics. Wiley-Interscience, New York, 1972.
15. J. S. Rogers and A. Klute. The Hydraulic Conductivity-Water Content Relationship During Nonsteady Flow Through a Sand Column. Proc., Soil Science Society of America, Vol. 35, 1971, pp. 695-700.
16. D. Hillel. Soil and Water, Physical Principles and Processes. Academic Press, New York, 1973, p. 51.
17. H. P. Hutchinson, I. S. Dixon, and K. G. Denbigh. The Thermo-osmosis of Liquids Through Porous Materials. Discussions, Faraday Society, Vol. 3, 1948, pp. 86-94.
18. J. R. Philip and D. A. de Vries. Moisture Movement in Porous Materials Under Temperature Gradients. Trans., American Geophysical Union, Vol. 38, 1957, pp. 222-232.
19. S. A. Taylor and J. W. Cary. Linear Equations for the Simultaneous Flow of Matter and Energy in a Continuous Soil System. Proc., Soil Science Society of America, Vol. 28, 1964, pp. 167-172.
20. S. A. Taylor and J. W. Cary. Soil Water Movement in Vapor and Liquid Phases. Methodology of Plant Eco-Systems, UNESCO Arid Zone Research, Vol. 25, 1965, pp. 59-165.
21. D. K. Cassel. Soil-Water Behavior in Relation to Imposed Temperature Gradients. Univ. of California, Davis, PhD thesis, 1968.
22. J. W. Cary. Soil Moisture Transport Due to Thermal Gradients: Practical Aspects. Proc., Soil Science Society of America, Vol. 30, 1966, pp. 428-433.
23. P. Hoekstra. Moisture Movement in Soils Under Temperature Gradients With Cold-Side Temperature Below Freezing. Water Resources Research, Vol. 2, 1966, pp. 241-250.
24. A. R. Jumikis. Experimental Studies on Moisture Transfer in a Silty Soil Upon Freezing as a Function of Porosity. Cushing-Malloy, Ann Arbor, Mich., 1969.

25. A. Klute. A Numerical Method for Solving the Flow Equation for Water in Unsaturated Materials. Soil Science, Vol. 73, 1952.
26. B. G. Richards. An Analysis of Subgrade Conditions at the Horsham Experimental Road Site Using the Two-Dimensional Diffusion Equation on a High-Speed Digital Computer. Proc., Symposium on Moisture Equilibria and Moisture Changes in Soils Beneath Covered Areas, Butterworth, Australia, 1965.
27. H. M. E. Selim. Transient and Steady Two-Dimensional Flow of Water in Unsaturated Soils. Iowa State Univ., Ames, PhD thesis, 1971.
28. R. L. Lytton and R. K. Kher. Prediction of Moisture Movement in Expansive Clays. Center for Highway Research, Univ. of Texas at Austin, Research Rept. 118-3, May 1970.
29. R. L. Rollins, M. G. Spangler, and D. Kirkham. Movement of Soil Moisture Under a Thermal Gradient. Proc., HRB, Vol. 33, 1954, pp. 492-508.
30. B. J. Dempsey. A Heat-Transfer Model for Evaluating Frost Action and Temperature Related Effects in Multilayered Pavement Systems. Department of Civil Engineering, Univ. of Illinois, Urbana, PhD thesis, 1969.
31. B. J. Dempsey and M. R. Thompson. A Heat-Transfer Model for Evaluating Frost Action and Temperature Related Effects in Multilayered Pavement Systems. HRB, Highway Research Record 342, 1970, pp. 39-56.
32. R. L. Berg. Energy Balance on a Paved Surface. U.S. Army Corps of Engineers Cold Regions Research and Engineering Laboratory, Hanover, N.H., Technical Rept. 226, 1974.

Unsaturated Transient and Steady-State Flow of Moisture in Subgrade Soil

Atef Elzeftawy and Barry J. Dempsey, Department of Civil Engineering, University of Illinois at Urbana-Champaign

A general procedure for determining the soil-water properties necessary for predicting moisture movement in subgrade soils is described. A gamma-ray transmission method was used for the nondestructive measurement of the water content and a tensiometer-pressure transducer arrangement to measure the soil-water pressure (suction); the unsaturated hydraulic conductivity, diffusivity, and soil-water characteristic functions were evaluated for AASHO A-4 subgrade soil. The soil was compacted in a column at uniform density and moisture content and tested under isothermal conditions. A water table was established at the bottom of the soil column and the transport of water through the subgrade soil studied. The mathematical procedures for determining the soil-water properties from the laboratory data are described, and the use of the experimentally determined hydraulic conductivity, soil-water diffusivity, and soil-water characteristic functions in the prediction of moisture changes in an AASHO A-4 soil is demonstrated.

In 1973 the Federal Highway Administration conducted five workshops to study the effects of moisture on pavement systems. Also in 1973, a research group sponsored by the Organization for Economic Cooperation and Development discussed the importance of predicting and controlling the effects of moisture in pavement systems and published a report (15) that recommended that the procedures shown in Figures 1 and 2 be used to develop research for predicting and controlling moisture effects in pavement systems.

The properties of soil-water systems must be known in order to predict and control moisture content and movement in pavement systems. Extensive studies of the resilient behavior of fine-grained soils, conducted by Robnett and Thompson (21), have shown the detrimental effects of moisture on the repeated-load resilient modulus. Fine-grained soils display various degrees of moisture sensitivity that depend on certain of their inherent characteristics. In general, much of their strength can be explained by changes in the soil-water pressure (suction), which is related to its water content as shown in Figure 3. The absolute magnitude of change in the resilient modulus caused by an increase in the soil-moisture content will not be constant for all soils, but will vary with the accompanying change in soil-water pressure. The understanding and quantification of soil-water properties are important not only to drainage analysis and design but also to studies of frost action.

The study of a moisture movement requires knowledge of the initial and boundary conditions that describe the specific moisture-flow situation, and of the hydraulic conductivity, diffusivity, and water-capacity functions that characterize the soil or the subgrade. With these, it is possible to predict the behavior of the flow system using an approximate analytical or numerical solution of the moisture-flow equation. A few not very successful attempts to predict the moisture conditions in a pavement profile have been made, but a satisfactory and realistic procedure for the study of moisture movement in pavements is needed to solve the engineering problems associated with the behavior of pavement systems in response to moisture changes. Therefore, the objectives of this study are

1. To investigate unsaturated transient moisture flow in subgrade soils,
2. To demonstrate a general procedure for determining the subgrade soil-moisture properties such as hydraulic conductivity, diffusivity, and the soil-moisture-suction characteristic function necessary for predicting moisture movement; and
3. To show how the soil-moisture parameters can be used to provide a comprehensive procedure for predicting moisture conditions in pavement profiles.

LITERATURE REVIEW

Darcy's Law and the Continuity Equation

In 1822, Fourier (8) published his very complete mathematical theory of heat transport in conducting materials. In 1827, Ohm (16) published his law that the rate of transport of electricity in a conductor is proportional to the electrical potential difference between its ends, i.e., that the electric current is proportional to the electrical potential gradient. In 1822, Navier (14) developed equa-

Publication of this paper sponsored by Committee on Subsurface Drainage.

tions describing the flow of viscous fluids in terms of the distribution of hydraulic potential. These equations were later derived by Stokes (23) in a more general way. By using the Stokes-Navier equations, the rate of flow can be derived in terms of the dimensions of the conductor and the hydraulic potential difference between the ends. Poiseuille's experimentally derived equation for the flow of a fluid through a tube (18) can be readily obtained from the earlier theoretical work. This equation can be written in the form

$$Q/t = (\Delta\phi/L)(\pi/8\eta)R^4 g\rho \quad (1)$$

where

- Q = volume passing in time, t,
- L = length of the tube between the ends of which the potential difference is $\Delta\phi$ (i.e., $\Delta\phi/L$ is the hydraulic potential gradient),
- η = viscosity of the fluid,
- ρ = its density,
- g = gravitation constant, and
- R = radius of the tube.

Figure 1. Research needs for prediction and control of moisture in pavement systems.

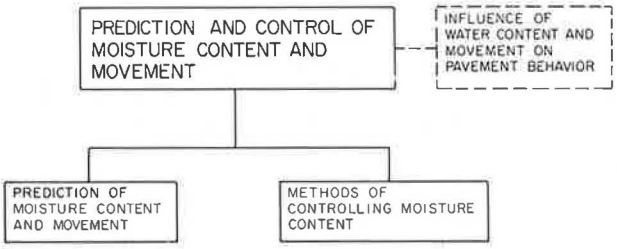

Figure 2. Approach for predicting moisture in pavement systems.

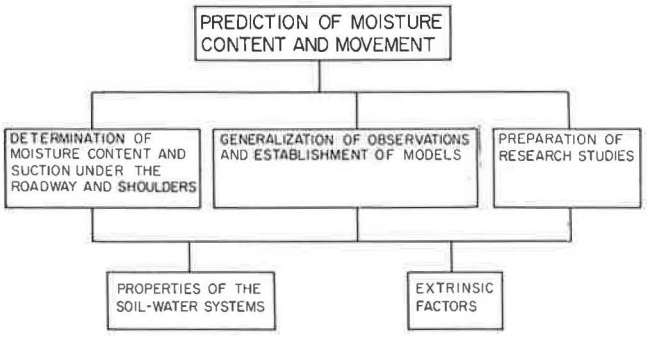

Figure 3. Soil-water characteristic function for AASHO A-4 subgrade soil.

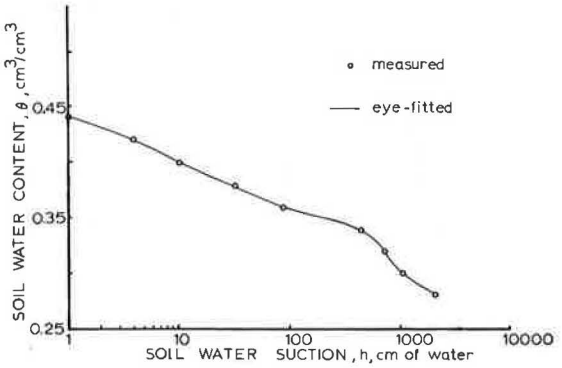

The configuration of the pore space in a porous material such as soil is far too complicated to permit the rate of flow of a fluid to be calculated by the Stokes-Navier equations. However, Darcy (3), from experiments on the infiltration of water through filter beds of sands, formulated a law that has been widely accepted as the basis for describing the flow of a liquid in a saturated porous material. In 1950, Childs and Collis-George (2) introduced the soil-water diffusivity concept as a way to describe the flow in a water-unsaturated soil. Their theory for the unsaturated flow of water assumes that Darcy's law can be written as a diffusion-type water-flow equation in homogeneous soils, where gradients of water content rather than gradients of total potential are expressed as

$$q = D(\theta)\nabla\theta - K(\theta) \quad (2)$$

where

- q = water flux,
- θ = soil-water content on a volume basis,
- $K(\theta)$ = soil hydraulic conductivity,
- $D(\theta)$ = $K(\theta)/C(\theta)$, the soil-water diffusivity,
- $C(\theta)$ = $\partial\theta/\partial h$, the specific soil-water storage capacity where h is the soil water pressure head having negative values, and
- $\nabla\theta$ = water-content gradient.

Both $D(\theta)$ and $K(\theta)$ are functions of the soil-water content, θ.

Equation 2 resembles Fick's law of diffusion with a concentration dependent diffusivity, except for the $K(\theta)$ term, which arises from the gravitation component of the total hydraulic head. If this equation is combined with the equation of continuity (i.e., the conservation of mass), a diffusion-type equation for flow in porous media under isothermal conditions is obtained (13). This can be written in the form

$$\partial\theta/\partial t = \partial[D(\theta)\partial\theta/\partial Z]/\partial Z + \partial K(\theta)/\partial Z \quad (3)$$

where t is the time and Z is the vertical space coordinate. The term $\partial K(\theta)/\partial Z$ in equation 3 is normally referred to as the gravitational component. The validity of equation 3 in describing the flow of water in unsaturated soils has been demonstrated by several workers (5, 17, 22, 25), and, more recently, by Dempsey and Elzeftawy in a paper in this Record.

LABORATORY MATERIALS AND METHODS

Materials

The soil-water properties were determined for an AASHO A-4 soil, which was compacted in a plexiglass column 150 cm (60 in) high and having a cross section of 20 by 20 cm (8 in by 8 in). The composition and properties of the soil as compacted in the column are given below.

Component	Percent	Component	Percent
Sand	62.00	Plastic limit	14.70
Silt	20.00	Optimum water content, W_{opp}	11.00
Clay	18.00	W_{HYGR}	1.40
Liquid limit	22.20		

Property	Value
Maximum dry density ($\gamma_{d\,max}$)	1016 kg/m^3
Saturated hydraulic conductivity (K_s)	0.31 cm/h
Bulk density (ρ_s)	1.72 g/cm

The particle size distribution showed a predominance of sand (more than 60 percent); however, the clay content (18 percent) and the compacted nature explain the low value of the saturated hydraulic conductivity.

Equipment

The gamma-ray attenuation method (11) can be used experimentally to investigate most moisture-movement problems in soils and subgrade materials. As shown in Figure 4, this method uses a radioactive source on one side of the soil column and a scintillation counter on the other for the nondestructive measurement of the water content. The assembly of source and detector must be positioned at the elevation at which the measurement of the water-content change is to be made. The general design requirements of the traversing mechanism are as follows:

1. The mechanism must be strong enough to move the source and detector, together with the heavy shielding involved, up and down the column with a minimum of vibration and with accurate horizontal positioning of the collimation slit relative to the column center line.
2. The source and detector assembly must be capable of being stopped precisely at any graduation mark on the column.
3. The movement from one elevation to another must be as rapid as possible (keeping in mind the accuracy of positioning required by 2 above).

Water Content Measurements

The full and desirable specifications for water content measurements for the unsaturated transient-flow type of problem are

1. Measurement over a small thickness of the sample to approximate as closely as possible a planar measurement,
2. Determination by nondestructive means,
3. Measurement over a very short time interval, and
4. Rapid means of making measurements at different parts of the soil column.

Ferguson (7), Rawlings (19), and Gurr (11) have shown that the principle of gamma-ray absorption can be used to infer the moisture content of the soil from changes in its density. The attenuation equation for a moist soil, and for a collimated, monoenergetic beam is

$$I_m/I_o = \exp - [(\mu_\theta \rho_\theta \theta) + (\mu_s \rho_s)x] \quad (4)$$

where

I_m/I_o = ratio of incident to transmitted flux for moist soil,
μ_θ = mass attenuation coefficient for water,
μ_s = mass attenuation coefficient for soil,
x = thickness of soil,
θ = volume of water/unit volume of soil,
ρ_s = bulk density of the soil, and
ρ_θ = density of water.

Study of equation 4 shows that its use in determining θ requires (a) values of the mass attenuation coefficients, (b) a uniform and known bulk density of the soil in the column (this can be achieved by special packing techniques), and (c) a constant thickness dimension along the column length.

Figure 4 also shows the source-detector assembly. A cesium-137 source, a scintillation probe, and a scaler unit are used to determine changes in the moisture content of the soil along the length of the column. The ^{137}Cs source and scintillation probe-preamplifier unit, with the required lead shielding, is moved along the length of the soil column by the use of three threaded screws that are part of the supporting frame. The scintillation probe, which absorbs the gamma radiation after it has passed through the soil column, is connected to a decade scaler and a pulse-height analyzer.

Soil-Water Pressure Measurement

A tensiometer system for the measurement of rapidly changing soil suction (negative pressure) should have the following features: (a) a high gauge sensitivity, (b) a response time of the order of a few seconds or less, (c) rapid means of reading, and (d) convenience of recording. The achievement of a very rapid response in the tensiometer system to pressure changes in the soil inherently implies a negligibly small exchange of water between the soil and the tensiometer. Klute and Peters (13) and Watson (24) have reported the satisfactory use of a pressure transducer for soil-water measurements requiring rapid response with minimum transfer of water between the soil water and the measuring system. Their approach has been further developed in the present tensiometer-transducer system, which can be used for a suction head range up to 900 cm of water (350 in).

A porous cup with as large a pore size as possible, yet with an air entry value greater than the maximum pressure (or suction) to be encountered, should be used to increase the response of the measuring system. The ceramic porous cups (fine porosity) used here as tensiometers were 1.0 cm (0.39 in) in diameter and 3.0 cm (1.2 in) in length with an air entry value (bubbling pressure) of approximately 800 cm (315 in) of water. The tensiometers were installed at eight positions and were saturated with boiled, distilled water. All of the tensiometers were connected by 1.6-mm ($\frac{1}{16}$-in) OD nylon tubing to a single pressure transducer by way of a common rotary switching valve. The output signal of the pressure transducer was measured by a demodulator and continuously recorded on a strip chart recorder.

A constant-head water column was used as a standard to calibrate the transducer. The ratio of the signal voltage to the differential pressure was 1 mV/cm of water pressure head.

The response-time constant of the tensiometer-transducer system when the flow system was water-saturated was 0.5 s, but became quite large (≥20 s) when the flow system was unsaturated. Richards (20) has defined the tensiometer conductance as the volume of water passing through the tensiometer cup per unit of time per unit of pressure difference: For a given time and pressure difference, the cup conductance depends primarily on the area of contact with the soil and the pore size of its porous material. He has also defined the gauge sensitivity s as the pressure change per unit volume of displacement. Watson (24) has shown that the gauge sensitivity, for the equipment used here, could more precisely be described as the transducer sensitivity. The response-time constant is thus related to the tensiometer cup conductance and the gauge sensitivity by the equation

$$\tau = 1/ks \quad (5)$$

where τ is the response-time constant, k is the tensiometer conductance, and s is the gauge sensitivity. [The pressure transducer used throughout this study has a volumetric displacement of 4.92×10^{-3} cm^3 (3.0×10^{-4} in^3); for a maximum pressure of 850 cm (335 in) of water and a gauge sensitivity of 1.7×10^5 cm^{-3} (1.1×10^6 in^{-3}), the tensiometer cup conductance can be calculated from equation 5 for any specified response-time constant.]

RESULTS AND DISCUSSION

The measured gamma-ray mass adsorption coefficient for water, μ_θ, of 0.0832 ± 0.0006 cm^2/g agreed with the theoretical value of 0.0857 cm^2/g calculated by Grodstein (10). In water content calculations an average bulk density ρ_s value of 1.72 g/cm^3 (107.1 pcf), and an optimum soil-water content W_{opp} of 11.0 percent, as reported by Gurr (11), were used.

Figure 3 shows the soil-water content on a volume basis as a function of the soil-water suction expressed as cm of water head for AASHO A-4 soil. The solid line was eye-fitted to connect all of the measured values of the $h(\theta)$ relation. (The particular data shown are for the case of transient water flow during the wetting of the soil column.) A value of 1.0 cm of water pressure head (suction) was considered to be the value at which the soil was saturated. The water content of this soil at saturation, θ_s, was 0.44 cm^3/cm^3 (in comparison to 0.28 cm^3/cm^3 at -2066 cm (-813.4 in) of soil-water pressure head, h. Thus, the soil has lost approximately 36 percent of its water content in response to a pressure head of -2066 cm of water.

Campbell (1) has shown that if the water characteristic function $h(\theta)$ can be expressed by the equation

$$h = h_e(\theta/\theta_s)^{-b} \quad (6)$$

where h_e is the air entry water potential and b is an empirically determined constant, then the hydraulic conductivity is given by

$$K = K_s(\theta/\theta_s)^{(2b+3)} \quad (7)$$

where K_s is the saturated hydraulic conductivity of the soil. Since equation 6 is assumed to describe the water characteristic curve for the AASHO A-4 soil, equation 7 can be expected to give valid estimates of $K(\theta)$. The measured and calculated unsaturated hydraulic conductivity of the AASHO A-4 soil is shown in Figure 5. $K(\theta)$ was calculated by using equation 7 of Campbell (1) and by the Elzeftawy and Mansell method (4), which is a modification of the Green and Corey method (9) that includes a spline function technique (6) to provide a smooth continuous soil-water characteristic function. The measured value of the hydraulic conductivity corresponding to water saturation ($\theta_s = 0.44$ cm^3/cm^3) was used as a matching factor to determine the calculated curve for the $K(\theta)$ function. Figure 5 shows that the revised method (4) calculating K versus θ gives better agreement with the measured values of the unsaturated hydraulic conductivity than does that of Campbell (1). The divergence of the Campbell method from the measured conductivity may be related to the assumption that the pore size distribution function is the same throughout the porous body.

Just as the flow of heat can be expressed in the form of a diffusion equation with a diffusivity expressed in terms of the thermal conductivity, density, and specific heat of the material, so Darcy's law may be put into a diffusionlike form with the water diffusivity $D(\theta)$ given by

$$D(\theta) = K(\theta)/C(\theta) \quad (8)$$

where $C(\theta) = \partial\theta/\partial h$, the specific water capacity of the soil. Figure 6 shows the AASHO A-4 soil-water diffusivity as a function of the soil-water content for a wetting case. As the soil-water content increases from 0.28 to 0.42 cm^3/cm^3, the soil-water diffusivity increases from 3.2×10^{-1} to 5.4×10^1 cm^2/h. For the same range of water content, the soil hydraulic conductivity increased from 3.1×10^{-7} to 1.9×10^{-1} cm/h (Figure 5). Recent studies (21) with a large number of soils from the Midwest, Oklahoma, Georgia, and the Carolinas have shown that a water-content change of 1 or 2 percent by weight can have considerable influence on the strength of the AASHO Road Test subgrade soil.

Dempsey and Elzeftawy, in a paper in this Record, have used numerical solutions of equation 3 to develop a moisture model to predict moisture movement in subgrade soils. The model can be used for one-dimensional or two-dimensional moisture flow through homogeneous or multilayered subgrade soil and pavement systems under iso or nonisothermal conditions. The experimentally determined relations of h versus θ (Figure 3), K versus θ (Figure 5), and D versus θ (Figure 6) were used in this model to predict the upward moisture movement into compacted subgrade soil columns having uniform initial water contents and a water table at the bottom of the soil column. Figure 7 shows the calculated and measured soil-water distributions for AASHO A-4 subgrade soil as a function of soil height after 6, 13, 36, and 60 d from establishing a water table at the bottom of the soil column. The soil-water content at the water table position increased from the initial value of 0.21 cm^3/cm^3 to 0.44 cm^3/cm^3, which is equal to the saturated soil-water content. After 13 days, the water front reached 40 cm (15.75 in) above the water table. The decreasing soil-water content with height at a specific time ($t > 0$) is due to the increase in the negative soil-water pressure (suction). At equilibrium, the soil-water content distribution profile should be similar to that of the soil-water characteristic function, $h(\theta)$. The agreement between the measured and calculated soil-water content distributions in AASHO A-4 subgrade soil is good, and thus the Dempsey-Elzeftawy moisture model can be used to predict the water movement in a subgrade soil.

SUMMARY AND CONCLUSIONS

A water table was established at the bottom of a compacted subgrade soil column, and the movement of water through the soil was studied under isothermal conditions. A gamma-ray method was used for the nondestructive measurement of the water content, and a tensiometer-pressure transducer arrangement to measure the soil-water pressure (suction); the unsaturated hydraulic conductivity, diffusivity, and soil-water characteristic parameters were evaluated from these data and used as input data for the Dempsey and Elzeftawy moisture model to predict the movement of moisture through subgrade soil. The following conclusions were made:

1. Darcy's law and the continuity equation can be used to describe and explain soil-moisture flow through compacted subgrade soil in both saturated and unsaturated flow.
2. Soil moisture moves through subgrade soil under unsaturated transient-flow condition.

Figure 4. Soil-moisture column and source-detector assembly.

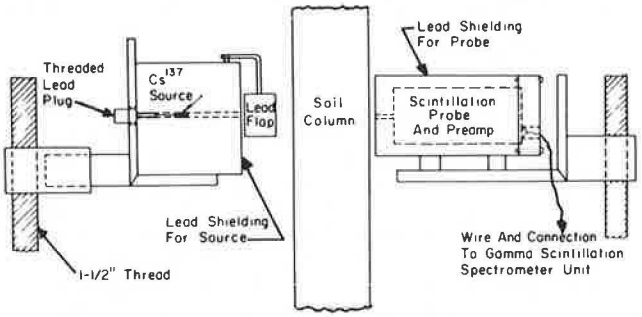

Figure 5. Measured and calculated unsaturated hydraulic conductivity of AASHO A-4 soil.

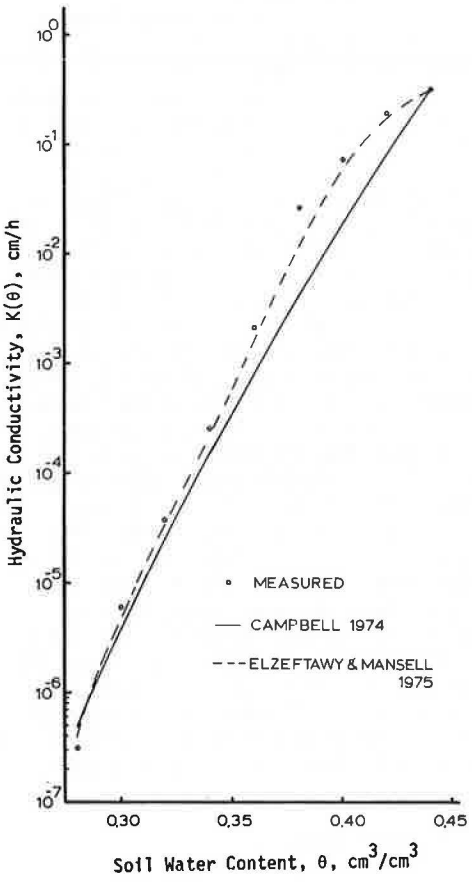

Figure 6. Soil-water diffusivity for AASHO A-4 subgrade soil.

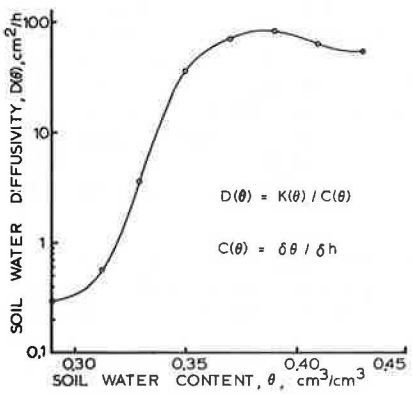

Figure 7. Soil-water distribution for AASHO A-4 subgrade soil as a function of soil height.

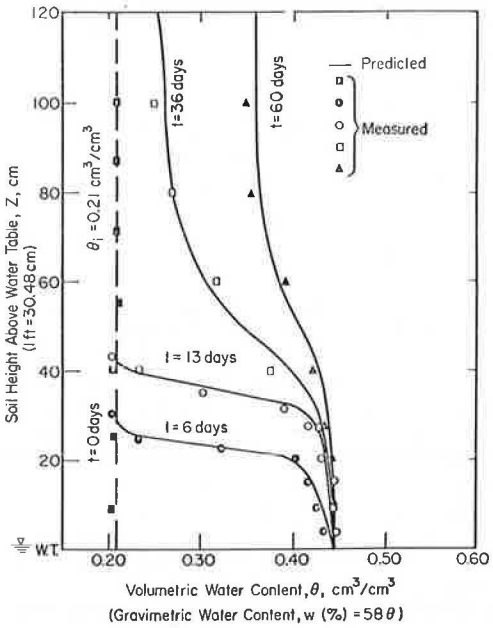

3. The experimentally evaluated soil-moisture parameters are necessary for the prediction of moisture content and its movement in subgrade soil.

ACKNOWLEDGMENTS

This report was prepared as a part of the Illinois Cooperative Highway Research Program, Moisture Movement and Moisture Equilibria in Pavement Systems, by the Department of Civil Engineering, Engineering Experiment Station, University of Illinois at Urbana-Champaign, in cooperation with the Illinois Department of Transportation and the Federal Highway Administration, U.S. Department of Transportation.

REFERENCES

1. G. S. Campbell. A Simple Method for Determining Unsaturated Conductivity From Moisture Retention Data. Soil Science, Vol. 117, No. 6, 1974, pp. 331-314.
2. E. C. Childs and N. Collis-George. The Permeability of Porous Materials. Proc., Royal Socicty, Vol. 201A, 1950, pp. 392-405.
3. H. Darcy. Les fontaines publiques de la ville de Dijon. Dalmont, Paris, 1856.
4. A. Elzeftawy and R. S. Mansell. Measured and Calculated Values of Hydraulic Conductivity of Partially-Saturated Lakeland Sand. Proc., Soil Science Society of America, Vol. 39, No. 4, 1975.
5. A. Elzeftawy. Water and Solute Transport in Lakeland Fine Sand. PhD thesis, Univ. of Florida, Gainesville, 1974.
6. K. T. Erh. Application of the Spline Function of Soil Science. Soil Science, Vol. 114, No. 5, 1972, pp. 333-338.
7. A. H. Ferguson. Movement of Soil Water as Inferred From Moisture Content Measurements by Gamma-Ray Absorption. PhD thesis, Washington State Univ., 1959.
8. J. B. J. Fourier. Theorie Analytique De La Chaleur. Firmin Didot Pere et Fils, Paris, 1822.

9. R. E. Green and J. C. Corey. Calculation of Hydraulic Conductivity: A Further Evaluation of Some Predictive Methods. Proc., Soil Science Society of America, Vol. 35, 1971, pp. 3-8.
10. G. W. Grodstein. X-Ray Attenuation Coefficients From 10keV to 100 meV. National Bureau of Standards Circular 583, 1957.
11. C. G. Gurr. Use of Gamma Rays in Measuring Water Content and Permeability in Unsaturated Columns of Soil. Soil Science, Vol. 94, No. 4, 1962, pp. 224-229.
12. D. Kirkham and W. L. Powers. Advanced Soil Physics. Wiley-Interscience, New York, 1972.
13. A. Klute and D. B. Peters. A Recording Tensiometer With a Short Response Time. Proc., Soil Science Society of America, Vol. 26, 1962, pp. 87-88.
14. C. L. M. H. Navier. Memoir Sur Les Lois Du Mouvement Des Fluids. Memoires de L'Academie des Sciences, Vol. 6, 1822, p. 389.
15. Water in Roads: Prediction of Moisture Content of Road Subgrades. Organization for Economic Cooperation and Development, Paris, 1973.
16. G. S. Ohm. Die Galvanische Kette Mathematisch Bearbeitet. T. H. Riemann, Berlin, 1827.
17. A. J. Peck. The Diffusivity of Water in a Porous Material. Australian Journal of Soil Research, Vol. 2, 1964, pp. 1-7.
18. J. L. M. Poiseuille. Recherches Experimentales Sur Le Mouvement Des Liquids Dans Les Tubes De Tres Petits Diametres. Comptes Rendu Général des Académies et Sociétés Médicales de la France et de l'Etranger, Vol. 2, 1842, pp. 961-967 and 1041-1048.
19. S. L. Rawlins. A Theoretical and Experimental Examination of the Validity of Diffusion Analysis as Applied to Unsaturated Flow of Water. PhD thesis, Washington State Univ., 1961.
20. L. A. Richards. Methods of Measuring Soil Moisture Tension. Soil Science, Vol. 68, No. 1, 1949, pp. 95-112.
21. Q. L. Robnett and M. R. Thompson. Development of Testing Procedure, Phase 1 Interim Report, Resilient Properties of Subgrade Soils. Civil Engineering Studies, Transportation Engineering Series No. 5, Illinois Cooperative Highway Research Program Series No. 139.
22. H. M. Selim, R. S. Mansell, and A. Elzeftawy. Simulation of Herbicide and Water Movement During Infiltration and Redistribution in Soil. Agronomy Abstracts, American Society of Agronomy, p. 115.
23. G. G. Stokes. On the Theories of the Internal Friction of Fluids in Motion and the Equilibrium and Motion of Elastic Solids. Proc., Cambridge Philosophical Society, Vol. 1, 1845, pp. 16-18.
24. K. K. Watson. Some Operating Characteristics of a Rapid Response Tensiometer System. Water Resources Research, Vol. 1, 1965, pp. 577-586.
25. E. G. Youngs. Moisture Profiles During Vertical Infiltration. Soil Science, Vol. 84, No. 4, 1957, pp. 283-290.

Evaluation of Freeze-Thaw Durability of Stabilized Materials

Marshall R. Thompson and Barry J. Dempsey, Department of Civil Engineering, University of Illinois at Urbana-Champaign

A suggested procedure for evaluating the freeze-thaw durability of stabilized materials is developed. Pertinent background information and previous related studies are summarized. The residual strength concept is used in the suggested evaluation procedure. Quantitative characterization of cyclic freeze-thaw action, freeze-thaw testing procedures and techniques, durability criteria, and construction influences are considered. Detailed data are presented for Illinois conditions, and the applicability of the proposed procedure is illustrated. It is demonstrated that current technology is sufficient to develop a realistic approach for evaluating the freeze-thaw durability of stabilized materials.

Methods of durability testing of stabilized materials were studied to develop a satisfactory and realistic procedure for evaluating the freeze-thaw (FT) durability of partially cemented highway materials such as soil-cement, lime-fly ash-aggregate, and soil-lime mixtures.

An illustrative example for a typical Illinois condition is presented.

DEVELOPMENTAL ACTIVITIES

Freeze-Thaw Cycles and Testing Procedures

A heat-transfer model for evaluating frost action and temperature effects developed for multilayered pavement systems (1) was used to establish relevant quantitative frost-action parameters for stabilized pavement systems for five locations in Illinois. The frost-action parameters were determined by statistically analyzing pavement temperatures for 30 years of past climatic data (2). The parameters generated by the model (a standardized FT cycle) were programmed into a unique FT testing unit (3, 4, 5, 6). The FT cycle was representative of field conditions in the more severe environments of Illinois (the central to northern parts of the state).

A vacuum saturation durability testing procedure was also developed (6). This procedure is much more rapid than the rather lengthy (48-h) FT test.

Laboratory Testing Program

A wide range of typical Illinois stabilized materials (soils, gravels, and crushed stone) was included in the laboratory testing program (6). The stabilizing agents considered were lime, lime-fly ash, and cement. Other factors considered were compaction density effects, curing time effects, and percent additive effects.

The various soil-stabilizer mixtures were subjected to 5 and 10 cycles of the standard FT cycle. The evaluation techniques used to measure the durability included measures of compressive strength, length change, and moisture change.

The laboratory data have shown that 5 and 10-cycle FT strengths can be predicted based on the strength of the stabilized material after curing (prior to FT testing) or on the vacuum saturation strength of the cured material. Figures 1 and 2 show the 10-cycle FT relations developed. Those factors that influence the cured strength (density, percent additive, curing time) affect the FT strength in the same manner.

DEVELOPMENT OF FREEZE-THAW DURABILITY CRITERIA

General

The results of the early phases of the FT durability project provided valuable information and data concerning field conditions and the response of typical stabilized materials to realistic FT exposure. However, in the development of tentative FT durability criteria, it is not only important that use be made of laboratory data and information but also essential that consideration be given to the many aspects of stabilized material use such as mix design, construction operations, pavement behavior, climatic factors, and curing conditions.

The Residual Strength Concept

The concept of residual strength has been used in estab-

Publication of this paper sponsored by Committee on Frost Action.

lishing quality requirements for soil-lime stabilization (7). The residual strength is the strength of a stabilized material following the equivalent of the first winter FT cycles. If the residual strength is adequate to ensure the desired level of structural pavement response, and the material displays a projected strength-time history that will ensure that the field strength will always be greater than some minimum strength requirement, then pavement performance will be satisfactory. The residual strength concept is illustrated in Figure 3. Field experience with partially cemented highway materials has shown that if the cured material possesses sufficient durability to survive the first winter FT cycles, the probability of durability problems during subsequent years is quite low. The additional curing and autogenous healing that may develop during the summer following construction and during subsequent summers are beneficial in developing additional strength in the stabilized mixture (especially in properly designed lime-fly ash and soil-lime mixtures).

Residual Strength Durability Criteria

The development of durability criteria based on the residual strength concept requires several steps.

1. Establish the minimum tolerable strength.
2. Estimate the cured strength of the stabilized material prior to cyclic FT action.
3. Estimate the residual strength following the first winter cyclic FT action.
4. Consider the projected strength-time profile for the material.
5. Check the adequacy of the residual strength and the strength-time profile.

The various factors are discussed in detail below.

Minimum Tolerable Strength

If a given set of pavement design parameters such as subgrade support, traffic loading, and design life is assumed, most pavement thickness design procedures consider the strength of the component pavement layers in establishing the required layer thicknesses. The strength of the stabilized materials must therefore be established for field service conditions. For such materials as soil-cement and lime-fly ash-aggregate mixtures, the most critical field service condition in FT areas is during the spring following the first winter of exposure to FT cycles. The strength during that period is therefore probably the strength that should be considered as a minimum strength for assessing the structural capacity of the pavement section.

Regardless of the thickness design procedure used to design a pavement section containing a stabilized layer, it should be possible (assuming the design procedure has some quasi-rational basis) to establish some minimum tolerable strength that corresponds to the lowest strength required to ensure the structural adequacy of the pavement during the critical spring period. An alternate approach for establishing minimum tolerable strength levels is to consider field performance and job history data.

Cured Strength

The cured strength that a stabilized mixture develops prior to cyclic FT action is dependent on many factors, but particularly on the mixture proportioning and mixing, the density, and the curing.

1. Field correction factors. Field correction factors must be applied to laboratory strengths to correct for mixing inefficiencies and the nonuniformity of field-mixed material. For equivalent mixture proportions the strength of field-mixed material is less than that for laboratory-mixed: For mixed-in-place operations the ratio of the field-mixed strength to that of the laboratory-mixed strength ranges from about 0.6 to perhaps 0.8. Plant mixing is more efficient than field mixing, but although ratios approaching 1 are sometimes achieved, a realistic range is perhaps 0.75 to 0.95. The variability in field mixture strength due to deviations from mix design proportions (primarily of additive and water contents) is substantial. Unpublished data (Barenberg, Department of Civil Engineering, University of Illinois) for lime-fly ash-aggregate plant-mixed material indicated coefficients of variation of strength from 7.7 to 18.2 percent with an average of approximately 11.5 percent. Similar data (8) for a cement-treated base (California type A material plant mix) indicated a coefficient of variation of 16 percent. The coefficient of variation for the compressive strength of a California specification class C cement-treated base constructed by using blade mixing techniques was about 19 percent (8). [There are limited data concerning the strength variability of field-mixed materials, although another California study (9) considers in detail various items of mixed-in-place field operations including additive content and depth of mixing.] Thus it is reasonable to conclude that plant-mixed materials will be more uniform than mixed-in-place materials and to assume a coefficient of variation of 10 to 15 percent for plant-mixed material and 20 to 25 percent for mixed-in-place material.

2. Density effects. The compacted density of stabilized materials substantially influences their cured strength and FT durability (6, 10). Density effects must be carefully considered in the development of a durability evaluation system. If it is assumed that field quality control is adequate to ensure complete compliance with the applicable specifications, the minimum acceptable specification density should be used for the laboratory preparation of specimens. In most instances, the stabilized mixtures are field compacted at approximately optimum moisture content, and a similar moisture content should be used in laboratory specimen preparation. If extensive field data for compaction density and water content are available, such data should be considered in establishing laboratory preparation procedures.

3. Curing effects. The influence of time and temperature on the strength development of soil-lime, soil-cement, and lime-fly ash-aggregate mixtures is well documented. For adequately proportioned mixtures, increases in the temperature and time of curing result in higher strengths. The problem of accurately predicting the combined temperature-time influence on the strength development of a field-cured material is complex. The field temperature in the stabilized layer is quite variable within any 1 year and also shows substantial variability from year to year. The critical consideration in the use of stabilized materials in FT climates is that adequate curing must be provided to ensure sufficient strength development in the material prior to the cyclic FT action. If the cured strength is not adequate at this point, the residual strength of the material after it experiences FT cycles will not be adequate (i.e., the residual strength will be less than the minimum tolerable strength). It is possible to develop information for establishing construction cutoff dates, as illustrated by MacMurdo and Barenberg (11) for various materials and geographic locations. The heat-flow model is readily available for use, although it requires extensive labora-

tory testing of the different materials to establish the minimum curing necessary to ensure adequate strength development. Such a procedure is cumbersome, but it represents the best current approach for considering curing effects. In the absence of such quantitative data, it is necessary to arbitrarily set the cutoff construction date sufficiently early in the fall to ensure attaining the curing essential to achieving the desired cured strength.

Figure 1. Relation between strength after curing and 10-cycle freeze-thaw strength.

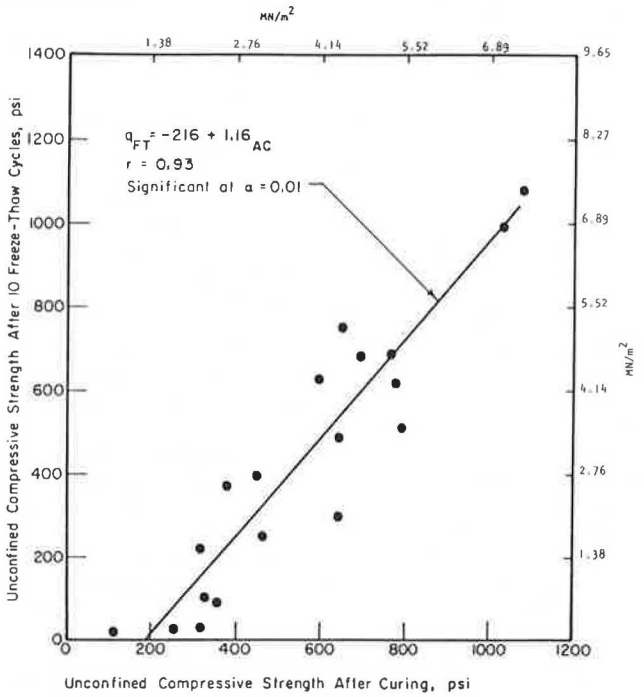

Figure 2. Relation between vacuum saturation strength and 10-cycle freeze-thaw strength.

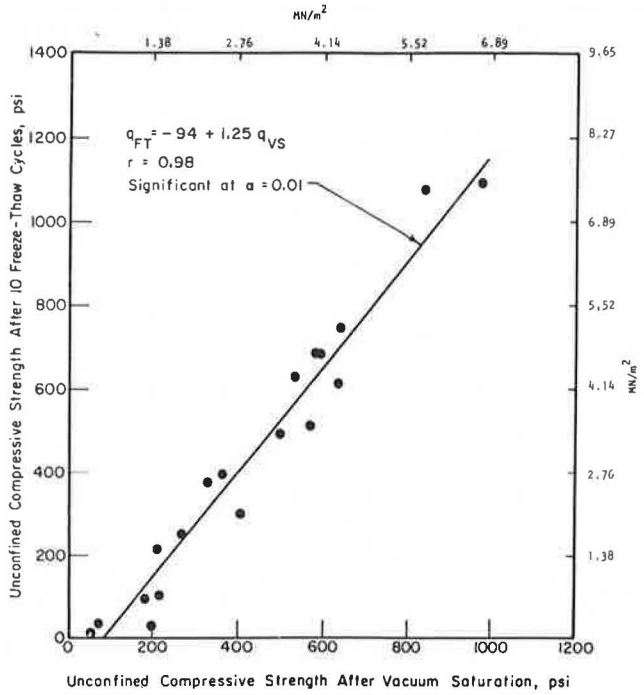

Residual Strength

Two basic factors must be considered in predicting the residual strength of a stabilized material. The first factor is the determination of the number of FT cycles the material will experience during the first winter. The second is the prediction of the residual strength based on the number of FT cycles and some property(ies) of the stabilized mixture.

1. Prediction of the number of FT cycles. The number of FT cycles a particular point in a pavement will experience is affected by many factors, of which the major ones are geographic location and climatic variability, and the pavement system characteristics.

(a) For a given pavement system, the number of FT cycles for a particular reference point will depend on its geographic location. The intensity of cyclic FT action varies from year to year. Figure 4 (2) shows the degree of variability ($\bar{X}$) associated with cyclic FT for various Illinois locations: The standard deviations (σ) are approximately 5 to 6 for northern and central Illinois and

Figure 3. Residual strength concept of freeze-thaw durability.

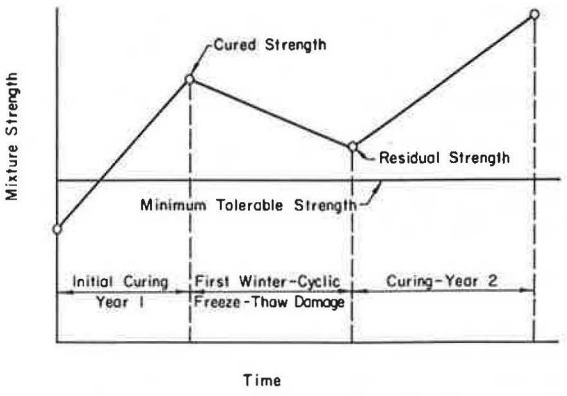

Figure 4. Freeze-thaw cycle data for a stabilized base with an asphalt concrete surface course.

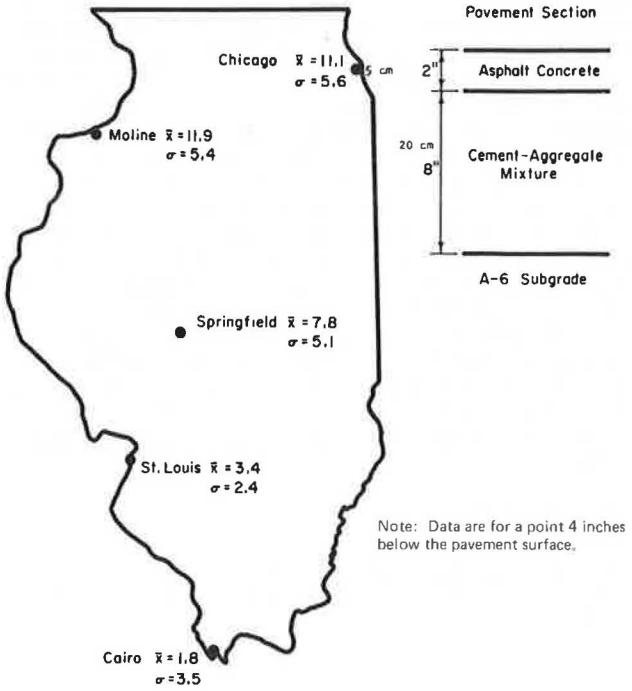

about 3 for southern Illinois. The data developed in the Thompson-Dempsey study (2) were analyzed using the hydrologic statistical concepts employed by Dempsey (12). In this procedure, a relation between the number of FT cycles and the recurrence interval (in years) is established, and by using the recurrence interval concept, it is possible to determine in a rational manner the number of FT cycles that should be considered for FT durability evaluation purposes. The recurrence interval selection should be based on a comprehensive consideration of such factors as economy, field construction practices, pavement design, and performance factors. If a recurrence interval of 2 years is used, that number of FT cycles is exceeded on the average once every 2 years. As illustrated in Figure 5, the cyclic FT-induced strength decreases are not linearly related to the number of FT cycles (6), and later FT cycles are not as detrimental as those initially experienced. This means that FT cycle prediction errors are not necessarily critical.

(b) The thickness of the component pavement layer, the characteristics such as thermal properties and color of the paving materials, and the subgrade soil properties all affect the number of FT cycles experienced by a pavement system. The major uses of stabilized materials are for base courses in flexible pavements with asphalt concrete surface courses or bituminous surface treatments, or for stabilized subbases beneath PCC pavements. Only flexible pavements are considered here. Many subgrade soils are fine-grained, and subgrade soil is not considered as a variable in the following discussions. The FT cycle data shown in Figure 4 were developed for a 20-cm (8-in) base course of a stabilized aggregate mixture (cement-aggregate mixture, pozzolanic aggregate mixture). Similar data were also developed (13) for 30 years of climatic data at three locations (Chicago, Springfield, and St. Louis) and for 1 year of climatic data for Moline for a pavement section in which the base course was 20 cm (8 in) of a stabilized fine-grained soil (soil-cement, soil-lime). Fewer FT cycles were experienced in the stabilized fine-grained soil base. On the average, the ratio of the number of FT cycles for a stabilized fine-grained soil to the number of FT cycles for a stabilized granular soil was 0.70. The effect of the base course thickness was also evaluated (13). The basic pavement section examined is that shown in Figure 4. The thickness of the stabilized granular base was varied from 10 to 20 cm (4 to 8 in). Ten years of climatic data for Springfield, Illinois, were evaluated. The data indicated an insignificant effect (0.7 FT cycle maximum difference) of base course thickness on the number of FT cycles. Thus, no adjustment is required for base course thickness variations if the thickness is within the 10 to 20-cm (4 to 8-in) range. The thickness of the asphalt concrete surface course overlying the stabilized base also influences the number of FT cycles experienced by the base course. As the surface course thickness increases, fewer FT cycles are experienced. If the reference surface course thickness is taken as 5 cm (2 in), an adjustment factor (FT cycles for x inches of surface course/FT cycles for 2 in of surface course) can be developed as shown in Figure 6. The surface course thickness and stabilized material type will substantially affect the number of FT cycles for a pavement system with an asphalt concrete surface course and a stabilized base course. These effects should also be considered in evaluating FT durability.

2. Prediction of residual strength. Three techniques have been developed for predicting residual strength (6). Any of the procedures (FT testing, FT strength-cured strength relations, FT strength-vacuum saturation strength relations) can be used.

(a) The standard FT testing procedure outlined by Dempsey and Thompson (6) is the most realistic and direct procedure for evaluating the FT durability of a stabilized material. The major constraints of the proposed procedure are that the programmable FT testing unit is not a common piece of laboratory equipment, and that the procedure is very time consuming (48 h/cycle).

(b) Cured strength data for the mixture can be used to predict the 5 and 10-cycle FT strength as shown in Figure 1. The standard error of estimate for the regression equation given in Figure 1 is 869 kPa (126 lb/in^2) for 10 cycles.

(c) Vacuum saturation strength data developed according to the testing procedures of Dempsey and Thompson (14) can also be used to predict the 5 and 10-cycle FT strengths, as shown in Figure 2. The standard error of estimate here is 462 kPa (67 lb/in^2) for 10 cycles.

The most direct approach for evaluating residual strength is obviously the FT testing procedure. However, in view of its limitations, the cured strength and vacuum saturation strength correlations are both very attractive. However, since the errors of estimate for the vacuum saturation strength correlations are lower than those for the cured strength correlations, better predictions can be made based on vacuum saturation strength data. Also since the time and equipment required to conduct the vacuum saturation test are nominal, the FT strength-vacuum saturation strength correlations are better (more accurate predictions of FT strength that are only slightly more expensive) than the cured strength correlations.

The major advantage of using the cured strength correlation is that cured strength criteria are commonly used in materials and construction specifications. If FT strength-cured strength correlations are used, residual strengths can be estimated quite readily (assuming that the specification strength is equal to the cured strength).

Strength-Time Profile

A major premise of the residual strength concept is that the stabilized material is capable of developing additional strength following the first winter of FT action. The additional curing (provided favorable temperature conditions prevail) experienced after the first winter is beneficial in developing additional strength in the stabilized material.

Typical strength relations (field data for areas with FT action) for soil-cement and lime-fly ash-aggregate mixtures have shown that the net effect of cyclic FT action and additional curing is a general strength increase (13). Cyclic FT damage is therefore not cumulative on a year-to-year basis. The general increasing strength with time relation for stabilized materials is further supporting evidence for the earlier statement that "if the cured material possesses sufficient durability to survive the first winter FT cycles, the probability of experiencing durability problems during subsequent years is quite low."

It is essential in developing mixture designs for stabilized materials that the mixture be capable of developing additional strength following the first winter. It may be appropriate to use laboratory curing conditions to simulate (a) curing prior to the first winter and (b) additional curing. The additional strength increase must be achieved with increased curing to ensure an adequate mixture design.

If the residual strength of the mixture is greater than the minimum tolerable strength and the mixture is capa-

ble of developing additional strength following the first winter of FT action, then the durability properties of the mixture should be considered adequate.

Other Considerations

In using the residual strength concept, due consideration must be maintained for good mixture design, quality control, and construction practices. If it is assumed that acceptable quality stabilizing additives (lime, cement, and fly ash) are used, and that adequate quality control is being achieved in mixture preparation and construction, then the mixture design becomes a very important and key process.

Freeze-thaw durability evaluation is but one aspect of the mixture design problem, but it is a critical part of the process. An acceptable mixture must meet not only durability requirements, but also other applicable criteria. For properly proportioned and constructed stabilized mixtures, the cured strength normally correlates well with FT durability.

The mixture durability is controlled primarily by the

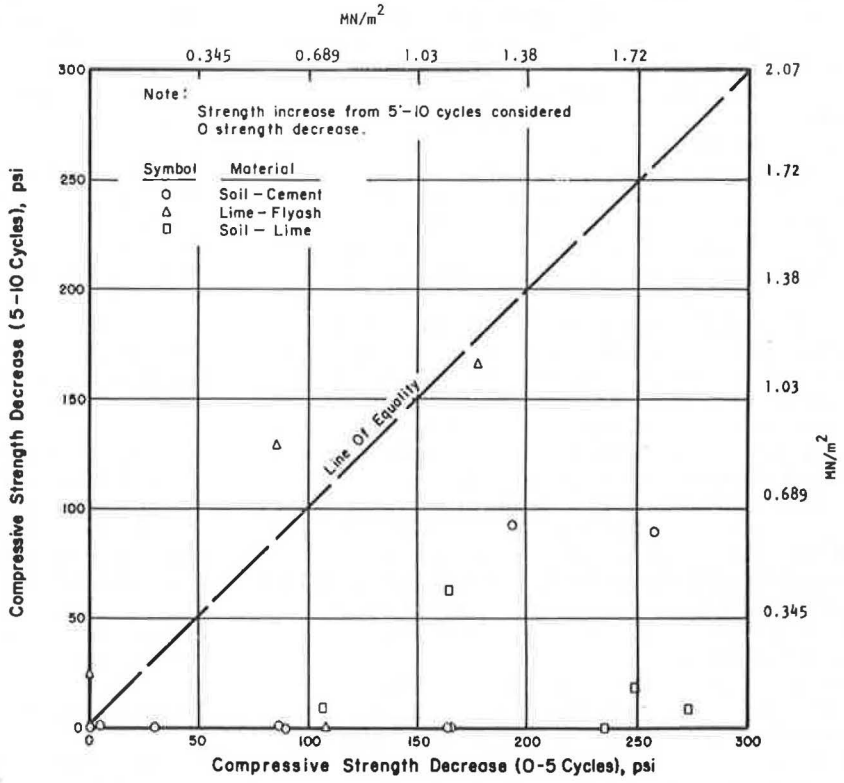

Figure 5. Effect of cycle interval on freeze-thaw strength decrease.

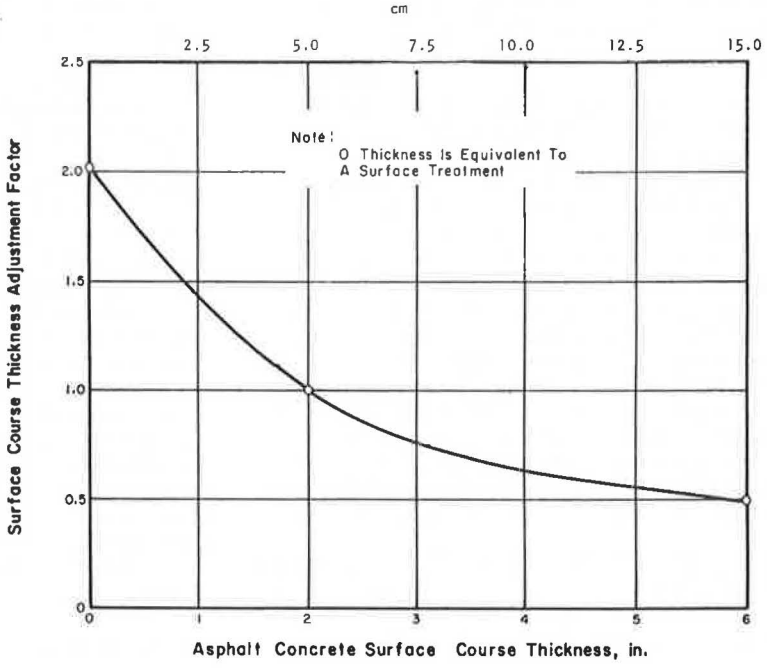

Figure 6. Adjustment factor for asphalt concrete surface course thickness effect.

Figure 7. Mean winter temperature data and freeze-thaw durability zones in Illinois.

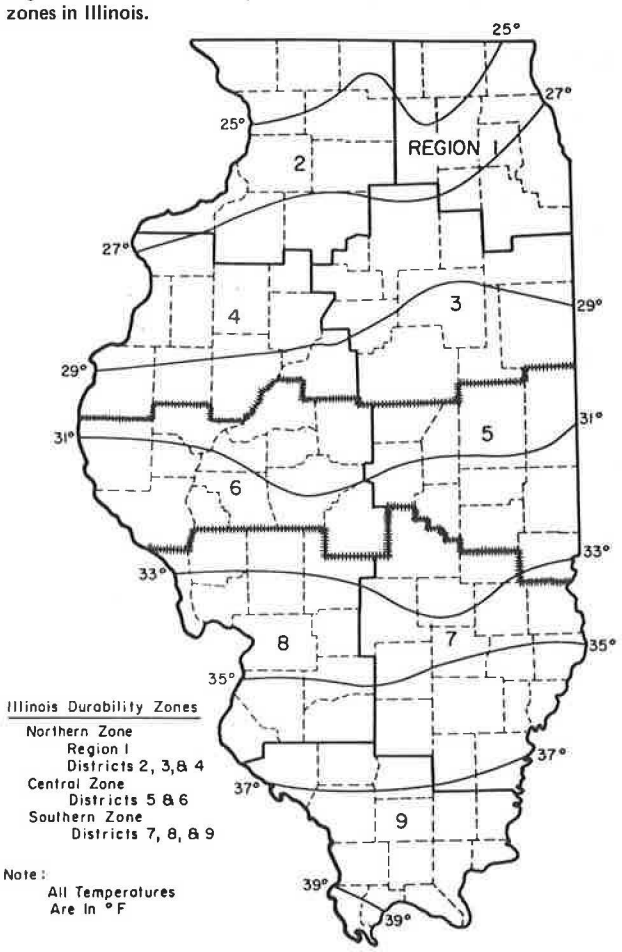

quality of the matrix material in the stabilized granular materials (cement-aggregate mixtures and lime-fly ash-aggregate mixtures). In order to ensure the development of a highly durable matrix fraction in the mixture, it is essential to ensure the development of a floating aggregate mixture in which the larger aggregate particles are separated and the matrix material (the stabilizing additives plus the fraction passing through a No. 4 sieve) is a continuous phase.

The gradation criteria shown below have been developed for cement-aggregate mixes to ensure a floating aggregate mixture.

Sieve	Percentage Passing
No. 4	55
No. 10	37
Nos. 10 to 200	25

Good quality lime-fly ash-aggregate mixtures normally contain sufficient quantities of fines, fly ash, and lime to achieve a floating aggregate condition. In some cases, for example with a uniformly graded sand, increased quantities of lime and fly ash are required to fill the voids in the sand and form a continuous phase, high-quality matrix material.

PROPOSED ILLINOIS PROCEDURE

The following procedure, which is based on the residual strength concept, has been developed for Illinois conditions:

1. Establish the minimum tolerable strength.
2. Determine the number of FT cycles to be expected during the first winter following construction.
3. Establish minimum field-cured and laboratory-cured strength requirements.

Durability Zones

To develop reasonable and realistic durability criteria for Illinois, it is essential to subdivide the state into various durability zones. Based on a consideration of the FT cycle data for various locations in Illinois (Figure 4) and the mean winter temperature data for December, January, and February, the state was divided into the three durability zones (northern, central, and southern) shown in Figure 7. The corresponding FT cycle-recurrence interval relations are shown in Figure 8 (13).

Minimum Tolerable Strengths

A key element in a residual strength-based durability concept is the establishment of a realistic minimum tolerable strength. Various approaches to establishing minimum tolerable strength levels have been discussed earlier in this report.

Cured strength requirements (laboratory conditions) and estimated 10-cycle FT strengths (based on the relation shown in Figure 1) are summarized in Table 1 for typical stabilized materials used by the Illinois Department of Transportation. The approximate 10-cycle FT strength groupings are 1.03 MPa (150 lb/in^2), 1.72 MPa (250 lb/in^2), 2.41 MPa (350 lb/in^2), and 3.79 MPa (550 lb/in^2). These strengths can be used as minimum tolerable strength groupings. (These values could also be based on material properties for pavement thickness design or on field performance data.)

First Winter FT Cycles

Only pavements with asphalt concrete surface courses and stabilized bases are considered in this paper. A similar approach has been developed for stabilized subbases beneath portland cement concrete pavements (13). The FT cycle predictions are based on data previously generated in the University of Illinois study (6) although it may be desirable, in some applications, to actually consider a particular pavement system and the local climatic conditions in more detail by using the heat-flow model techniques developed by Dempsey and Thompson (1).

The following FT cycle prediction procedure is proposed:

1. Select an appropriate frequency-of-return period. (If a 2-year return period is used, that number of FT cycles will be exceeded on the average once every 2 years).
2. From the FT frequency-of-return chart (Figure 8) for the appropriate durability zone, determine the number of FT cycles for the standard pavement structure.
3. Modify the FT cycle value by using the materials factor. (This factor is 1.0 for stabilized granular material and 0.70 for stabilized fine-grained soils.)
4. For an asphalt concrete surface course thickness different from 5 cm (2 in), modify the FT cycle value in accordance with Figure 6. [The thickness of the stabilized base or subbase material is not a significant factor (within normal ranges of thickness), and a modifying factor for this is not needed.]

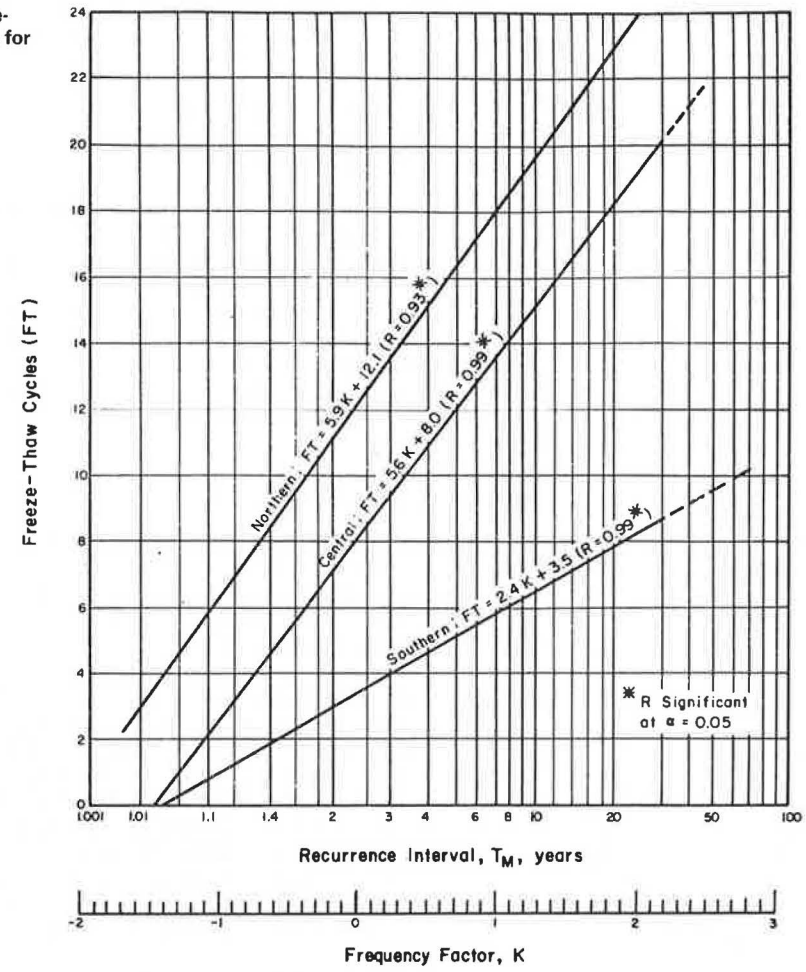

Figure 8. Freeze-thaw cycle-recurrence interval relations for Illinois durability zones.

Table 1. Minimum laboratory strengths and estimated residual strengths for stabilized materials.

Material	Minimum Laboratory Compressive Strength (MPa)	Curing Conditions	10-Cycle FT Strength[a] (MPa)
Cement aggregate base course (bureau of local roads and streets)	"Not less than the design strength specified" (4.48)	7 days—moist	3.71
Pozzolanic base course, type A	2.76	7 days at 38°C	1.71
Soil cement (Illinois DOT flexible pavement design)	2.07	7 days—moist	0.91
Soil cement (bureau of local roads and streets)	2.07 or 3.45	—	0.91 or 2.51
Stabilized shoulders and subbases, cement-aggregate mixture, pozzolan-aggregate mixture	2.76 (FT durability criteria)	7 days at 38°C	1.71

Note: 1 MPa = 145 psi; 1°C = (1°F - 32) 1.8.
[a] Estimate based on the relation shown in Figure 1.

Strength Requirements

It is possible to establish a field-cured strength requirement based on the minimum tolerable strength level and the predicted number of FT cycles. The relations shown in Figure 9 can be used to estimate the field-cured strength requirement (i.e., the strength corresponding to 0 FT cycles). This should then be adjusted (increased) sufficiently to account for mixing efficiency, field variability, and curing considerations. The adjusted strength requirement can be considered as a laboratory strength requirement for the material when it is cured under simulated field conditions; and as more information and experience are developed concerning these important factors, further refinements in strength requirements should be made.

Illustrative Example

The following example of the application of the residual strength procedure is illustrative in nature. A similar approach could be used to establish cured and laboratory strength requirements for different applications. The tools and concepts have been developed, but careful study and judgment are required to establish specific requirements.

Assume the following conditions: (a) The minimum tolerable strength = 1.72 MPa (250 psi), (b) the predicted number of FT cycles (first year) = 10, and (c) the material is plant mixed. In accordance with the suggested procedure:

1. Estimate the required field-cured strength. From Figure 9, the field-cured strength (prior to the first

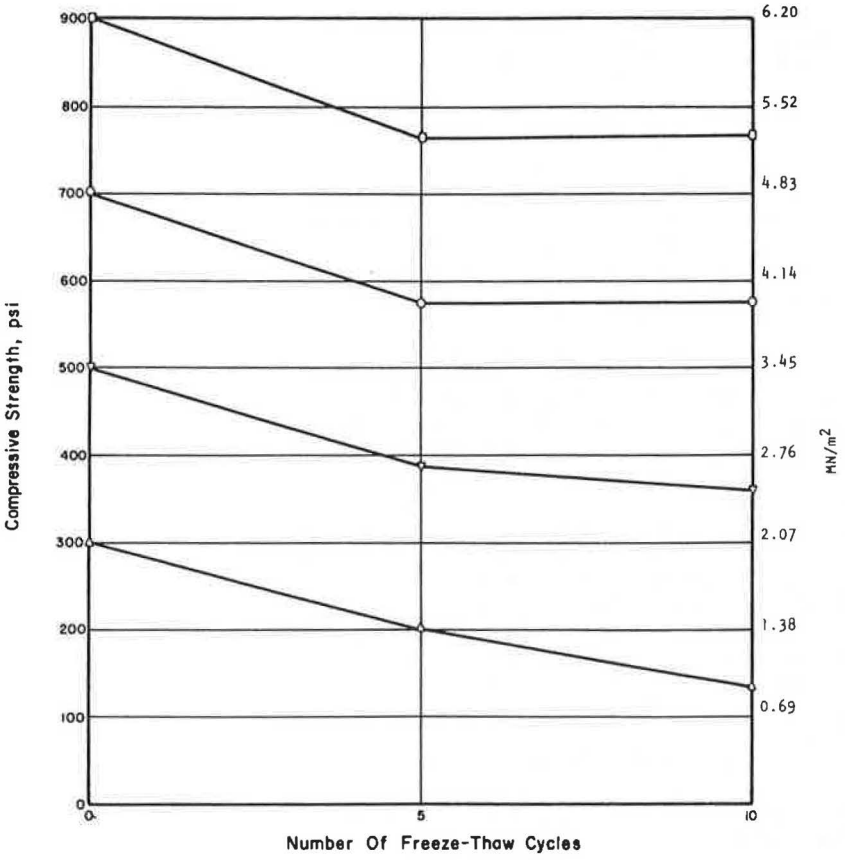

Figure 9. Generalized relation between compressive strength of stabilized materials and number of freeze-thaw cycles.

winter) should be approximately 2.76 MPa (400 psi).

2. Adjust for field variability. If the coefficient of variation for the field compressive strength is assumed to be 15 percent, in order for 84 percent of the material to have a strength greater than 2.76 MPa (400 psi), the average field-cured strength should be

$\overline{X} - 1\sigma = 2.76$ MPa (400 psi)

$\sigma = 0.15\,\overline{X}$

$\overline{X} - 0.15\overline{X} = 2.76$ MPa (400 psi)

$\overline{X} = 2.76/0.85 \cong 3.24$ MPa (470 psi)

3. Adjust for mixing efficiency. For plant mixing operations with a mixing efficiency of 0.85, the adjusted strength is

3.24/0.85 = 3.81 MPa (553 psi)

It it is assumed that field density and curing will be approximately equivalent (i.e., develop similar strength) to laboratory conditions, then the 3.81-MN/m^2 (550-psi) strength requirement can be considered as the laboratory strength requirement for the field material to have a strength of 1.72 MN/m^2 (250 psi) after 10 FT cycles for the conditions and assumptions previously stated.

SUMMARY

Freeze-thaw durability evaluation of stabilized materials and the development of durability criteria are considered by using the residual strength concept. Since so many factors influence the FT durability of stabilized materials and the field FT environment is so variable, the use of this type of procedure is justified. Freeze-thaw durability is not an inherent material property, but relates to the conditions (geographic location, position in the pavement, type of pavement, mixture variables, construction variables, and curing) under which the material is used.

REFERENCES

1. B. J. Dempsey and M. R. Thompson. A Heat Transfer Model for Evaluating Frost Action and Temperature Related Effects in Multilayered Pavement Systems. HRB, Highway Research Record 342, 1970, pp. 39-56.
2. M. R. Thompson and B. J. Dempsey. Quantitative Characterization of Cyclic Freezing and Thawing in Stabilized Pavement Materials. HRB, Highway Research Record 304, 1970, pp. 38-44.
3. B. J. Dempsey and M. R. Thompson. Development of a Programmed Freeze-Thaw Durability Testing Unit for Evaluating Paving Materials. Department of Civil Engineering, Engineering Experiment Station, Univ. of Illinois at Urbana-Champaign, Interim Rept., Phase 2, 1971.
4. B. J. Dempsey. A Programmed Freeze-Thaw Durability Testing Unit for Evaluating Paving Materials. ASTM, Journal of Materials, Vol. 7, No. 2, 1972.
5. B. J. Dempsey and M. R. Thompson. Effects of Freeze-Thaw Parameters on the Durability of Stabilized Materials. HRB, Highway Research Record 379, 1972, pp. 10-18.
6. B. J. Dempsey and M. R. Thompson. Durability Testing of Stabilized Materials. Civil Engineering Studies, Transportation Engineering Series No. 1, Illinois Cooperative Highway Research Program, Univ. of Illinois at Urbana-Champaign, Series No. 132, Sept. 1972.

7. M. R. Thompson. Lime-Treated Soils for Pavement Construction. Journal of Highway Division, Proc., ASCE, Vol. 94, No. HW2, Nov. 1968, pp. 191-217.
8. Soil Stabilization With Portland Cement. HRB, Bulletin 292, 1961.
9. E. Zube, C. G. Gates, and J. A. Matthews. Investigation of Machines Used for Road Mixing. California Division of Highways, Department of Public Works, Research Rept. 633296, Feb. 1970.
10. M. R. Thompson. Engineering Properties of Lime-Soil Mixtures. ASTM, Journal of Materials, Vol. 4, No. 4, Dec. 1969.
11. F. P. MacMurdo and F. J. Barenberg. Determination of Realistic Cutoff Dates for Late Season Construction With Lime-Fly Ash and Lime-Cement-Fly Ash Mixtures. HRB, Highway Research Record 442, 1973, pp. 92-101.
12. B. J. Dempsey. A Heat-Transfer Model for Evaluating Frost Action and Temperature Related Effects in Multilayered Pavement Systems. Department of Civil Engineering, Univ. of Illinois at Urbana-Champaign, thesis, 1969.
13. M. R. Thompson and B. J. Dempsey. Durability Testing of Stabilized Materials. Civil Engineering Studies, Transportation Engineering Series No. 11, Illinois Cooperative Highway Research Program, Univ. of Illinois at Urbana-Champaign, Series No. 152, June 1974.
14. B. J. Dempsey and M. R. Thompson. A Vacuum Saturation Method for Predicting the Freeze-Thaw Durability of Stabilized Materials. HRB, Highway Research Record 442, 1973, pp. 44-57.

Designations of Excavation Characteristics for Materials Identified in Field Investigations

David L. Royster, Division of Soils and Geologic Engineering, Tennessee Department of Transportation

This paper describes a system whereby geologic materials could be categorized according to their excavation difficulty during preconstruction field investigations and defines designations of excavation characteristics for each of the types of materials. It is based on the premise that geologic formations, by their very nature, have rippability characteristics that are traceable, and thus predictable, from one locality to the next. The information obtained within right-of-way limits as a part of geologic mapping would be supplemented by numerous closely spaced auger borings. Examples of road and drainage excavation costs in various geologic environments and of costs of field investigations relative to total project costs are given.

In recent years many legal questions about representations of subsurface conditions relative to the design and construction of transportation facilities have arisen. The entire June 1972 issue of the NCHRP Research Results Digest was devoted to the subject (1). In it, the problem was summed up as follows:

> Contractual representations of subsurface conditions to be encountered in highway construction, which prove to be incorrect after the contract has been let and work has begun, frequently become costly burdens on highway construction programs and even serious impediments to the orderly course of planning and development.

As a result of such problems and the growing number of cases that have gone to litigation, government agencies have become more and more reluctant to reveal all that they know about the subsurface at a given site, and plans and specifications that do contain subsurface data are often accompanied by statements disclaiming guarantees of the accuracy of the information that is supplied. The thinking seems to be that the less information that is furnished concerning conditions at a construction site, the less likely is the possibility of being held liable for misrepresentation. However, while disclaimers and policies that disallow or discourage the inclusion of all available subsurface data may be one way of attempting to avoid litigation, nondisclosure, or failure to provide all of the available information, may be just as contestable in court as information that is incorrect.

This paper discusses some of the factors that may have caused the increasing number of legal problems associated with subsurface investigations and offers suggestions as to how they might be resolved or minimized.

ROOT OF THE PROBLEM

Aside from the fact that the states are weakening in their claim of sovereign immunity, there are a number of reasons why misrepresentation suits are increasing. One reason may be traced to the building boom that began soon after World War II and reached its peak in the last 15 years with the construction of the Interstate system. In the rush to prepare projects for contract, there was simply not enough time to investigate the subsurface in the necessary detail. There has also been a tendency to cut short investigations and handle unforeseen problems arising during construction with supplemental agreements, but while supplemental agreements are an expedient way of handling such problems, they usually result in greatly increased costs. They are also rarely to the advantage of the contracting agency in that they must be negotiated from a disadvantageous position.

Furthermore, soil engineering in its fullest definition did not gain significant acceptance by the highway construction industry until about the middle 1960s. Contractors and construction engineers, for the most part, have been inclined to view many aspects of soil engineering as impractical, too theoretical, and a deterrent to the mass production approach to grading operations. Even now, many individuals without training in soil mechanics or engineering geology tend to underestimate the frequently complex nature of the subsurface. In this regard, soil engineers and engineering geologists (geotechnical personnel)—because they are so few in number—have had difficulty in publicizing the virtues of their trades.

Another factor in all this is that subsurface investigations historically have been almost totally design-oriented. Information from such investigations that can be used by construction people is, in most cases, only a

Publication of this paper sponsored by Committees on Earthwork Construction and Exploration and Classification of Earth Materials.

by-product of the design work. This is a failing of the geotechnical personnel who have not geared their investigations to maximize construction information. Nor have they developed a language that can be understood by others. For example, a contractor who is told that he must move 250 000 m^3 (327 000 yd^3) of Bodine cherty silt loam, residuum from the Pennington shale, or even an A-7-6 with a group index of 25 may be no better informed than if he were told nothing at all. This communication problem, on the other hand, may be directly attributable to the role and position of the geotechnical staff in the total department operation, who may be so situated in the structure of the department that they cannot function to their fullest capabilities.

Still another reason is that subsurface investigations, if done correctly, usually require a large inventory of specialized equipment and a staff of technicians to operate it. Subsurface investigations, whether they be for deep mineral or petroleum exploration or for relatively shallow foundation studies, involve difficult, oftentimes complex, and always very dirty work. Furthermore, the work continues year-round. While construction workers may hibernate, so to speak, during the winter months, geotechnicians must continue their work to prepare for the next construction season. People who do this work and are good at it become harder and harder to find.

Subsurface investigations—to borrow terms from the medical profession—involve both diagnosis and prognosis. But since geotechnical engineering is not as precise, exacting, and predictable a science as medicine, a great deal more interpretation is required. This, then, is the root of the problem as well as the key to its solution. For, if wrong interpretations or no interpretations at all have created an increase in misrepresentation and nondisclosure cases, correct interpretations should result in a decrease in such cases.

IMPROVING COMMUNICATIONS

Part of the solution to the problem may be the development of a language or a method of depicting subsurface materials and conditions that is both design and construction oriented.

In this period of soaring construction and maintenance costs, it is more and more important that the contractor have as much advance information as possible about the soil and rock materials and the conditions at a construction site. This applies not only to highways but also to all types of civil engineering projects such as airfields, dams, canals, buildings, and reservoirs. For bidding purposes, as well as for scheduling and equipment selection, the contractor must be aware of any excavation and grading problems that may be peculiar to the conditions or materials at a particular site. It is incumbent upon the contracting agency to furnish such information, for, after all, how can a design be conceived and be considered safe and feasible to build, without knowledge of the subsurface? Such information, if adequate for the design, will in most cases be adequate for construction. There are times, however, when the area to be excavated may need more thorough exploration with conventional augering equipment, to further delineate variances that may affect the kinds of equipment and the time involved in the excavation process itself. It may be necessary to express or present this information in a different manner. While the designer may be interested in shear strengths and bearing values, the contractor may be more interested in moisture contents and rippability characteristics.

NEED FOR ACCURATE GEOLOGIC INFORMATION

It is not always possible to precisely determine excavation characteristics from subsurface investigations alone, but such investigations, coupled with experience in construction in various geologic environments, can be used to evolve fairly accurate interpretations. Geologic formations, by definition, have characteristics that are consistent from one location to another. These include strata thickness, color, structure, grain size, texture, topographic expression, associated soil types, and weathering characteristics. It is logical to assume that a given type of formation would also have similar excavation characteristics that would be predictable from one site to another. This, then, is a major premise in the applicability of the excavation designations proposed in this paper, for, in addition to a thorough auger-boring program, the geology of an area must be known if its subsurface is to be properly and accurately interpreted for construction purposes.

It is no doubt possible to develop an approximately quantitative approach to the classification of materials that is based on a gauged drilling resistance that could be correlated to the measured ability of that same material to be moved by various types and sizes of earth-moving equipment. There are so many variables in a scheme such as this, however, that it would probably be unreliable. The best approach seems to be a simple qualitative system in which numbers are assigned, based on field investigation and past observations as to the relative ease or difficulty of excavation of the various materials that constitute the particular geologic formation. Such a scheme includes only the materials; it does not include other factors such as terrain conditions and the type or denseness of the vegetative cover. (If desired, these factors could be assigned values that would be added exponentially or in some other manner to the primary excavation difficulty value.)

In devising such a system it is necessary to begin by thinking in terms of the extremes in excavation situations, while at the same time considering the equipment and methods available for use in such excavations. In highway construction, the simplest major excavation is that which can be accomplished with a self-loading scraper. Relatively dry, loosely compacted silts and sands are the easiest and simplest materials to excavate. At the other extreme are the various types of solid rock that require blasting for removal: Unweathered granites and limestones are in this category. On a scale of 1 to 10, the dry silt and sand condition would be assigned a value of 1, and the granite and limestone, the essentially solid rock condition, would be assigned a rating of 10. The main problem, of course, is in deciding on the numerous combinations of materials and conditions that make up the eight other values between. Nevertheless, the following is an example of how a classification system of this type might be set up.

Excavation Index	Degree of Excavation Difficulty	Examples
1	May be easily scraped	Relatively dry sand or silt; some clays
2	May be scraped or bladed	Moist gravel, sand or silt; most clays
3	May be easily bladed or may be scraped with difficulty	Moist clay with minor—less than 25 percent—small disseminated rock particles; some highly weathered

Excavation Index	Degree of Excavation Difficulty	Examples
		shales; some organic materials
4	May be bladed with difficulty	Clay with moderate to heavy—25 to 50 percent—small disseminated rock particles, or with minor pinnacle and/or boulder content; some moderately weathered shales; colluvium with minor boulder content; sanitary landfill material; alluvial boulders
5	May be bladed with great difficulty; or may be easily ripped, dredged, or draglined	Clay with heavy disseminated to some bedded chert; slightly weathered shale; talus or colluvium with heavy boulder content; saturated clay, silt, sand, or gravel
6	May be ripped with some difficulty	Very slightly weathered shale; thin and slabby, disjointed limestones and siltstones; saprolite (rotten igneous or metamorphic materials)
7	Rippable with great difficulty	Thin-bedded chert with clay seams; thin-bedded limestone or siltstone with interbedded shale
8	Requires blasting (up to 25 percent)	Weathered granite, slate, and other igneous or metamorphic rocks; friable sandstone; medium- to thick-bedded limestone with cutters, or disjointed with clay or shale seams; soils with rock pinnacles or large boulders
9	Requires blasting (25 to 50 percent)	Hard shale; thin- to medium-bedded sandstone, siltstone or limestone with interbedded shale; soils with numerous rock pinnacles or large boulders
10	Requires blasting (greater than 50 percent)	Thin- to thick-bedded sandstone, siltstone, and limestone; granite, slate, and other well-indurated or fresh igneous, metamorphic, and sedimentary rocks

Each state or agency would have to prepare, more or less by trial and adjustment, its own criteria for the materials and conditions that would fall into each category of excavation difficulty. These categories would then be incorporated into the profiles and sections that are normally used to depict subsurface conditions (Figure 1). At some later time it might even be possible to standardize such a system, at least on a regional basis, so that contractors who work on projects in those areas could develop a more confident and consistent approach to bidding.

The creation and successful application of a classification system such as this will depend on the position, role, staffing, and overall competency of the geotechnical units responsible for field investigations. Correct interpretations will depend on a great deal of field work on the part of the professionals in the organization. Not only must the soils engineers and the engineering geologists be on hand during the drilling and sampling program, but they must also be constantly observing ongoing grading operations on nearby projects, noting and comparing the construction methods used and the excavation efforts required in the various geologic formations that occur in the area. They must also spend considerable time on the project once it has been let to contract to check the accuracy of their interpretations and to make adjustments and refinements in the system.

UNIT COSTS VERSUS SITE GEOLOGY

Many things go into establishing a bid price: the proximity, type, size, and location of the project, the number of projects being worked by the bidder, the specialty areas of the bidder, and the degree of competition are all important, but a principal factor, though it may not be consciously defined as such, is the site geology. This involves such things as the rock and associated soil types, the extent of weathering, the terrain and drainage conditions, and the structure (faulting, jointing, and direction and angle of dip of the strata). All of these are directly related to the ease or difficulty of excavation of the site and, thus, to the grading and drainage costs.

In Tennessee, as in most other states, the geologic structure may vary considerably over a given area, but, at least on a small scale, certain broad assumptions and predictions can be made about the excavation characteristics of the materials present in a given area. For example, Tennessee is divided into six major physiographic provinces; that is, there are six regions with their own distinct patterns of geologic structure, relief features or landforms, and climatic conditions. These are, from east to west, the Unaka Mountains, the Valley and Ridge, the Cumberland Plateau, the Highland Rim, the Central Basin, and the Coastal Plain as shown in Figure 2 (2). The Highland Rim, the Central Basin, and the Coastal Plain are often further subdivided, but for the purposes of this paper only the major divisions will be considered. The most complex province physiographically, as well as geologically, is the Unaka Mountains province. The least complex is the Coastal Plain. As might be expected, highway construction costs in the Coastal Plain province are significantly less than those in the mountainous province. Some relationships of physiographic areas, probable excavation indexes, and excavation costs for recent projects are indicated below.

Area	Excavation Index Range	Recent Costs ($/m^3)
Coastal Plain	1 to 5	0.84 to 1.33
Highland Rim	3.5 to 6	1.64
Central Basin and edges of Cumberland Plateau	3 to 9	2.22
Cumberland Plateau	6 to 7.5	2.03
Valley and Ridge	4 to 7	1.44
Unaka Mountains	5 to 10	2.62

This kind of correlation could be used as a reference for creating a classification system based on the excavation difficulty of specific geologic formations.

The next step would involve the collection of information about individual projects in each province according to the geologic formations that are traversed. This involves detailed surface mapping along the alignment, a detailed subsurface investigation program, and a comparison of the materials and conditions found along the alignment with those of nearby projects that traverse the same geologic formations that are traversed. This involves detailed surface mapping along the alignment, a detailed subsurface investigation program, and a comparison of the materials and conditions found along the alignment with those of nearby projects that traverse the same geologic formations. The subsurface investigation should be accomplished primarily with power augers. In some cases, geophysical methods may be used but only

Figure 1. Schematic of boring pattern in plan and profile.

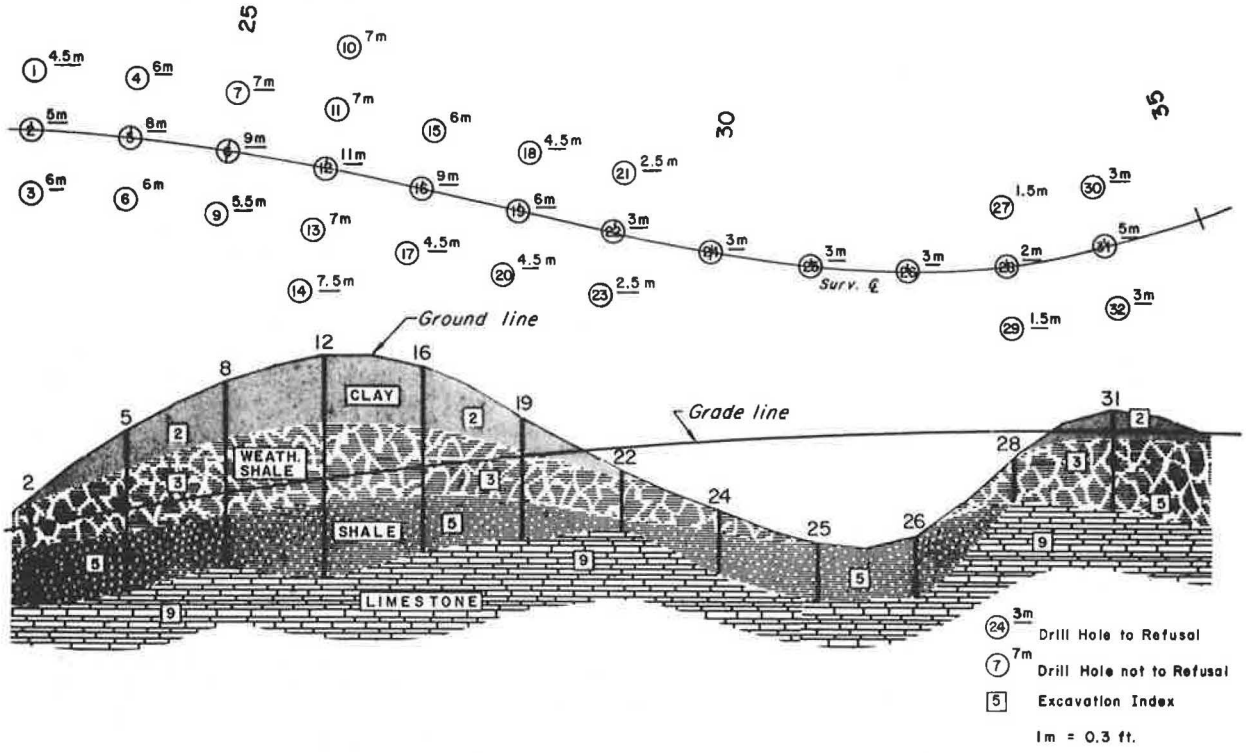

Figure 2. Generalized physiographic map of Tennessee.

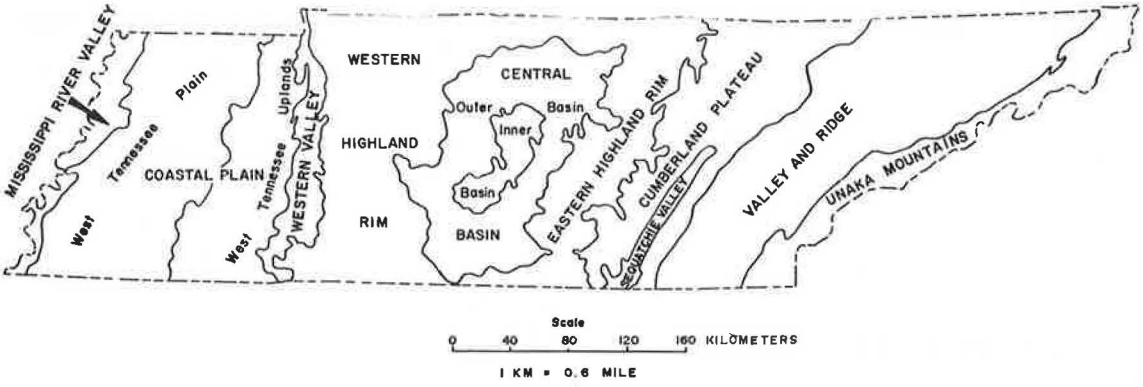

to supplement the borings. The drilling should follow a pattern commensurate with the geology, terrain conditions, right-of-way limits, and proposed roadway gradient (Figure 1). In most cases, borings on 30-m (100-ft) centers will be adequate; however, there are times when 15-m (50-ft) centers or less will be required. This, again, will depend on the geology of the area and the degree of accuracy that is desired. Furthermore, occasional core borings may be required to further delineate variances in materials and conditions at a given site.

Samples for the determination of in-place moisture should be taken periodically by the standard penetration test method (AASHTO T206-74). The number of samples required for this will depend on the depth, width, and length of the interval to be excavated, as well as on the geology of the drilling site. An approximate rule might be to sample every fifth hole along the centerline. This procedure can determine not only the amount of moisture, but also the resistance to penetration by the sampler, which may be useful in developing designations of excavation characteristics for the project.

All of this information could then be depicted graphically in plan and profile (Figure 1), and typical cross sections, as well as detailed sections of the more complex areas, could be developed. The subsurface information displayed in this manner would relieve the contractor of the time-consuming chore of studying the boring and geophysical records and reports to make his or her own determinations of the materials to be excavated.

At first consideration, field investigations in this detail may appear to be too expensive of both time and money. However, the costs of overdesign or the sometimes catastrophic results of underdesign, as well as the construction problems that result from simply not knowing what to expect, make detailed site investigations the most realistic approach.

As a percentage of the total costs involved, the costs of adequate field investigations on most projects are not significant. This is especially the case when auger

borings are the principal means of investigating the subsurface. Some typical cost examples are given below.

Example	No. of Holes Drilled	Total Depth Drilled (m)	Drilling Cost ($)	Percentage of Total Project Cost
1	298	915	8 400	0.34
2	309	1525	14 000	0.31
3	272	1186	10 900	0.30

In Tennessee, where almost all subsurface investigations are conducted by state employees, total costs, including all borings, samplings, analyses, and evaluations, rarely exceed 0.75 percent of total project costs, with most ranging between 0.35 and about 0.60 percent.

PREBID SITE INVESTIGATIONS BY CONTRACTORS

There is a trend, at least in Tennessee, toward fewer geotechnical investigations by contractors prior to bidding on highway construction projects. There are several reasons for this. The principal one is that the benefits are no longer considered worth the time, effort, and costs involved if a reasonable amount of information is supplied by the contracting agency. A forthcoming NCHRP synthesis on subsurface investigation practices by highway and transportation departments will indicate that at present only 15 to 25 percent of contractors make a geotechnical investigation prior to bidding. Of those who do so, most do so primarily to determine for themselves the rippability and general nature of the materials to be excavated.

It is logical to assume that most contractors would forgo the effort and expense of prebid subsurface investigations if they were more confident about the information furnished by the contracting agency. It is logical to assume that, the more subsurface information supplied, the more realistic and competitive the bids will be. A contractor would be more confident about bidding on projects for which the subsurface information was depicted in a manner similar to that shown in Figure 1. This should be reflected in road and drainage excavation unit prices: If excavation costs could be reduced as little as 1 to 5 cents/m^3, this would amount to hundreds of thousands or millions of dollars for all projects during a year.

CONCLUSION

Obviously, the more time, effort, and money expended on subsurface investigations, the more information will be gained, and the more information gained, the more appropriate and realistic will be the design. Further, the more information supplied the contractor, the greater will be his confidence and the more realistic will be his bid. This information, however, must be presented in a form that is oriented to construction. A classification system such as that described here would seem to meet this criterion. Such a system should help to close the communications gap that exists between the contractor and geotechnical engineers, and this, in turn, should reduce the number of misrepresentation and nondisclosure cases brought to litigation in the future.

REFERENCES

1. Legal Aspects of Representations as to Subsurface Conditions. NCHRP, Research Results Digest 39, June 1972.
2. Robert A. Miller. The Geologic History of Tennessee. Tennessee Division of Geology, Bulletin No. 74, 1974.

Pore Structure of Selected Hawaiian Soils

R. A. Lohnes, E. R. Tuncer, and T. Demirel, Civil Engineering Department and Engineering Research Institute, Iowa State University

Many studies have emphasized that the structure or fabric of deeply weathered tropical soils has important influences on their engineering behavior. This study attempts to characterize the structure of five soils from the island of Oahu, Hawaii, by mercury injection porosimetry. All the soils were derived from basalt, but each had weathered under a different mean annual rainfall. A comparison of air-dried, oven-dried, and freeze-dried samples showed that the method of drying has little effect on the pore size distribution and is interpreted as evidence that the structure of these soils is more stable than that of soils in which the main bonding material is clay. From 89 to 72 percent of the voids in these soils fall within a size range greater than 0.004 μm. Although the void ratio variations between these soils do not show any systematic trends, the pore size distributions do. The soils that had developed under wetter climates have higher percentages of pores smaller than 2 μm in diameter and a more uniform pore size distribution. The pore size distributions can be related to the mineral and chemical contents of the soils in that soils weathered in wetter environments are higher in sesquioxide content and lower in kaolinite content.

The engineering behavior of deeply weathered tropical soils in the undisturbed state is largely controlled by their structure, which appears to result from the cementation of the clays by iron oxides (2, 11, 13, 16, 21, 22, 23, 24, 27). For this reason, the Unified and AASHO classification systems, which are based on engineering index tests using disturbed samples, are inadequate to predict the field performance of these soils (7, 8, 10, 14, 28), and an engineering classification based on parent material and degree of weathering (4, 9, 10, 15) has been recommended.

In an effort to better understand the structure of such soils in relation to their weathering environment, the porosity of five soils, all derived from basalt but weathered under a wide range of mean annual rainfalls, was measured by mercury injection porosimetry tests.

THE SOILS

The soils used in this study were Paaloa, Manana, Wahiawa, Lahaina, and Molokai soils from Oahu, Hawaii. All were derived from the Koolau basalt series on the leeward side of the Koolau mountain range. Since this basalt series is uniform chemically and petrologically (26) it may be assumed that all of the soils were derived from essentially the same parent rock. These rocks are described as Pliocene olivine basalt flows, which dip from the crest of the mountain range at angles of 3 to 10 deg. The basalt has a high permeability, resulting from interstitial spaces in the clinkers, shrinkage cracks, and gas vesicles (18, 19).

The soils are classified as Oxisols and Ultisols. All have a seasonal high water table deeper than 150 cm and bedrock at depths greater than 150 cm. A complete morphologic description and other physical and chemical data are given by Foote and others (7).

The sample locations are along a 5-km traverse on the divide between Kipapa Stream and Panakauki Gulch about 5.5 km northwest of Pearl City. The elevations of the sample sites range from about 165 to 365 m. Since the rainfall is orographic, there is a mean annual precipitation of 58 to 216 cm/year. The slopes on which the soils formed range from 2 to 7 percent. The pedologic classification and environmental factors are given below.

Soil Series	Pedologic Classification	Mean Annual Rainfall (cm/year)	Slope (%)
Molokai	Typic torrox	58	2
Lahaina	Typic torrox	71	2
Wahiawa	Tropeptic eutrustox	127	2
Manana	Orthoxic tropohumult	158	7
Paaloa	Himoxic tropohumult	216	7

Samples were collected from the B horizon of each soil series at depths of 25 to 135 cm in thin-walled Shelby tubes 7.62 cm in diameter and about 25 cm long. Three borings were made at each location and samples taken from various depths. The range of sampling depths for each series is shown in Table 1. The engineering index properties of these soils are also listed in Table 1 although they do not correlate with the porosimetry data.

Publication of this paper sponsored by Soil and Rock Properties and Geology Section.

METHOD

The use of mercury injection porosimetry to characterize the pore size distribution of soils in order to relate the soil structure to its engineering properties was introduced by Diamond (6). Since then several related studies on compacted soils (1, 3, 17) have been conducted. The technique is based on the Washburn (25) equation

$$P = (-2T \cos \theta)/r \quad (1)$$

where P is the pressure, T is the surface tension, θ is the angle of contact, and r is the pore radius. The soil samples were dried and placed in the sample cell of the porosimeter, and the sample space was then evacuated with a vacuum pump so that air would not block the flow of mercury into the pores of the sample. After evacuation of the pressure chamber, mercury was allowed into it to immerse the soil sample. Since the volume of the chamber is known and the volume of mercury that flows into it can be measured, the total volume of the sample can be calculated. Then, as pressure is applied, the mercury penetrates the sample. Both the volume of mercury penetrating the soil and the pressure required to cause this penetration are measured, and these data are used in equation 1 to compute the pore radius that is being penetrated at a given pressure. These results are then plotted to give the pore size distribution curve.

The instrument used in this study has a pressure range of 0.035 to 3500 kg/cm^2. With it, if the surface tension of mercury is taken as 47.4 mN/m and a contact angle of 140 deg is used, it is possible to measure pore radii between 105.4 and 0.00210 μm. This porosimeter also has the capability to empty the pores by reducing the pressure to produce a vacuum at the end of the penetration phase. This allows measurement of the pore size distribution on the extrusion cycle and, from those data, a characterization of the irregularity of the pores.

OBSERVATIONS

The influence of drying methods was evaluated for all of the soils by taking three portions of soil from the same boring and depth, and air-drying one, oven-drying the second at 100°C, and freeze-drying the third. Figure 1 shows that there is little or no difference in the pore size distribution curves for samples of the same soil dried by the different techniques. The same behavior is true of all five soil series and contrary to the results of Ahmed and others (1). This observation supports the conclusions of other studies on tropical soils that the clays are cemented together by iron oxides. If the clays themselves were the main source of bonding in these soils, significant volume changes would result from air- and oven-drying as compared with freeze-drying.

Pore size distribution determinations were made for 6 to 10 samples from various depths and borings of each series. Figure 2 shows the range of pore size distribution curves for 9 samples of the Paaloa soil series, which is typical for all of the series. The variation in pore size characteristics within a soil series is fairly small.

On the other hand, when the pore size characteristics of the various series are compared, there is a wide range in the curves as shown in Figure 3. From these curves, each of which is representative of a soil series, it is possible to generate a set of parameters to characterize the pore structure of each series.

Some similarities in the curves are observed. For example, the Molokai, Lahaina, and Wahiawa series all show a distinct bimodal distribution, one in the 10 to 20-μm size range and the other in the 0.01 to 0.1-μm range. The other two soils show only the smaller size range. These quantitative data support earlier qualitative studies made with a scanning electron microscope (23).

The extrusion curves were plotted to describe the pore diameter versus volume relation as the mercury was removed from the soil. In all soils there is a considerable hysteresis loop that indicates the necking down of the pores. A typical curve having a hysteresis loop is shown in Figure 4. The volume of mercury that is retained in the sample at the end of the evacuation is a measure of the nonuniformity of the pore size distribution. The percentage of the total amount of mercury injected into the samples that was retained in the soil varied from 36 to 55 percent. The values for each series are shown in Table 2. Table 2 also shows the following other pore size characterization parameters: the median (50 percent) and small mode pore diameters, the uniformity coefficient, the percentage of pores smaller than 2 μm, and the void ratios computed both from mercury injection data and from measurements of the bulk geometry of the Shelby tube samples and the dry weight of the samples. The uniformity coefficient is defined, by analogy with the uniformity coefficient calculated from particle size distribution curves, as the ratio of the minimum pore diameters corresponding to 60 and 10 percent of the total pore volume penetrable by mercury respectively.

Comparison of the void ratios calculated from the mercury injection data with those calculated from the bulk density measurements shows that not all of the voids were intruded by the mercury. That is, there is a considerable volume of pores having diameters smaller than 0.004 μm. The portion of pore volume not intruded by mercury, expressed as a percentage of the total volume as measured by bulk density, is about 11 percent for the Molokai soil and ranges from about 21 to 28 percent for the other four. From these data the pore size parameters can be computed on the basis of the total pore volume rather than on the basis of the pore volume intruded by the mercury; but, although there are small changes in the values of the parameters such as the percentage of pores smaller than 2 μm and median pore diameter, the trends, which are observed as the five soil series are compared, do not change. For convenience, all of the pore size parameters reported here are based on the volume of pores intruded by mercury.

RELATIONSHIP OF PORE SIZE TO WEATHERING AND MINERALOGY

The soils are listed in Table 2 in order of increasing mean annual precipitation. Although there is no apparent relation between the void ratio and the amount of rainfall, there are trends between other pore size parameters and rainfall. This emphasizes the usefulness of information related to pore size as opposed to information based on total pore volume only. Data both on the percentage of mercury retained at the end of the withdrawal cycle and on the uniformity coefficient show that the soils that have developed under wetter climates have a more uniform distribution of pore sizes than those developed under drier climates. The small pore mode diameters range from 0.014 to 0.031 μm, and the wetter soils have larger mode pore sizes. There is no clear trend for the median diameter or for the total pore volume. The percentage of pores smaller than 2 μm increases systematically from soils developed under drier climates to those developed in wetter areas. The mineral and other chemical constituent contents of the soils (based on B horizon data of the Soil Conservation Service) are shown below.

Table 1. Engineering index properties.

Soil Series	Gradation Sand (%)	Silt (%)	Clay (%)	Liquid Limit	Plasticity Index	Specific Gravity	Range of Sample Depths (cm)
Molokai	28.7	51.1	20.3	45.5	6.8	2.946	43 to 135
Lahaina	31.0	38.8	30.3	49.1	10.6	2.937	48 to 122
Wahiawa	10.7	45.6	43.8	51.3	15.3	2.989	34 to 104
Manana	69.3	16.7	14.0	67.1	16.7	2.991	25 to 124
Paaloa	27.8	39.3	33.0	57.1	17.8	3.098	38 to 135

Note: 1 cm = 0.4 in.

Table 2. Pore size parameters.

Soil Series	Void Ratio by Mercury Injection	Void Ratio by Bulk Measurement	Median Pore Diameter (μm)	Small Pore Mode Diameter (μm)	Uniformity Coefficient ($\times 10^{-1}$)	Mercury Retained (%)	Pores ≤2 μm (%)
Molokai	0.960	1.085	0.037	0.015	4.3	55.2	61.5
Lahaina	0.919	1.276	0.019	0.014	8.4	47.6	70.5
Wahiawa	0.723	1.011	0.017	0.015	8.9	50.0	79.0
Manana	0.978	1.237	0.023	0.022	28.1	36.1	84.0
Paaloa	1.029	1.321	0.038	0.031	30.7	40.4	85.0

Note: 1 μm = 4 x 10^{-5} in.

Figure 1. Effect of drying method on cumulative pore size distribution.

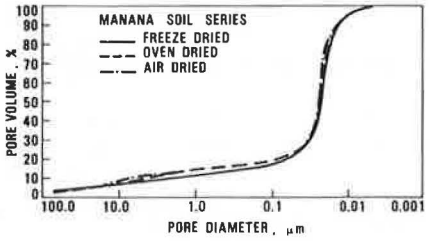

Figure 2. Example of variation of pore size distribution within Paaloa soil series.

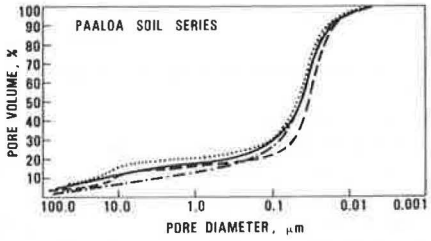

Figure 3. Cumulative pore size distribution curves for five soil series.

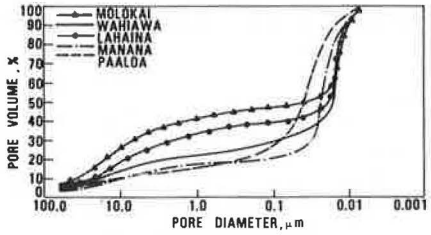

Figure 4. Typical pore size distribution curve including hysteresis loop.

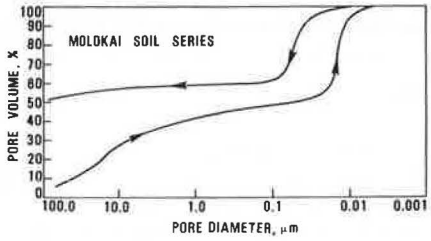

Soil Series	Kaolinite	Gibbsite	Iron Oxide	Kaolinite Gibbsite + Iron Oxide
Molokai	53	0	12.1	4.38
Lahaina	52	2	16.0	2.89
Wahiawa	53	6	13.6	2.70
Manana	30	11	20.9	0.94
Paaloa	12	34	25.8	0.20

The kaolinite content decreases with increasing rainfall (5, 12, 20), and the gibbsite and total iron oxide contents both increase with increasing rainfall. The systematic trend is indicated by the variation of the kaolinite to gibbsite plus iron oxide ratios with rainfall. From these trends it appears that both the aluminum and iron oxides may be involved in the cementation of the clays. According to the weathering model of Alexander and Cady (2), as the kaolinite is weathered to gibbsite there may be more cementation, which would result in a higher percentage of smaller pores and a more uniform size range of those pores.

SUMMARY AND CONCLUSIONS

Tests on five basalt-derived soils from Oahu showed that mercury injection porosimetry can be used to characterize the pore size distribution of these deeply weathered tropical soils. The method of drying the soil has little effect on the pore size distribution. This is interpreted as evidence that the structure of these soils is more stable than that of soils in which the main bonding material is clay. From 89 to 72 percent of the voids are within the size range greater than 0.004 μm. Although the void ratio of the soils does not show any systematic trends in relation to the mean annual rainfall, the soils that developed under wetter climates have higher percentages of smaller pores and pores of a more uniform size distribution. These data can also be related to the mineral contents of the soils in that the soils that had weathered in wetter environments are higher in sesquioxide content and lower in kaolinite content.

ACKNOWLEDGMENTS

The authors gratefully acknowledge the support for this work by a grant from the Army Research Office and the additional support of the Engineering Research Institute at Iowa State University. They also thank Oran Bailey, U.S. Department of Agriculture, who helped select the sampling sites and provided pedogenic and chemical data on the soils studied.

REFERENCES

1. S. Ahmed, C. W. Lovell, Jr., and S. Diamond. Pore Sizes and Strength of Compacted Clay. Journal of the Geotechnical Engineering Division, Proc., ASCE, Vol. 100, 1974, pp. 407-425.
2. L. T. Alexander and J. G. Cady. Genesis and Hardening of Laterite in Soils. U.S. Department of Agriculture Technical Bulletin 1282, 1962.
3. W. W. Badger and R. A. Lohnes. Pore Structure of Friable Loess. HRB, Highway Research Record 429, 1973, pp. 14-23.
4. H. S. Bhatia. Discussion of Engineering Characteristics of Laterites. Proc., Specialty Session of Engineering Properties of Lateritic Soils, 7th International Conference on Soil Mechanics and Foundation Engineering, Mexico City, Vol. 2, 1970, pp. 75-80.
5. L. A. Dean. Differential Thermal Analysis of Hawaiian Soils. Soil Science, Vol. 63, 1947, pp. 95-105.
6. S. Diamond. Pore Size Distribution in Clays. Clays and Clay Minerals, Vol. 18, 1970, pp. 7-23.
7. D. E. Foote, E. L. Hill, S. Nakamura, and F. Stevens. Soil Survey of the Islands of Kauai, Oahu, Maui, Molokai, and Lanai, State of Hawaii. Soil Conservation Service, U.S. Department of Agriculture, and Agricultural Experiment Station, Univ. of Hawaii, 1972.
8. B. Fruhauf. A Study of Lateritic Soils. Proc., HRB, Vol. 26, 1946, pp. 579-589.
9. M. D. Gidigasu. The Importance of Soil Genesis in the Engineering Classification of Ghana Soils. Engineering Geology, Vol. 5, 1971, pp. 117-161.
10. A. L. Little. The Engineering Classification of Residual Tropical Soils. Proc., Specialty Session on Engineering Properties of Lateritic Soils, 7th International Conference on Soil Mechanics and Foundation Engineering, Mexico City, Vol. 1, 1969, pp. 1-10.
11. R. A. Lohnes, R. O. Fish, and T. Demirel. Geotechnical Properties of Selected Puerto Rican Soils in Relation to Climate and Parent Rock. Geological Society of America, Vol. 82, 1971, pp. 2617-2624.
12. R. A. Lohnes and R. L. Handy. Shear Strength of Some Hawaiian Latosols. 6th Annual Symposium on Engineering Geology and Soil Engineering, Boise, Idaho, 1968.
13. R. A. Lohnes and T. Demirel. Strength and Structure of Laterites and Lateritic Soils. Engineering Geology, Vol. 7, 1973, pp. 13-33.
14. Z. C. Moh and F. M. Mazhar. Effects of Method of Preparation on Index Properties of Lateritic Soils. Proc., Specialty Session on Engineering Properties of Lateritic Soils, 7th International Conference on Soil Mechanics and Foundation Engineering, Mexico City, Vol. 1, 1969, pp. 23-36.
15. D. G. Moye. Engineering Geology for the Snowy Mountains Scheme. Civil Engineering Transactions, Institution of Engineers, Australia, Vol. 27, 1955.
16. S. Sivarajasingham, L. T. Alexander, C. G. Cady, and M. G. Cline. Laterite. In Advances in Agronomy, Academic Press, New York, Vol. 14, 1962, pp. 1-60.
17. A. M. Sridharan, A. G. Altschaeffl, and S. Diamond. Pore Size Distribution Studies. Journal of the Soil Mechanics and Foundations Division, Proc., ASCE, Vol. 97, No. SM5, 1971, pp. 771-787.
18. H. T. Stearns. Geology of the State of Hawaii. Pacific Books, Palo Alto, Calif., 1966.
19. H. T. Stearns and K. N. Vaksvid. Geology and Ground-Water Resources of the Island of Oahu, Hawaii. Hawaii Division of Hydrography Bulletin, No. 1, 1935.
20. T. Tanada. Hawaiian Soil Colloids. Agricultural Experiment Station, Univ. of Hawaii, Rept., 1942-1944, pp. 56-57.
21. K. Terzaghi. Design and Performance of Sasumua Dam. Proc., Institute of Civil Engineers, Vol. 9, 1958, pp. 369-395.
22. F. C. Townsend, P. G. Manke, and J. V. Parcher. Effects of Remolding on the Properties of the Lateritic Soil. HRB, Highway Research Record 284, 1969, pp. 76-84.
23. G. Y. Tsuji, R. T. Watanabe, and W. S. Sakai. Influence of Soil Microstructure on Water Characteristics of Selected Hawaiian Soils. Proc., Soil Science Society of America, Vol. 39, 1975, pp. 28-33.
24. K. B. Wallace. Structural Behaviour of Residual Soils of the Continually Wet Highlands of Papua New Guinea. Geotechnique, No. 2, 1973, pp. 203-218.
25. E. W. Washburn. Note on a Method of Determining the Distribution of Pore Sizes in a Porous Material. Proc., National Academy of Sciences, Vol. 7, 1921, pp. 115-116.
26. C. J. Wentworth and H. Winchell. Koolau Basalt Series, Oahu, Hawaii. Bulletin of the Geological Society of America, Vol. 58, 1947, pp. 46-78.
27. H. F. Winterkorn and E. C. Chandrashekharan. Laterite Soils and Their Stabilization. HRB, Bulletin 44, 1951, pp. 10-29.
28. F. L. D. Wooltorton. The Scientific Basis of Road Design. Edward Arnold Publishers, London, 1954.

Insulated Road Study

E. Penner, Division of Building Research, National Research Council of Canada

The results of a 3-year insulated road study showed that frost penetration inward from the edge of an insulated area is about the same as the downward penetration on a control section. Moisture accumulated in the frost-susceptible subgrade after the frost line penetrated the insulation. During periods of rapid cooling, the temperature of the surface above an insulated pavement may be lowered sufficiently to permit surface icing if atmospheric moisture conditions are suitable. Terminating the insulation without feathering induces abrupt changes in elevation in the roadway as a result of heaving.

Thermally insulated roads attenuate frost penetration in winter by reducing ground heat loss to the air. The pavement thickness of such roads can be reduced in areas where frost penetration and its subsequent damage are critical factors. Since base course material is becoming scarce in some areas, the use of insulation may reduce the cost of road construction.

Insulated road sections have been constructed in Canada and the northern regions of the United States (1, 2, 3, 4, 5). In Ontario insulation is now used as a standard method for repairing frost-damaged highway sections, although it has not yet been used in new highway construction. The information in the literature is still sparse on some aspects of the field performance of insulated roads despite the general acceptance of the technique for the fast and efficient repair of busy highways. Among the less understood aspects are (a) the extent of ice lensing when the frost line penetrates and remains below the insulation layer in frost-susceptible soil for a considerable period and (b) the thermal pattern in the soil at the transition zone between the insulated and uninsulated sections.

The first is particularly significant if an insulated section has been underdesigned, either in error because of a lack of air temperature information or intentionally to keep construction costs as low as possible or to decrease the likelihood of surface icing. Information about the thermal regime at the transition zone is important for extending the insulation a sufficient distance beyond the protected area to prevent abrupt changes in elevation at the ends.

SOIL CONDITIONS

The experimental work was conducted on the grounds of the National Research Council of Canada in Ottawa. The soil is a postglacial clay of marine origin that is commonly referred to as Leda clay (6). It consists of about 70 percent clay-size and 30 percent silt-size particles. Frost heaving is approximately 9 to 12 cm (0.3 to 0.4 ft) during most winters in snow-cleared areas.

DESIGN OF INSTALLATION

Figure 1, a plan of the 30.5-m (100-ft) test road, shows the location of the instrumentation, which consists of thermocouple strings, survey plates, and access holes for neutron moisture measurements. The pavement design for the 15-m (50-ft) insulated section is shown in Figure 2. The procedure for preparing the subgrade for placement of the insulation boards was to fine grade it, then hand rake the surface. The 0.6 by 1.2-m (2 by 4-ft) insulation boards were staggered and held in place with 15-cm (6-in) wooden dowels. The crushed rock base was end-dumped from trucks and spread by hand.

MEASUREMENT TECHNIQUES

Temperatures were measured by 0.8-mm (20-gauge) copper-constantan thermocouples attached to 4-cm (1.5-in) diameter wooden dowels. A 0.3-m (1-ft) length of thermocouple lead was wrapped around the dowel in a groove at each measurement position to minimize conduction errors. At each location in the control section at which temperatures were measured, thermocouples were placed 0.076, 0.3, 0.6, and 1.2 m (3, 12, 24, and 48 in) from the surface; in the insulated section thermocouples were placed 0.076, 0.2, 0.3, 0.6, and 1.2 m (3, 10, 12, 24, and 48 in) from the surface.

Subgrade moisture contents were determined with a neutron moisture meter near the center of each section (7, 8). The access holes of the neutron meter probe were

Publication of this paper sponsored by Committee on Frost Action.

cased with 4-cm (1.5-in) diameter aluminum tubes sealed with rubber stoppers; desiccant was kept inside the tubes to prevent moisture condensation on the inner walls. Elevation surveys for heave measurements were carried out with a precise level on metal plates embedded in the surface of the asphaltic concrete at the locations shown in Figure 1 and referenced to a stable benchmark.

RESULTS AND DISCUSSION

The thermal pattern for the time of maximum frost pene-

Figure 1. Plan of test road.

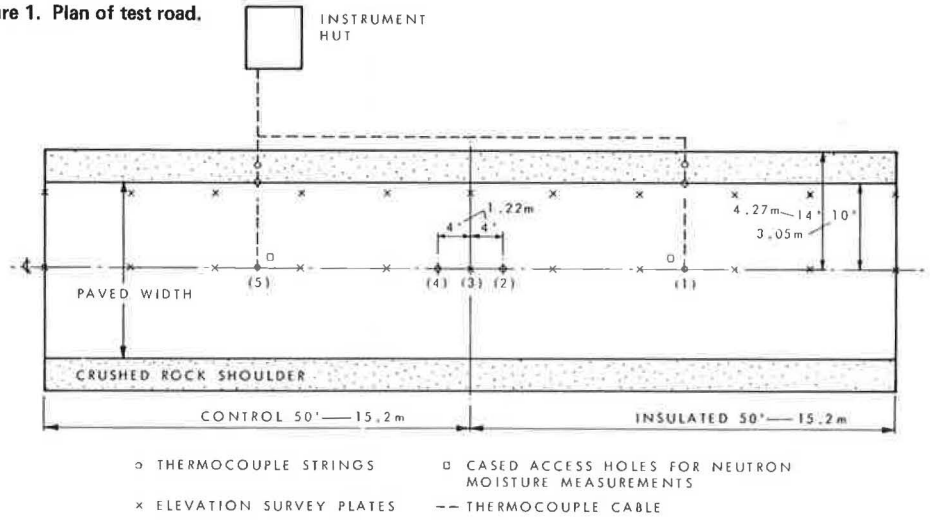

Figure 2. Cross section of insulated road section.

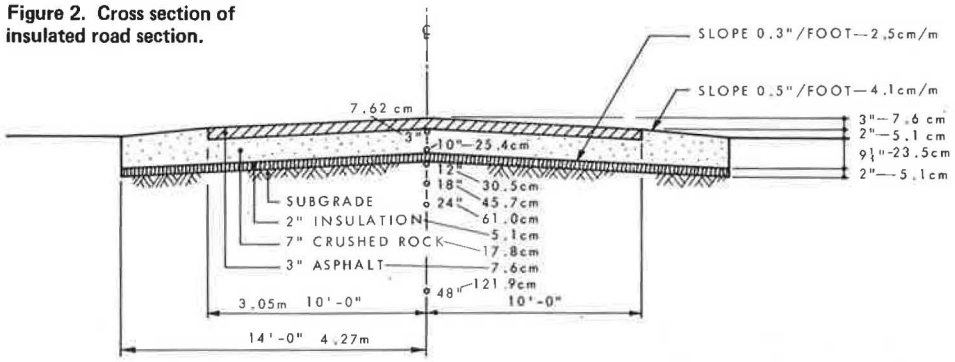

Figure 3. Isotherms near time of maximum frost penetration at end of insulated section on centerline of snow-cleared road.

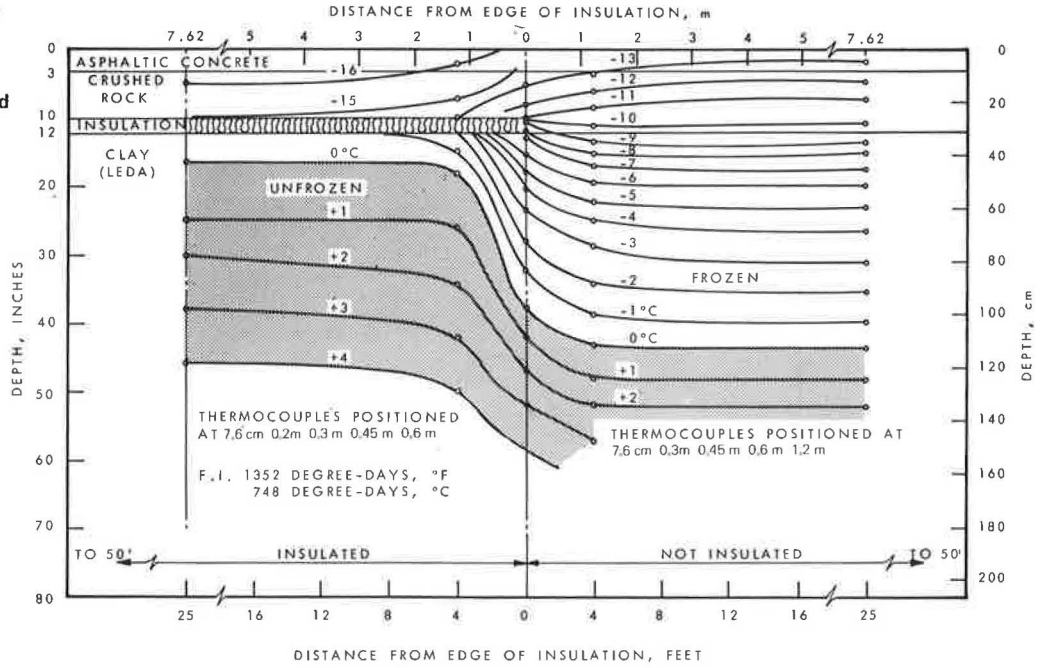

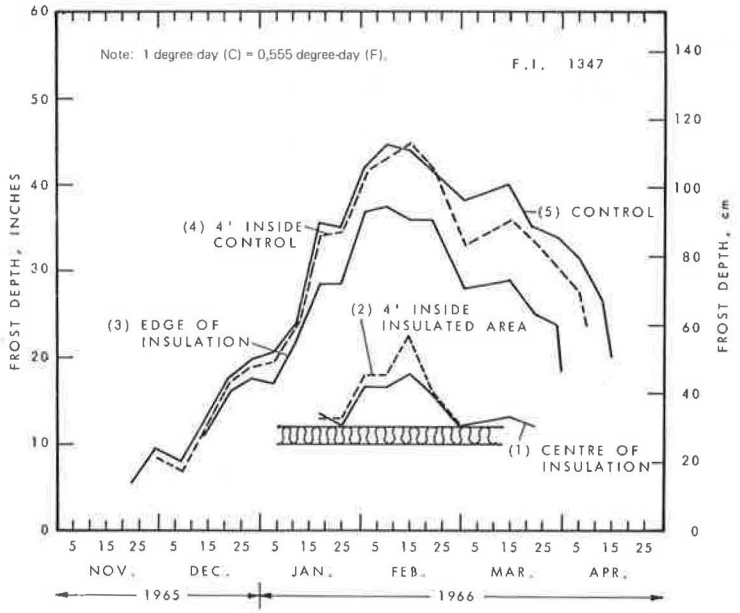

Figure 4. Depth of frost line at various locations as given in Figure 1 for winter 1965-66.

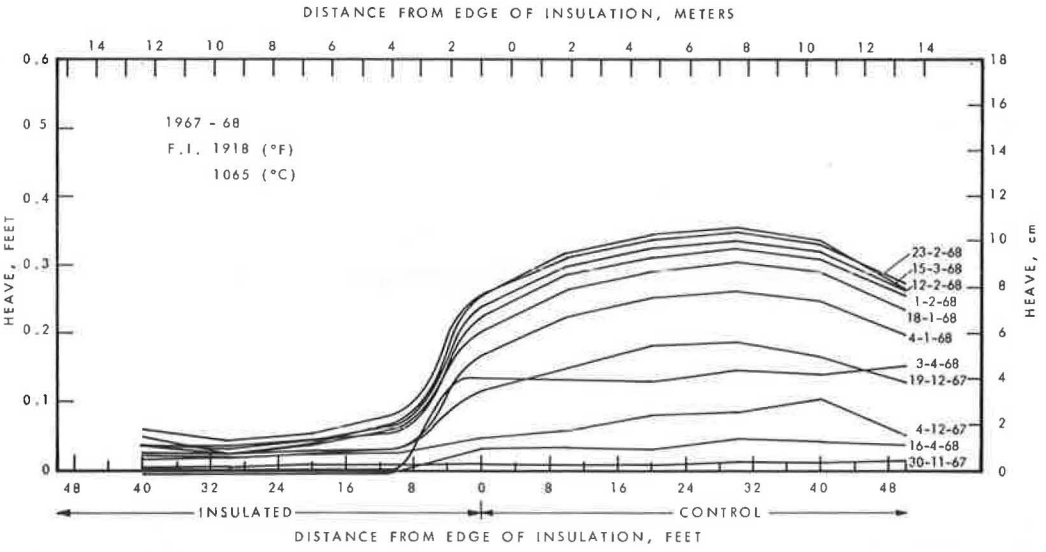

Figure 5. Frost heave on road centerline of insulated section and adjacent control.

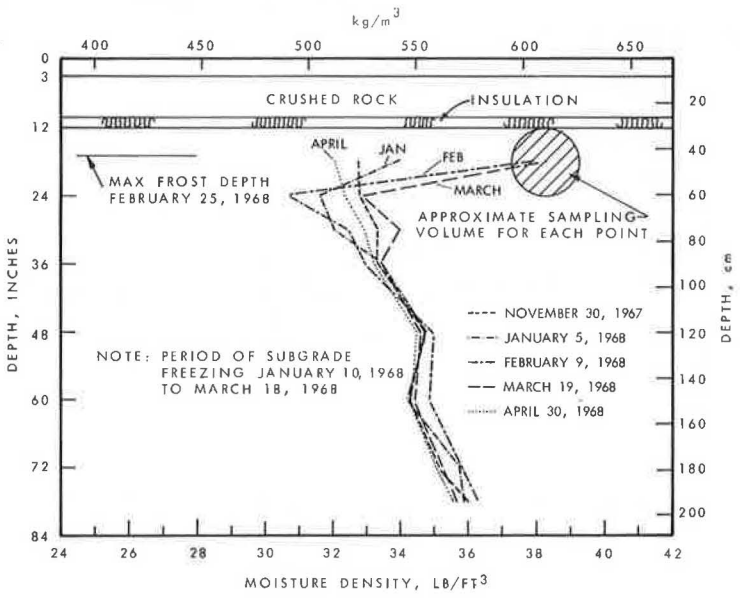

Figure 6. Moisture density profile in subgrade, 1967-68.

tration, at the transition zone between the insulated and control sections on the road centerline, was similar for the 3 consecutive years, 1965-66, 1966-67, and 1967-68. Figure 3 gives such a pattern for 1 year. The base course above the insulation was colder than the surface of the control section, but differences in the temperatures of the surfaces would depend on the air temperature prior to the measurements. The thermal response of the base course above the insulation to changes in the air temperature gave warmer temperatures for the insulated sections in the summer and colder temperatures in the winter.

Figure 4 shows the frost penetration at the edge of the insulation 1.2 m (4 ft) inside the insulated area, 1.2 m (4 ft) inside the control area, and at the center of each section. In all cases, the frost penetration at the center of the control area and that at a point 1.2 m (4 ft) from the edge of the insulation were similar. During the 3-year period when the measurements were made, the frost penetration in the control area ranged from about 1.1 to 1.5 m (45 to 55 in). Thus, at a distance inside the insulated area equal to the depth of frost penetration almost all end effects due to insulation have disappeared.

The heave pattern for the three winters shows the severity of frost heave in Leda clay. Figure 5 gives the results for 1967-68. Heaving was observed in the insulated area as well as in the control section since 5 cm (2 in) of insulation does not provide complete frost protection for the subgrade. The water table at the site characteristically rises to the ground surface in the fall; as the surface of the pavement is level with the surrounding terrain, this results in a fully saturated base course. The small heave above the insulation measured during the period of freezing is attributed solely to expansion of water. Normal ice lens growth is thought to be responsible for the measured heave that takes place after the frost line has passed through the insulation into the subgrade. The measure of moisture increase below the insulation is given in terms of moisture density in Figure 6, which also shows the position of the frost line at a maximum penetration in relation to the depth at which the moisture was measured.

Two final items are of particular interest. The thermal equivalents of soil versus insulation for the Ottawa trials and for those at another test site in Sudbury, Ontario, are shown in the table below, which also lists the cumulative degree-days for each year at each site.

Location and Year	Penetration Into Subgrade Below Insulation (cm)	Penetration Into Subgrade in Control (cm)	Insulation Equivalents (cm)	Degree-Days
Ottawa				
1965-66	15	84	14	748
1966-67	20	104	17	988
1967-68	13	105	19	1065
Sudbury				
1964-65	30	119	18	1443
1965-66	13	94	16	1127
1966-67	33	107	15	1212
1967-68	46	117	14	1476

The values range from 14 to 19 cm of soil per centimeter of insulation. The average thermal conductivity of the insulation (measured in the laboratory) was 0.39 W/m·K (0.27 Btu·in/h·ft^2·°F) after 10 years burial at the Ottawa test site. After 6 weeks drying at 41°C (105°F) this value was reduced to 0.35 W/m·K (0.24 Btu·in/h·ft^2·°F). The moisture absorbed and retained was 6.8 percent by volume, which appears entirely acceptable after 10 years of exposure in the ground.

CONCLUSIONS

Although the heat extraction rate is slow when the frost line is in wet frost-susceptible soil below insulation, moisture flow is induced and heaving occurs. Under the soil and climatic conditions of this study, frost penetration inward from the edge of the insulation was about the same as that downward in an uninsulated area. Abrupt heaving at the edge of the insulation was well demonstrated and can be avoided by feathering the insulation at the ends of the insulated sections.

ACKNOWLEDGMENTS

The author wishes to express his appreciation to his colleagues for assisting with the work carried out in this study and for their many helpful suggestions. This paper is a contribution from the Division of Building Research, National Research Council of Canada, and is published with the approval of the director of the division.

REFERENCES

1. Performance Study Report on Insulation Board (Polystyrene). AASHO-ARBA Subcommittee on Development, Evaluation, and Recommendation of New Highway Materials, 1970.
2. M. D. Oosterbaan and G. A. Leonards. Use of Insulating Layer to Attenuate Frost Action in Highway Pavements. HRB, Highway Research Record 101, 1965, pp. 11-27.
3. F. D. Young. Experimental Foamed Plastic Base Course. HRB, Highway Research Record 101, 1965, pp. 1-10.
4. E. Penner, M. D. Oosterbaan, and R. W. Rodman. Performance of City Pavement Structures Containing Foamed Plastic Insulation. HRB, Highway Research Record 128, 1966, pp. 1-17.
5. E. Penner. Experimental Pavement Structures Insulated With a Polyurethane and Extruded Polystyrene Foam. Proc., International Conference on Low Temperature Science, Sapporo, Japan, Vol. 1, Part 2, 1967, pp. 1311-1322.
6. C. B. Crawford. Quick Clays of Eastern Canada. Engineering Geology, Vol. 2, No. 4, 1968, pp. 239-265.
7. K. N. Burn. Design and Calibration of a Neutron Moisture Meter. ASTM, STP 293, 1961, pp. 14-26.
8. K. N. Burn. Calibration of a Neutron Moisture Meter in Leda Clay. Canadian Geotechnical Journal, Vol. 1, No. 2, 1964, pp. 94-103.